The University Of Sheffield

The impact and regulatory function of Tribbles on metabolic homeostasis

By

Zabran Ilyas

A thesis submitted in partial fulfilment of the requirements for the degree of

Doctor of Philosophy

The University of Sheffield

Faculty of Medicine, Dentistry and Health

Department of Infection, Immunity & Cardiovascular Disease (IICD)

March 2018

In memory of my beloved Father, Mohammed Ilyas.

‘This PhD is dedicated to my Father, Mohammed Ilyas (May his soul rest in peace), who has been a powerful influence in my life. His discipline, support and love gave me the ability and strength to prosper.’

Publications arisen from work presented in this thesis

Conference abstracts

- **Ilyas Z** , Angyal A, Szilli D, Johnston J and Kiss-Toth E. (2016) *MIRNA202 is a Novel Regulator of Tribbles-1 Expression.* Heart 101(4)
- **Ilyas Z** , Al-Ghamdi J, Tan A and Kiss-Toth E. (2016) *Trib3 is a novel regulator of lipid metabolism*. Heart 18(3)
- Angyal A, **Ilyas Z**, Hadadi E, Johnston J, Ariaans M, Kraus R, Wilson H, Bauer R, Rader D, Francis S and Kiss-Toth E. (2015) *Does myeloid expression of TRIB1 regulate plasma lipid levels?* Atherosclerosis 241(1), 34

Reviews

- Johnston J, Basatvat S, **Ilyas Z**, Francis S & Kiss-Toth E (2015) *Tribbles in inflammation*. Biochemical Society Transactions , 43(5), 1069-1074

Oral presentations

- 'Trib3 a novel regulator of lipid handling'. Tribbles 2nd conference- Beijing
- 'miR202 novel regulator of TRIB1'- Singapore

Abstract

Metabolic syndrome significantly increases the risk of developing chronic inflammatory diseases including coronary artery disease, stroke and type 2 diabetes. Obesity is a major risk factor for many facets of metabolic diseases which lead to significant morbidity and mortality worldwide. The family of Tribbles pseudokinases, including Trib3 have been implicated in the development of many chronic inflammatory diseases.

Previous human genetic studies have shown a Q84R polymorphism of TRIB3 to be associated with insulin resistance, dyslipidaemia and increased risk of developing diabetes. Furthermore, patients with type 2 diabetes (T2DM) were shown to have elevated levels of TRIB3 in the pancreas compared with healthy patients. TRIB3 was also implicated in the diabetic atherosclerosis process. Silencing Trib3 in apolipoprotein E (apoE)/LDR receptor (LDLR) double-knockout (ApoE$^{-/-}$/LDLR$^{-/-}$) mice with diabetes reduced atherosclerotic burden and stabilised the plaque in mice. All the evidence above indicates that Trib3 is an important regulator of insulin resistance and cardiovascular disease. However, the mechanisms of how Trib3 plays a part in chronic inflammatory diseases are unexplored.

Development of metabolic syndrome is driven by a combination of different metabolic tissues becoming dysfunctional. While it is clear that the various organs may be affected differently, our insights into the role of Trib3 in various organs remains limited. This study is aimed to use a systemic approach, for the first time on a whole body Trib3^{ko} mice to decipher a role for Trib3 in metabolic dysfunction.

Full body Trib3^{ko} mice were created using the gene-trap system. Male Trib3^{ko} mice were obese with elevated plasma levels of HDL and total cholesterol. These knockout mice also displayed a fatty liver phenotype, an increased macrophage influx in the liver and dysregulated proliferation in the adipose tissue. Comparative gene expression microarray analysis was performed on the liver, adipose and muscle tissues from Trib3^{ko} and WT littermates. Gene Ontology and Pathway Analysis were performed using Ingenuity Pathway Analysis software. This analysis revealed multiple metabolic pathways in the liver, adipose and muscle tissues were altered, suggesting a dysregulated inter organ communication underpinning obesity. Key signalling regulators, such as PPARα, CEBPα and Akt were altered in the liver of Trib3^{ko} compared with WT mice as evidenced by qPCR and western blots. Interestingly, a concurrent increase in GLUT2 levels were detected in Trib3^{ko} liver, pointing to a possible cross-regulation between liver lipid and glucose metabolisms via Trib3.

Although Trib3 is implicated in lipid metabolism and insulin resistance, the isoform Trib1 has also been described as a regulator of inflammatory signalling and lipid metabolism. A genome-wide association study (GWAS) in a human patient had shown Trib1 to be associated with hyperlipidaemia and increase the risk of developing coronary artery disease (CAD)

Trib1 has also shown to be an important negative regulator of inflammation and acts to lower plasma lipid levels. The half-life of Trib1 mRNA is <1 h, so the aim of the second part of the project was to find ways to stabilise Trib1 mRNA levels which would, therefore, have beneficial effects on lipogenesis. The liver is the primary organ to modulate systemic cholesterol levels, so the aim was to stabilise TRIB1 levels in the liver. miRNA202 was shown to be a novel small non-coding RNA which can modulate TRIB1 protein levels, therefore representing a target by which TRIB1 levels could be raised in vivo, providing a mechanism to augment lipid levels and therefore the anti-atherosclerotic effects of this protein.

Declaration of Contribution

I can confirm that majority of the work presented in this thesis is my own. Data interpretation and analysis have been carried out by myself. I would like to acknowledge those people that have contributed their work, who either came before me or during my PhD. Data carried out by others have been acknowledged in the relevant figure legends.

I would like first to thank and appreciate **Dr.Jihan Al Ghamdi** who was a previous PhD student at Endre Kiss-Toth group for providing extensive lipid profile data for the Trib3^{ko} mice vs WT littermates, including the glucose tolerance test and Insulin tolerance test data. **Dr Steven Reynolds** for the MRI scans of Trib3^{ko} vs WT. Special appreciations go to **Dr Li Liang** and **Tan Ming Jie** who helped alongside myself carrying out the microarrays. The actual microarray was carried out at Denova sciences in Singapore. I would like to extend my gratitude to **Dr Zoe Bichler** for carrying out the metabolic cage experiments, and finally, I would like to thank **Chiara Niespolo** for the miRNA bioinformatics data, a PhD student in Endre Kiss-Toth group.

Acknowledgement

I would like to express my gratitude and appreciation to my supervisors: Professor Endre Kiss-Toth and Professor Tan Nguan Soon who gave me the opportunity to work in their lab and the support and advice to complete my PhD. I am immensely grateful to them for giving me the chance to travel the world for scientific conferences. It has been an amazing experience meeting new people, exchanging ideas and making new scientific discoveries. Again, thank you for all this, I am eternally grateful.

I would also like to especially thank Dr Adrienn Angyal and Dr Jessica Johnston, who have helped me in the Sheffield labs and have provided advice and support to me throughout my PhD journey. I am ever so grateful for their help, discussions and feedback. Furthermore, I would extend my wishes and thanks to the Kiss-Toth Group, past and present, whom I had enjoyed working with and had fruitful conversation with, especially at times when experiments were not working.

Additionally, I would like to thank my colleagues in Tan Nguan Soon group in the Singapore labs; especially appreciations go to Dr Liang Li, Dr Penchang Chu, Dr Zhen Wei and Tan Ming Jie, who have made my Singapore trip amazing and provided the help and support I required upon my time in Singapore. I will cherish the memories in Singapore, and as promised we shall meet up in Sheffield and re-live the fun times.

I would also like to thank Prof. Guillermo Velasco for giving me the opportunity to work in his lab and Dr Maria Lorento who supported me throughout my stay in Madrid. Thank you for showing me the ropes on Western blotting.

Finally, I would take this opportunity to thank my family, especially my mum, my brothers, and my wife and son; Rayan, who have been a strong moral support for me when things got difficult. Their endless love and motivation had kept me going. It has not been an easy journey, but was well worth it. Undoubtedly, the journey has not only developed me as a scientist, but also made me stronger as a person. Without the teachings of my father, all this would not be possible; he gave me the ambition and the encouragement to believe that I can achieve anything in life. It was that believe and ambition which resulted in where I am today.

Content page

List of Figures

List of Tables

;

.

Abbreviations

A	Adventitia
AAV	Adeno-associated virus serotype
ABC	ATP-binding cassette
ACC	Acetyl coenzyme A Carboxylase
AcLDL	Acetylated Low-Density Lipoprotein
AD	Alzheimer's disease
Akt	(PKB) Protein kinase B
AML	Acute myeloid leukaemia
AP-1	Activator protein 1
ApoE	Apolipoprotein E
Arg	Arginase
BAT	Brown adipose tissue
C/EBP	CCAAT-enhancer binding protein
CARE	Cholesterol and Recurrent events
cDNA	Complementary DNA
CE	Cholesterol ester
CETP	Cholesterol ester transfer protein
CHIP	Chromatin immunoprecipitation
CHOP	C/EBP homologous protein
COP1	Constitutive photomorphogenic 1
COPD	Chronic obstructive pulmonary disease
COX	Cyclooxygenase
CRP	C-reactive protein
CVD	Cardiovascular disease
DAPI	4',6-diamidino-2-phenylindole
DC	Dendritic cell
DMEM	Dulbecco's modified Eagle's Medium
DNA	Deoxyribonucleic acid
DNL	*De novo* lipogenesis
ER	Endoplasmic reticulum
ERK	Extra-cellular signal-regulated kinase
EVG	Elastic van Gieson
FABP	Fatty acid binding protein
FASN	Fatty acid synthase
FBS	Neutral buffered formalin
FC	Fibrous cap
FCS	Foetal calf serum
FFA	Free fatty acids
FFPE	Formalin fixed paraffin embedded
GFP	Green fluorescent protein
GWAS	Genome-wide association study

H	Human
H&E	Haematoxylin & Eosin
Hb	Haemoglobin
HDL	High density lipoprotein
Hem	Haemorrhage
HFD	High fat diet
HRP	Horse radish peroxidase
Hs	Homo sapiens
IC	Immune complex
IDL	Intermediate density lipoprotein
IFN	Interferon
IHC	Immunohistochemistry
IHD	Ischaemic heart disease
IKK	Inhibitor of IκB
IL	Interleukin
IL1R1	Interleukin 1 receptor
IMT	Intima-media thickness
INOS	Inducible nitric oxide synthase
IRAK	Interleukin-1 receptor associated protein kinase
IRF-5	Interferon regulatory factor-5
IVC	Individual ventilated caging
IκB	Inhibitor of κB
JNK	c-Jun N-terminal kinase
KCs	Kupffer cells
KO	Knockout
LAL	Lipoprotein lipase
LCAT	Lecithin cholesterol acyl transferase
LDL	Low-density lipoprotein
LDLR	Low-density lipoprotein receptor
LOX	Lectin-like oxidised low-density lipoprotein receptor
LPS	Lipopolysaccharide
LXR	Liver X Receptor
M	Media
Mm	Mouse
MAPK	Mitogen activated protein kinase
MARS	Monitored Atherosclerosis Regression Study
Mb	Mega base pairs
MCP	Monocyte chemo-attractant protein
MCSF	Macrophage colony stimulating factor
MDMs	Monocyte derived macrophages
MDP	Monocyte/macrophage cell progenitor
MI	Myocardial infarction
miRNA	micro-RNA
MKK	MAPK-Kinase
MMP	Matrix metalloproteinase
MMR	Macrophage mannose receptor

MPO	Myeloperoxidase
MPS	Mononuclear phagocyte system
mRNA	messenger RNA
MRI	magnetic resonance imaging
NAFLD	Non-alcoholic fatty liver disease
NCEH	neutral cholesteryl ester hydrolase
NEFAs	Non-esterified fatty acids
NEMO	NF-κB essential modifier
NF-κB	Nuclear factor kappa-light-chain enhancer of activated B cells
NICE	National Institute for Health and Care Excellence
NMR	Nuclear magnetic resonance
NO	Nitric oxide
OLR	oxLDL receptor
ORO	Oil red O
oxLDL	Oxidised low-density lipoprotein
PBS	Phosphate buffered saline
PCSK9	Proprotein convertase subtilisin/kexin type 9
PFA	Paraformaldehyde
PIL	Procedure individual license
PKB	(Akt) Protein kinase B
PL	Phospholipid
PPAR	Peroxisome proliferator-activated receptor
PPRE	PPAR response element
PRRs	Pattern recognition receptor
qPCR	Real-time polymerase chain reaction
RNA	Ribonucleic acid
ROI	Region of interest
ROS	Reactive oxygen species
RPMI	Roswell Park Memorial Institute Medium
RT	Room temperature
RXR	Retinoid X receptor
SDS	Sodium dodecyl sulphate
SEM	Standard error of the mean
siRNA	Small interfering RNA
SMCs	Smooth muscle cells
SNP	Single nucleotide polymorphism
SR	Scavenger receptor
SREs	Sterol regulatory elements
STAT	Signal transducer and activator of transcription
TBST	Tris-buffered saline-Tween
Tg	Transgenic
TG	Triglyceride (triacylglycerol)
TGF	Transforming growth factor
TH	T-helper cell
Thr	Threonine
TIMP	Tissue inhibitor of matrix metalloproteinase

TIR	Toll-interleukin-1 receptor
TLR	Toll-like receptor
TNF	Tumour necrosis factor
TRAF	TNF receptor activated factor
Trib	Tribbles
Trib1	Tribbles 1
Trib2	Tribbles 2
Trib3	Tribbles 3
VLDL	Very low-density lipoprotein
WAT	White adipose tissue
WHO	World Health Organisation
WT	Wild type

Chapter 1 General Introduction

1.1 Metabolic syndromes

Metabolic syndrome has been characterised by the World Health Organization (WHO) as the presence of insulin resistance in combination with two additional risk factors, including dyslipidaemia, obesity and elevated blood pressure that contribute towards developing cardiovascular disease (CVD) and type 2 diabetes (Alberti and Zimmet, 1998, Mayans, 2015). There have been several attempts to refine the clinical definition of metabolic syndrome, with the most commonly accepted definitions shown in **Appendix I**. It is essential to identify patients who develop metabolic syndrome because it is a tool for physicians to categorise patients who are at high risk of developing CVD and type 2 diabetes. Furthermore, it also allows scientist to understand the pathophysiology that links the components of metabolic syndrome together in developing CVD and further facilitates epidemiological and clinical studies for therapeutic treatments. Although environmental factors are essential in causing metabolic syndrome, genetic susceptibility is critical as well. Insulin resistance was first thought to be the primary cause of metabolic syndrome, however, more recently obesity has been linked to causal factors (Patel et al., 2016, Huang, 2009).

1.2 Epidemiology of obesity

Obesity, which is defined by the WHO as having a body mass index (BMI) greater than 30.0 kg/m^2, is a global epidemic. It is a growing health problem with a significant burden on the economy and the health service. In 2016, 1.9 billion adults were reported overweight and 650 million obese. Furthermore, the estimated figures for 2025 are that 2.7 billion adults will become overweight and over 1 billion will be affected by obesity (IASO/IOTF, 2016). Worldwide, at least 2.8 million people die each year as a result of being overweight or obese (2.3%). In addition, Worldwide, in 2013 an estimated 42 million children under the age of five years were estimated to be overweight or obese; In contrast 3.1 million child deaths annually of malnutrition (UNICEF, World Health Organization [WHO], & The World Bank, 2018), which accounts to 45% of child deaths in 2011. There is a growing concern for both adults and children because being overweight or obese leads to metabolic dysfunctions and increases the risk of developing CVD (Kaur, 2014). **Figure 1.1** shows the percentage of adults that are obese worldwide.

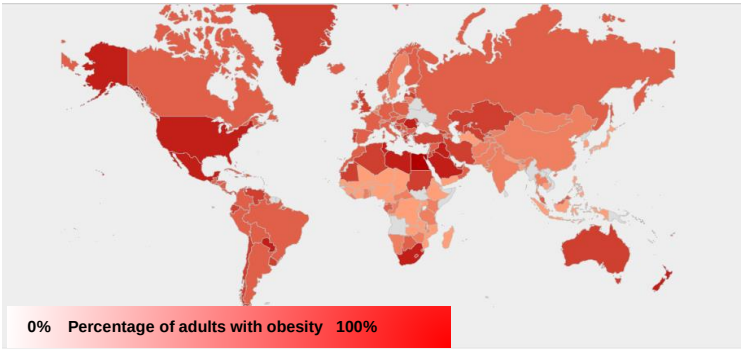

Figure 1.1: Map showing the percentage of adults that are obese worldwide. The red gradient marks the percentage of adults that are obese. A higher incidence of obesity is present in Western societies and Western-influenced countries (e.g., countries in the Middle East including Saudi Arabia). Adapted from (IASO/IOTF, 2016).

1.2.1 Consequences of Obesity

As mentioned before, being overweight or obese significantly increase the risk of developing chronic inflammatory diseases, including CVD, cancer, mental disorder and type 2 diabetes. All of these require treatment and some of them even surgery. In the UK, the NHS spends £5.1 billion per year on the treatment of ill-health caused by overweightness and obesity. Estimated figures by 2035 are in the region of £7–8 billion per year due to the alarming increase of patients with obesity-related disorders (Scarborough et al., 2011).

Some studies have reported that patients with obesity are divided into two pathological categories; the primary changes which are characterised by mental stress from obesity has been shown to have an impact on individuals' self-esteem, often accompanied by sleep apnea and osteoarthritis. The second is metabolic changes, which give rise to metabolic syndrome and cause secondary diseases, including type 2 diabetes, insulin resistance and hypertension, which increases the chances of endothelial damage causing stroke, thrombosis and a heart attack (Lawrence and Kopelman, 2004, Kopelman, 2000).

Obese patients have a poorer prognosis than healthy lean individuals if they develop cancer. A prospective study in the US has shown that obese adult men are 33% more likely to die from cancer than lean adult men (Calle et al., 2003). Epidemiological studies have also demonstrated that obesity is associated with lifelong expectancy (Hruby, 2015).

Furthermore, as mentioned, obesity and overweight have an impact on mental stress. Being overweight has been shown to increase the risk of developing Alzheimer's disease by 33% and this is significantly increased in obese individuals (Anstey et al., 2011).

A systematic review has highlighted evidence for an increased sick leave rate due to overweightness- and obesity-related illnesses in the workplace for affected individuals compared with healthy. The review assessed 50 studies on the indirect costs of overweightness and obesity and demonstrated that excess weight entailed substantial indirect costs. Having an impact in the workplace can overall have an impact on the economy (Goettler et al., 2016).

Being a source of physical and economic stress, obesity has social health impacts. A study by (Ostrovsky et al., 2013) has reported that social anxiety was significantly associated with obese and overweight people. However, this seems to diminish amongst extremely obese participants, compared with overweight and obese participants (Ostrovsky et al., 2013).

From the literature above, it can be seen that obesity gives rise to mental stress and secondary diseases, alongside having a huge burden on the economy. The metabolic changes in obesity lead to an increased risk of developing diseases, including CVD and cancer. Obesity increases the risk of developing diseases. Having just an increased BMI is not sufficient in some cases, it includes having excess adiposity that has an impact metabolically.

Hippocrates, the Greek philosopher and the fore-founder of medicine, said, 'Corpulence is not only a disease itself but the harbinger of others', first recognising that obesity is a medical disorder and gives rise to other disorders. Interestingly, scientists have provided more evidence on the impacts of obesity.

1.2.2 Defining obesity

Obesity is a complex but preventable disease with a heterogeneous group of conditions. Obesity is caused by an excessive amount of fat accumulation from excessive intake of calories which supersedes calories used. The excessive calories are then stored in the form of fat and triglyceride.

As suggested before, a person with a BMI of 30 or more is generally considered obese. A person with a BMI equal to or more than 25 is considered overweight. BMI is calculated by weight in kilogrammes divided by the square of the height in metres. BMI is used to predict body fatness levels by using a grading system. Furthermore, it allows comparisons of weight between populations, which can, therefore, identify the mortality rates. For a physician, it is a useful first-line tool used to evaluate whether intervention is required. **Table 1.1** shows the different methods of examining fat mass levels. Advantages and disadvantages of examining different methods of fat mass levels. The most common ways include BMI, waist circumference, skinfold thickness and bioimpedance.

Table 1.1: Different methods of examining fat mass levels.

Method	Definition	Advantages/limitations
BMI	It is the weight in kilogrammes (kg) divided by height in metres squared.	BMI has a correlation with densitometry measurements of fat mass. The limitations include being unable to distinguish fat mass from lean mass.
Waist circumference	Measured between the lower border of your ribs and the upper border of the pelvis in centimetres (cm)	Good for measuring the upper body fat deposition; however, it does not provide intra-abdominal (visceral) fat measurements.
Skinfold thickness	Measurement (in centimetres) using callipers, measures skinfold thickness (cm). Normally taken at multiple sites.	The measurements can be variable due to different observers and require accurate callipers. Limitations include no information on abdominal and intramuscular fat.
Bioimpedance	It is the measurement of resistance to a weak current applied across the body.	It is a simple way of measuring but not a more accurate predictor of fat compared with anthropometric measurements.

It is essential to understand that differences in gender, body proportions and the ethnic background will have an impact on the BMI and may not reflect the most accurate body fat levels. Alongside this, it is also worthwhile taking note of that defining a ‘healthy weight’ for a particular population can be sometimes misleading when using a BMI because different populations have different body size, weight, etc. The main limitation of using a BMI is the lack of the ability to differentiate between body fat composition and lean mass.

One of the ways clinicians can measure the amount of body fat is by body imaging such as magnetic resonance imaging (MRI) or computed tomography. MRI uses a combination of magnetic fields and radio waves to generate images of the body and its composition. These high-quality images will be able to be processed and differentiate and measure the amount and distribution of fat (Poonawalla et al., 2013). MRI would be the most accurate way of measuring body fat composition, however the limitations are the costs and time.

Having understood the limitations of BMI, there is a clear relationship between BMI and the relative risk of developing diabetes, CAD, hypertension and cholelithiasis (Willett et al., 1999). **Figure 1.2** reveals the relationship between BMI and relative risk of developing disease for both males and females. In women, there is a significant trend in developing type 2 diabetes with a BMI up to 25, while in men the critical BMI for the same condition is up to 28.

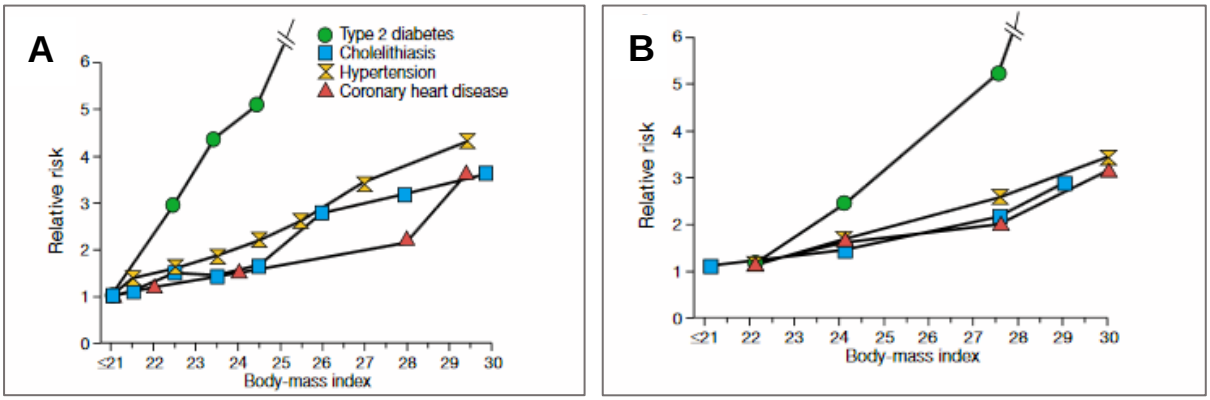

Figure 1.2: The relationship between BMI and relative risk of developing disease.

BMI and the relative risk of developing diabetes, coronary artery disease (CAD), hypertension and cholelithiasis A) In **women** Initially 30 to 55 years old, followed up for 18 years. B) In **men**. Initially 40 to 65 years old, followed up to 10 years. In women, there is a significant trend in developing type 2 diabetes with a BMI up to 25, while in men the critical BMI for the same condition is up to 28. Adapted from (Willett et al., 1999).

1.2.3 Causes of Obesity

Our body is a complex network mediated by interactions between genetic, environmental, psycho-behavioural and economic factors which all contribute to and influence physiological mediators of energy intake and expenditure. Susceptible genes increase the risk of developing obesity. However, it should be noted that these alone are not essential for disease initiation or disease progression (Nammi et al., 2004).

The most common model used to study obesity is caused by monogenic mutations involving leptin pathways. The *ob knock out* mouse is well studied and the ob locus is located at chromosome 6. The gene is expressed exclusively in the adipose tissue in the C57BL6 mice. The *ob* gene produces leptin, which is a crucial adipokine primarily produced in the white adipocytes and has been shown to be linked to appetite. Mutations that result in the expression of a constitutively active form of leptin result in profoundly obese mice with a mutant mouse that overeats (Zhang et al., 1994, de Luis et al., 2009).

A study by (Campfield et al., 1995) has shown that a leptin replacement in the *ob/ob* mice leads to a reduction in body weight, food intake, body fat composition and insulin sensitivity. In the *db/db* model, which is a diabetic, obese model with high levels of leptin, there was no effect on body fat composition and body weight, showing signs of leptin resistance.

There have been many mouse studies that have identified candidate susceptible genes which increase the risk of developing obesity. Many of these are associated with human obesity and metabolic dysfunction. A study by (Monda et al., 2010) has shown that if genes involved in the regulation of appetite become mutated, this could lead to an increased risk of developing obesity. Other models include the diet-induced models, polygenic models (Willett and Albright, 2004).

Animal models are important in studying and understanding the potential pathology of metabolic syndrome, especially murine models, because their whole genome has been sequenced and a large amount of transgenic and knockout models are readily available. However, there are limitations of these as well. The animal models can be expensive and lipid physiology can differ compared with humans. In mice, most of the cholesterol transport is carried by the high-density lipoprotein (HDL), whereas in humans, low-density lipoprotein (LDL) plays an important part in delivering cholesterol to the tissues. Thus, high HDL levels would be reasonable in mice (Jackson Laboratory) (Camus et al., 1983).

Although genetic susceptibility is paramount, it can be established that environmental factors influence the degree of obesity which is attenuated or exacerbated by non-genetic factors. These are known as obesogenic environmental factors (Kachur et al., 2017).

Physical activity has shown to be a significant factor in reducing energy expenditure. There have been cross-cultural studies showing a sevenfold increased risk of becoming overweight in those who have reduced the physical activity level to less than 1.8 per week (Ferro-Luzzi and Martino, 1996). A longitudinal study by a Finnish group has shown that the prevalence of obesity was inversely associated with the level of physical activity. Those reported doing physical activity 2–3 times per week had on average weight loss compared with those with little physical activity (Rissanen et al., 1991).

Furthermore, there is a strong correlation between the prevalence of overweightness and hours spent in front of the television. In the USA, youth who watch TV 5 h a day have a 4.6 times higher risk of becoming overweight than those watching 0–2 h (Gortmaker et al., 1996).

Evidence for the critical role environmental factors frequently play can be shown from studies on migrants and the impact of westernised diet and lifestyles. There is often an increase in BMI in migrant workers, where populations with a common genetic heritage live under new and different environmental circumstances. The Pima Indians who are living in the United States have been shown to be 25 kg heavier with an increase in BMI levels than the Pima Indians living in Mexico (Ravussin., 1995).

Cultural and educational background have also been shown to be associated with attributes of obesity. In industrial countries, there is a higher prevalence of overweightness and obesity observed in lower educational and low-income families. In England and Wales, there is a strong association between social class and obesity, especially in women. There is a risk of 10.7% for becoming overweight in high social class compared with 25% in low social class families (Zaninotto et al., 2009). **Figure 1.3** shows a summary of factors influencing obesity.

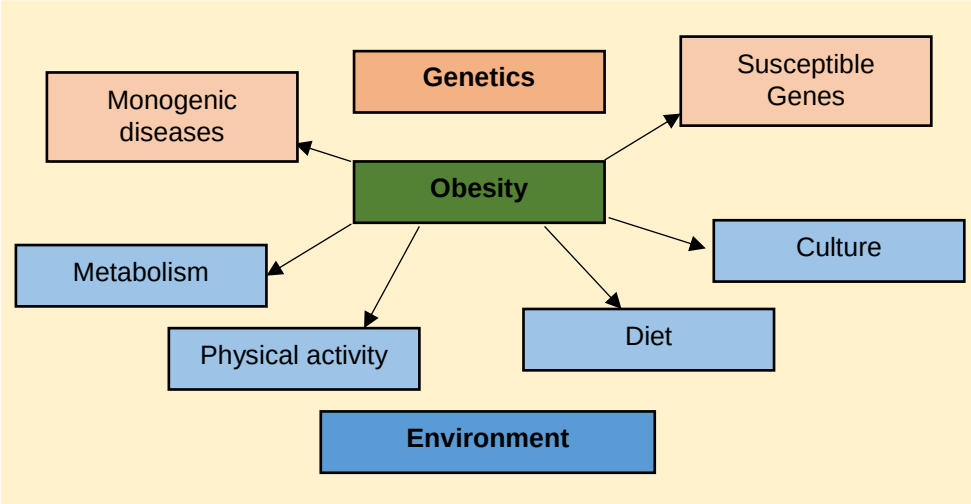

Figure 1.3: Summary of factors influencing obesity.

Environmental and genetic factors influence obesity, including metabolism, physical exercise, diet and culture which have been shown to be associated with an increased risk of developing CVD.

1.3 Adipose tissue WAT vs. BAT

In the classical view, adipose tissue was regarded as storage tissue for increasing energy intake only. However, it is now seen as an endocrine organ which releases free fatty acids (FFA), adipokines that act on other tissues including the brain, liver and muscle to regulate insulin sensitivity, food intake and energy balance. Adipose tissue can be separated into many different types. However, there are two main types, white adipose tissue (WAT) and brown adipose tissue (BAT). The WAT has been shown to store excess energy as triglycerides, and the BAT has been shown to dissipate energy through heat production. It is abundant in small mammals and newborns and also present in adult tumours (Saely et al., 2012).

The WAT appears pale white in colour and spherical in dimension, which is variable in size with a single lipid droplet inside the adipocytes for fat storage. The mitochondria are thin and elongated. The WAT is located at different anatomical sites, including the subcutaneous tissue located around the buttocks, thighs and abdominal region. The visceral fat is located around the organs inside and around the peritoneum. There has been a strong correlation between visceral WAT and increased risk of CVD (Golia et al., 2014, Luo and Liu, 2016, Esteve Rafols, 2014).

Furthermore, the ectopic fat is a store of triglycerides that resides in other tissues like the liver, skeletal muscle or around the heart (epicardial fat). It can interfere with cellular functions and organ function and is strongly associated with insulin resistance in type 2 diabetes (Esteve Rafols, 2014).

The BAT, in contrast, is darker in colour, with a high mitochondrial content which is largely spherical with laminar cristae. The BAT has higher capillaries and vascularisation due to higher oxygen demand. In adults, the BAT is primarily located around the cervical, supraclavicular, axillary, paravertebral, mediastinal and upper abdominal regions. The BAT has a unique mechanism for the vital organs which require oxygen and nutrients (Cypess and Kahn, 2010).

The BAT has a crucial role in regulating body temperature to ensure that cellular and physiological processes continue to work in cold temperature. In cold temperatures, the hypothalamus becomes activated, which induces blood flow towards the BAT and results in a release of noradrenaline, which can bind to β-adrenergic receptors that are present in the BAT. This leads to the activation of protein kinase A and p38. This activation results in the phosphorylation of transcriptional factors and the cAMP response element binding protein, which controls the expression of genes involved in BAT activation. PGC-1 belongs to a family of transcriptional coactivators which has been shown to increase biogenesis of the mitochondria and induce expression of Uncoupling protein 1 (UCP1). Acute thermogenesis leads to lipolysis, glucose uptake and activation of UCP1 and mitochondrial biogenesis. **Figure 1.4** shows the activation of brown adipocytes in the cold (van den Berg et al., 2017).

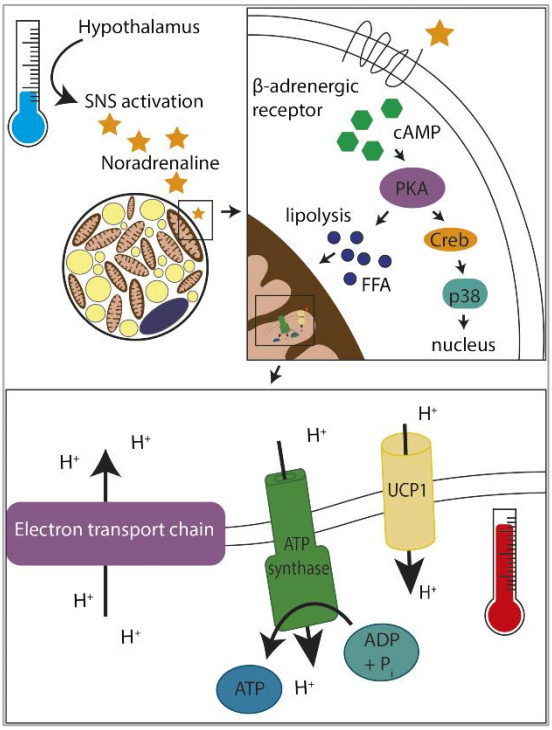

Figure 1.4: The activation of brown adipocytes in cold temperatures.

The hypothalamus gets activated by the cold, which activates the sympathetic nervous system to release noradrenaline. This can bind to the β-adrenergic receptors on the adipocytes of the BAT and results in fatty acid degradation by beta-oxidation and lipolysis. This causes activation of the UCP1.This is driven by a proton gradient. Adapted from (van den Berg et al., 2017).

UCP1 is a protein ubiquitously expressed in the BAT. It is localised in the mitochondria and its role is to uncouple oxidative phosphorylation from ATP, which results in dissipation of energy into heat. It has been shown that cold induces glucose uptake by a factor of 15 in the paracervical and supraclavicular adipose tissue in 5 healthy subjects. Upon mRNA examination, there was an increase in UCP1 (Virtanen et al., 2009). The morphological examination has shown an increase in intracellular lipid droplets.

Furthermore, 14 obese men have shown a significantly reduced BAT activity compared with 24 healthy individuals. BMI and percentage of body fat have a negative correlation with brown tissue, with a positive correlation for the resting metabolic rate. The activity was measured using an integrated FDG PET-CT scan (van Marken Lichtenbelt et al., 2009).

The primary role of WAT is to store energy in the form of triglycerides during an increase in energy intake and mobilising FFA to be used as fuel when energy expenditure increases. The adipocytes synthesise triglycerides as lipid droplets by combining glycerol molecules with FFA through a process known as esterification. The breakdown of triglycerides involves multiple hydrolysis steps mediated by

lipases. Both size and number can determine the WAT. It can undergo two processes—hypertrophy, which is the increase in cell size and hyperplasia, which is the increase in cell number. Hypertrophy is achieved via an increase in lipogenesis; lipid accumulation and decreased lipolysis; breakdown of triglycerides, whereas hyperplasia is a process involving adipogenesis, which includes the proliferation of preadipocytes to mature adipocytes (Rosen and OA., 2006). **Table 1.2** shows the comparison between WAT and BAT.

	White adipose tissue (WAT)	Brown adipose tissue (BAT)
Function	Many including mainly energy storage	Mainly including heat production
Morphology	Single lipid droplet A variable number of mitochondria	Multiple small vacuoles Abundant mitochondria
Characteristic protein	Leptin	UCP1
Human Data	An increase in WAT has been shown to be associated with a higher risk of obesity-related disorders	An increased in BAT has been shown to be associated with reduced risk of obesity-related disorders.
Impact of ageing	Increases	Decreases

Table 1.2: comparing WAT with BAT.

WAT is predominantly used as the main energy storage, it releases adipokines, important in regulating many physiological activities. The BAT is mainly for heat production and keeping you warm. Its characteristic proteins include the UCP1 and increased amount of BAT reduces CVD. Adapted from (Saely et al., 2012).

An increase in circulating non-esterified fatty acids (NEFA) is the reflection of the adipose tissue unable to store excess nutrient intake, which relates to a dyslipidemia state, a marker for metabolic syndrome. Upon overload in the subcutaneous adipose tissue (WAT), it spills to the liver, which increases production of Apo-B, which transports the excess lipids to other organs. The subcutaneous tissue has a larger capacity to store lipids, a protective buffer for excess lipid intake. Individuals who have a smaller compartment of the subcutaneous tissue (WAT) due to, for example, genetics will achieve an earlier storage limit of the subcutaneous tissue depot and will overspill to the visceral depot. Increase in visceral adipose tissue leads to hypertriglyceridemia, and further accumulation leads to overspill into other organs which are not able to store lipids efficiently and harms their functions, causing toxicity. These include the peripheral organs like the liver and the muscle (Monteiro and Azevedo, 2010).

1.3.1 Impact of adipose tissue on ageing

There is an age-related impact on adipocyte size and accumulation of fats. As we age, the lean mass decreases but ectopic fat accumulation occurs over time, which potentially leads to tissue dysfunction. The rate at which fat changes is different amongst different WAT and BAT. The subcutaneous fat is lost first, which means the excessive FFA is stored in the visceral fat, which increases the risk to CVD. This is one of the reasons CVD events occur more to aged individuals (Jura and Kozak, 2016).As we age, the preadipocytes lose their ability to become mature adipocytes. The BAT is also impaired, its ability to regulate temperature also diminishes. This causes a decrease in cold tolerance and impaired bodyweight. Ueno et al. (1998) showed the effect of ageing on BAT activity in lean and obese (ob/ob) mice. Unlike lean animals, old obese animals exhibited decreased expression of mRNA for UCP1 and therefore impaired thermogenic capacity in old obese mice (Ueno et al., 1998).

1.4 Adipogenesis

There is a wide range of evidence in the literature demonstrating that adipose tissue is essential in a number of roles, including lipid storage, energy homeostasis, insulin sensitivity and thermoregulation. WAT and BAT are derived from distinct precursor cells. The adipose tissue is comprised of a variety of cells, including fibroblasts, macrophages, pericytes and other immune cells, however, it is predominantly made up of mature adipocytes. There are several different transcription factors that control adipogenesis. However, two proteins have been especially well established in the literature, the peroxisome proliferator-activated receptor PPARγ and CCAAT-enhancer-binding protein CEBP.

PPARγ and CEBPα are master regulators of adipocyte differentiation and gene expression. PPARγ is a member of a superfamily of hormone receptors that has been shown to be essential for adipocyte development. The expression level of the two PPARγ isoforms, PPARγ1 and PPARγ2, varies depending on the tissue type. PPARγ2 is highly expressed in adipocytes and was found to be elevated in morbidly obese individuals. Both isoforms have been shown to impact adipogenesis. However, PPARγ2 shows an enhanced ability to impact adipogenesis due to its increased sensitivity to ligands and binding capacity. PPARγ1 is critical for fat development.

Conditional knock out mice lacking PPARγ in the adipose tissue displayed a decrease in fat disposition and insulin resistance in both adipose and liver tissue. Furthermore, PPARγ heterozygous mice responded with enhanced insulin sensitivity. Mice with mutations of PPARγ (P465L and L466A) exhibited defects in adipose tissue development. Furthermore, patients with dominant negative mutations in the PARPγ gene were diagnosed to display an abnormal body fat distribution (Harp, 2004, Davies et al., 2017).

The CEBPs are a family of leucine zipper transcriptional factors with six currently known isoforms. All of them have a highly conserved bZIP domain. CEBPα, CEBPβ and CEBPδ promote adipocyte differentiation and the loss of CEBPα causes a decrease in adipogenesis. Whole body CEBPα knockout mice die early due to liver defects and hypoglycaemia and failing to accommodate lipids in the WAT

and BAT. CEBPα have been shown to be induced late in adipogenesis and are important in glucose uptake.

Recent studies have shown that CEBPα binding sites seem to co-localise with those of PPARγ (Rosen et al., 2002). A study by Spiegelman has shown that PPARγ expression can completely rescue adipogenesis in CEBPα deficient mouse embryonic fibroblasts (MEFs) PPARγ (Rosen et al., 2002). Studies clearly show that PPARγ and CEBPα cross-regulate each other and help in mediating adipocyte differentiation: lack of CEBPα increases PPARγ expression levels and loss of CEBPα increases PPARγ levels (Lowe et al., 2011, Luo and Liu, 2016). **Figure 1.5** shows PPARγ and C/EBPα expression, in adipogenesis.

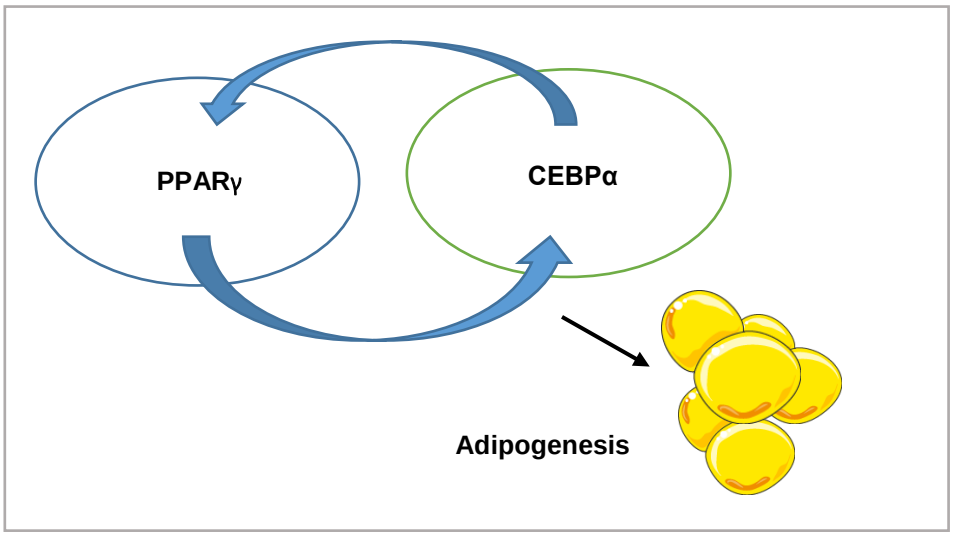

Figure 1.5: PPARγ and C/EBPα expression, in adipogenesis.

PPARγ and CEBPα are master regulators of adipocyte differentiation and gene expression. PPARγ and CEBPα cross-regulate each other and help in mediating adipocyte differentiation.

1.4.1 Structure and function of PPARs

PPARs form a nuclear receptor family which consists of three isotypes, namely PPARα, PPARβ and PPARγ; they play an important role in energy homeostasis and metabolic function. All of them have a unique expression pattern depending on the tissue. All PPARs have a conical domain with an AF-1 train-activation domain, followed by a DNA binding domain. The PPAR function as a heterodimer with a co-activator complex that binds to the DNA sequence PPRE, which then leads to the transactivation or transrepression of genes. PPARα is predominantly expressed in hepatocytes, enterocytes and macrophages (Tyagi et al., 2011). It plays a vital role in fatty acid oxidation in the liver and provides energy for the tissues (Tyagi et al., 2011).

1.5 Mechanism linking obesity to type 2 diabetes

Diabetes mellitus (DM), is a metabolic disorder which causes blood sugar levels to rise due to an insufficient amount of insulin being produced to regulate glucose levels. There are two main types of diabetes. Type 1 is an autoimmune condition caused by the malfunction of immune cells that destroy the pancreatic islets of Langerhans cells. Thus, the body will be unable to produce any insulin, and the patient will require insulin injections. Type 2 diabetes is a long-term metabolic disorder, which is the most common form of diabetes accounting for up to 90% of all diabetes patients. In type 2 diabetes, the body produces insufficient or no insulin. This could be due to several reasons, including genetics, obesity and lack of physical exercise. Lifestyle management; diet, exercise and drugs are usually prescribed to patients with this condition. In 2012, 382 million people worldwide were diagnosed with diabetes, and it is expected to increase to 592 million people by 2035. Diabetes has also significantly increased in the UK. One in 17 people in the UK has diabetes (diagnosed or undiagnosed) (diabetes.org.uk). Overweight people run an up to 7 times higher risk to develop diabetes than healthy individuals (diabetes/gov.uk) Furthermore, for every kilogramme of weight gained, the risk of diabetes increases between 4.5 and 9% (Al-Goblan et al., 2014). Despite these factors, some patients who are overweight and obese do not develop diabetes and the molecular mechanism is still unknown.

There are many different interactions occurring between the different metabolic organs, which contribute to the pathogenesis of obesity and diabetes (WHO). **Figure 1.6** shows the effects of insulin resistance on different organs. Impaired insulin resistance causes a reduced amount of insulin production, leading to activation of the hypothalamus to increase food intake, resulting in obesity. This further causes reduced output of glucose from the liver, alongside inhibition of glucose uptake from the muscle, with an increase in lipolysis in the adipocytes resulting in an increase in NEFA in the plasma. This leads to further suppression of pancreatic β-cell in the pancreas and resulting in glucotoxicity (Kahn et al., 2006).

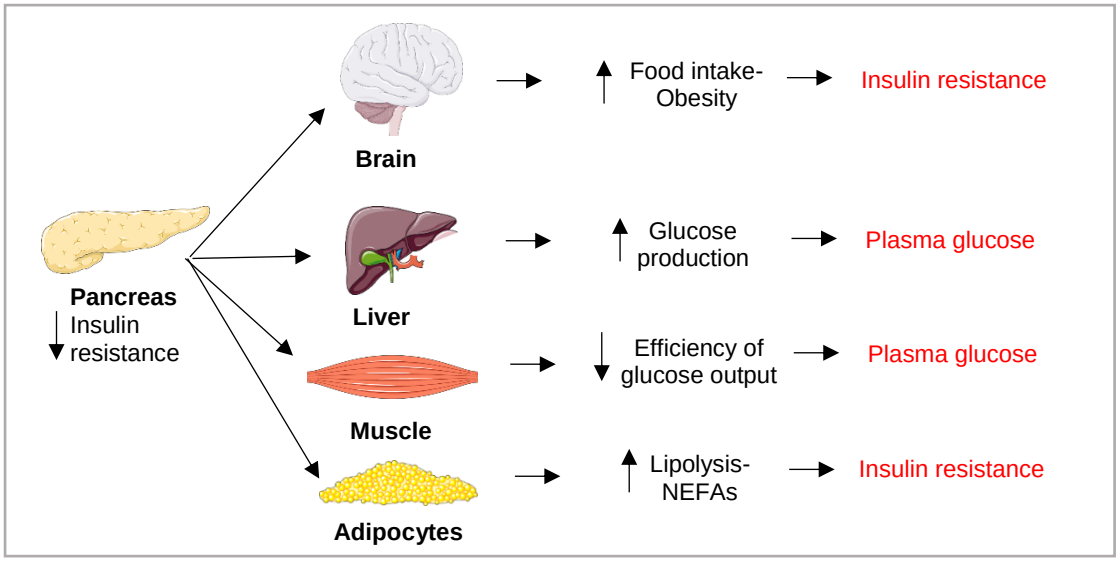

Figure 1.6: Effects of Insulin resistance on different organs.

Many different interactions occur between the different metabolic organs, to contribute towards the pathogenesis of obesity and diabetes. Adapted from (Kahn et al., 2006).

1.6 Insulin signalling and glucose homeostasis

Glucose is essential for the survival of all organs and is controlled by the primary metabolic organs which are the liver, fat and skeletal muscle. When glucose homeostasis becomes impaired, then it requires compensatory mechanisms from different organs.

One important pathway is the insulin signalling pathway. Insulin is an important hormone released by the pancreatic beta cells located at the islets of Langerhans. It is secreted to the bloodstream in response to high glucose levels in the blood. This then triggers the uptake of glucose to the main metabolic organs, like the liver, adipose and skeletal muscle to promote storage. Insulin promotes glucose uptake by stimulating the translocation of the glucose transporter GLUT4 from the intracellular compartment to the plasma membrane by the insulin signalling pathway. GLUT4 receptor concentration on the cell surface is low without the presence of insulin.

The insulin receptor is a receptor tyrosine kinase that is composed of two extracellular subunits, two transmembrane B subunits linked by disulfide bonds and the intracellular tyrosine kinase domains. Ligand-binding causes a conformational change in the extracellular subunits that activates the tyrosine kinase domain which autophosphorylates some tyrosine residues present in the B-subunit. The residues are recognised by the phosphotyrosine binding domains of the adaptor proteins like the insulin receptor substrates (IRS). The IRS-1 protein then, in turn, binds and activates phosphatidylinositol three kinases (PI3K) by the Src homology two (SH2) domain of the p85 regulatory subunit of the PI3K. This is then followed by a translocation of the PI3K to the membrane and the phosphorylation of phosphatidylinositol (PIP2) leading to the formation of phosphatidylinositol-3,4,5-triphosphate (PIP3). A pip3-dependent kinase (PDK) subsequently interacts with PIP3-activating protein kinase B, also known as Akt. Once Akt is phosphorylated and active, it enters the cytoplasm where it participates in several different processes. It causes the translocation of GLUT4 from intracellular vesicles to the plasma membrane to stabilise glucose levels. Upon glucose homeostasis in the blood and a reduction in insulin levels, GLUT4 is removed from the plasma membrane by endocytosis and recycled back into their compartment. Akt also promotes glucose storage as glycogen by phosphorylating forkhead box protein O1 (FoxO1) and facilitates glycogen synthesis by phosphorylating and inactivating glycogen synthase kinase (GSK)-3, which can no longer phosphorylate glycogen synthase and inhibits glycogen synthesis. In addition to promoting glucose storage, Akt can promote production and release of glucose by the liver by blocking gluconeogenesis and glycogenosis. Insulin is also able to increase lipogenesis and decrease lipolysis. Trib3 is a negative modulator and is able to bind to PI3K or AKT and inhibit and modulate its signal. APP1 competes with Trib3 as an antagonist (Kahn et al., 2006, Kahn et al., 2001). **Figure 1.7** shows the insulin signalling pathway.

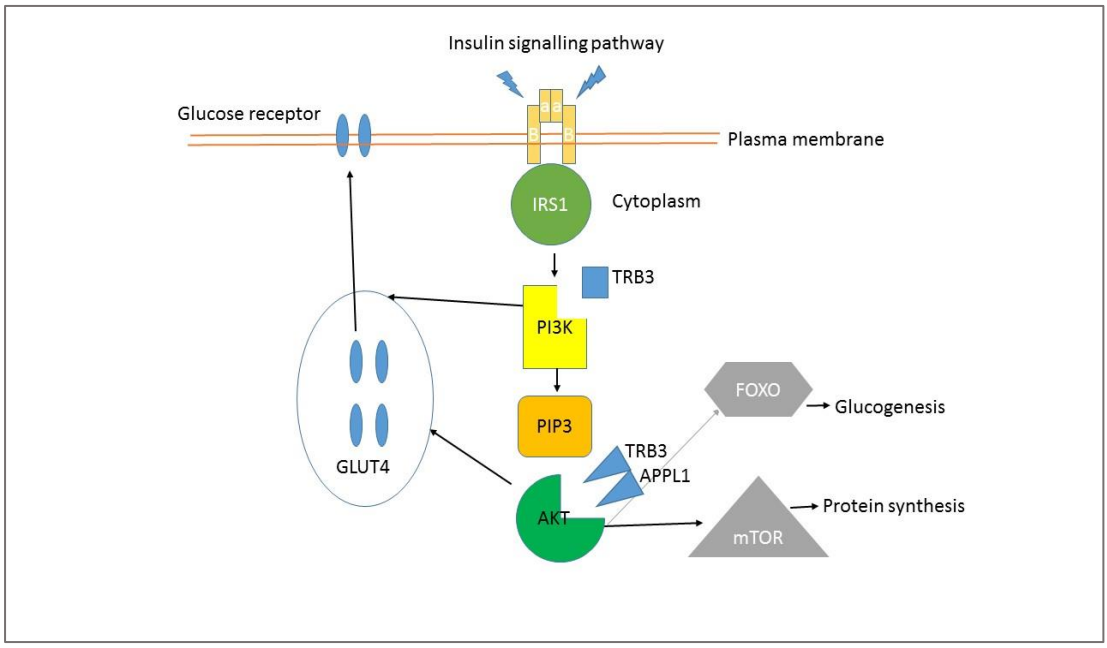

Figure 1.7: Schematic diagram representing the insulin signalling pathway.

A ligand binds to the transmembrane glycoprotein that contains two alpha and two beta subunits, which causes a signalling cascade and starts auto-phosphorylation. This then increases the tyrosine kinase activity and activates its substrates, IRS-1 and IRS-2. This, in turn, binds to the PI3K, which causes the production of PIP3. This acts as a secondary messenger and goes on to activate Akt, which acts as a secondary messenger and mediates insulin signalling, including translocation of GLU4, mTOR and FOXO. Trib3 is a negative modulator and has been shown to inhibit both Akt and P13K and modulate its signal. APP1 competes with Trib3 as an antagonist.

1.6.1 The role of skeletal muscle and adipose tissue in insulin resistance

Skeletal muscle is one of the most important energy sites of the body, as it is always in the disposal of energy. The skeletal muscle uses both glucose and FFA in uptake. However, when there is an imbalance between glucose and FFA, due to reduced oxidation and increased uptake, it can cause an accumulation of triglycerides which increases the risk of insulin resistance.

Type 2 diabetes (T2DM) patients have six times more fat in the muscle than non-diabetic patients. An excessive amount of FFA causes lipotoxicity that leads to insulin resistance. During fasting, the FFA in plasma is high, and glucose uptake is low, so the FFA is used as a primary fuel source for energy production in the skeletal muscle while glucose is reserved for the brain. In lean individuals, there is an increased uptake of glucose in a dose-independent manner. However, in patients with insulin resistance, the skeletal muscle has displayed a slow reduction of glucose uptake (DeFronzo and Abdul-Ghani, 2011).

Moreover, a study by Himsworth and Kerr has shown that using a glucose tolerance test, tissue sensitivity to insulin is diminished in T2DM patients (Himsworth and Kerr, 1939). Furthermore, it is reported that up to 80% of the total body glucose uptake occurs in the skeletal muscle under euglycemic conditions.

FFA induces insulin resistance in the skeletal muscle by blocking insulin activation of IRS-1-associated PI3K via the increased activation of protein kinase C and its downstream IRS-1 serine (307)

phosphorylation, which reduces the phosphorylation of tyrosine and the subsequent IRS-1-associated PI3K activity. This results in a decrease in GLUT4 translocation alongside a decreased insulin-stimulated glucose uptake (Yu et al., 2002).

Obesity causes excessive fat accumulation in many different tissues; most prominently in adipose tissues, but also in other peripheral organs, such as skeletal muscle and liver, predisposing these insulin-responsive organs to insulin resistance. An increase in lipolysis by the adipose tissues causes FFA to be released to the circulation. Hence, we can see obese patients with type 2 diabetes to have high levels of FFA in the bloodstream (Abdul-Ghani and DeFronzo, 2010).

1.6.2 Insulin resistance in the liver with and without HFD

The liver is the largest metabolic organ, which is associated with many functions including glycogen synthesis, manufacturing triglyceride and cholesterol and bile production. The liver is a key regulator of glucose homeostasis.

High-fat diet (HFD) in mice has shown hepatic steatosis, which is a fatty liver. Obese patients are not always insulin resistant, for example, patients with highly active antiretroviral therapy associated lipodystrophy lacking subcutaneous fat are not insulin resistant. However, they do have an increase in fat hidden in the liver. Ectopic fat in the liver has been shown to cause hepatic insulin resistance (Neuschwander-Tetri, 2007, Adiels et al., 2008, Yki-Jarvinen, 2010).

1.7 Obesity is a chronic inflammatory disease

Inflammation is the body's mechanism to respond to harmful physical, chemical or biological stimuli to maintain physiological homeostasis levels. Obesity is a chronic inflammatory condition that is often referred to as 'low-grade' inflammation. It is normally given the name Met-inflammation due to inflammation being triggered by metabolism.

Obesity has shown a positive association with inflammatory markers, like C-reactive protein (CRP) in adult participants (Maury and Brichard, 2010, Lau et al., 2005, Katsiki et al., 2017, Matsuzawa, 2010). In agreement with this study, weight loss of obese patients results in the decreased expression of inflammatory biomarkers including CRP (Heilbronn et al., 2001). Inflammation has a central role in the liver, as it consumes free fatty acids, it releases IL-6 by the adipose tissue, which triggers hepatocyte expression and release of CRP (Katsiki et al., 2017, Matsuzawa, 2010).

The pro-inflammatory cytokine TNFα was the first cytokine that had been identified as a link between obesity and inflammation. The study has shown induction of TNFα levels in the adipose tissue from four different rodent models (Hotamisligil, 2006, Hotamisligil et al., 1993). Furthermore, TNFα was shown to be increased in the adipose tissue of human obese individuals with macrophages co-localising with adipocytes (Lumeng, 2013).

Moreover, saturated fatty acids seem to activate the TLR2 and TLR4 receptors, and unsaturated fatty acids inhibit TLR mediated signalling and gene expression. There was an increase in IL-6 and TNFα upon exposure to diet-derived saturated fatty acids whereas unsaturated fatty acids did not have any impact on TNFα (Qatanani and MA., 2007). Activation of TLRs results in a pro-inflammatory state, with

an increase in NEFA obesity, it is likely that there is amplified inflammation contributing to the development of aggravation of Met syndrome (Aprahamian and Sam, 2011).
There is a marked increase in plasma makers upon high-fat meal in abdominally obese men (Blackburn et al., 2010). Other studies have shown the importance of microbiota in inflammation. High-fat feeding increases intestinal permeability and the plasma concentration of LPS, which has an impact on inflammation. Changes of gut microbiota control inflammation in obese mice through GLP2 driven mechanisms (Cani et al., 2009).

1.7.1 Inflammatory signalling

As mentioned before, the role of the inflammation is to respond to injury, infection or any other type of harm to promote healing and restore physiological homeostasis. The immune system initiates intracellular mediators which cause inflammatory signalling. Macrophages are important cells that secrete factors such as cytokines, which promote several processes such as phagocytosis to eliminate harmful debris. Each cell has essential cell signalling complexes which work together to co-ordinate responses allowing them to respond appropriately depending on its environment and development. In the adipose tissue, adipokines such as IL-6, TNF, adiponectin and leptin have been involved in lipid metabolism and inflammation. Dysregulation in adipokines leads to chronic inflammatory diseases, including atherosclerosis (Sherling et al., 2017).

1.7.2 Adipokines

Adipokines are metabolic mediators secreted by the adipose tissue to maintain homeostasis. An example of an adipokine is adiponectin, a protein derived from the adipose tissue which has been reported to have an impact on type 2 diabetes and atherosclerosis. High levels of adiponectin are found in the plasma of patients who suffer from metabolic syndrome. Adiponectin is a 247-amino acid peptide discovered in 1995 (Beltowski et al., 2008, Matsuzawa et al., 2004). The adiponectin levels were demonstrated to increase the expression of nitric oxide (NO), which is a vasodilator known to protect against endothelial dysfunction (Nakamura et al., 2004).

Furthermore, adiponectin reduces oxidative stress, and in the liver, adiponectin has been shown to improve insulin sensitivity by decreasing the uptake of NEFA and reducing gluconeogenesis (Gatselis et al., 2014, Lihn et al., 2005). Adiponectin levels are significantly reduced in obese patients (Engin, 2017), although the exact mechanism is yet unknown. However, an increase in serum level of IL-6 and TNFα inhibits and reduces the synthesis and secretion of adiponectin (Ellulu et al., 2017). Adiponectin was reported to have a negative association with obesity in both genders and a positive correlation with HDL cholesterol (Eglit et al., 2013).

Another cytokine, IL-6, which is produced by many different cell types including the adipose tissue also has been reported to mediate inflammatory responses (Guzik et al., 2006). Moreover, it was shown that FFA in obesity activates pro-inflammatory serine kinase cascades, such as I_kB kinase, which stimulates adipose tissue to release IL-6 that results in hepatocytes to secrete CRP (Ellulu et al., 2017). There is a positive correlation between IL-6 levels and BMI which significantly decreases 12 months after surgery (Illán-Gómez et al., 2012).

CRP is synthesised by the liver and is a sensitive marker of systemic inflammation. It has been reported that the level of CRP levels is positively related to obesity. It is regulated mainly by two cytokines, IL-6 and IL-1, which induce the farnesoid X receptor, which can influence many lipid metabolism genes such as PPARγ (Ellulu et al., 2017). **Figure 1.8** shows mechanisms on how obesity influences inflammation to cause metabolic syndrome.

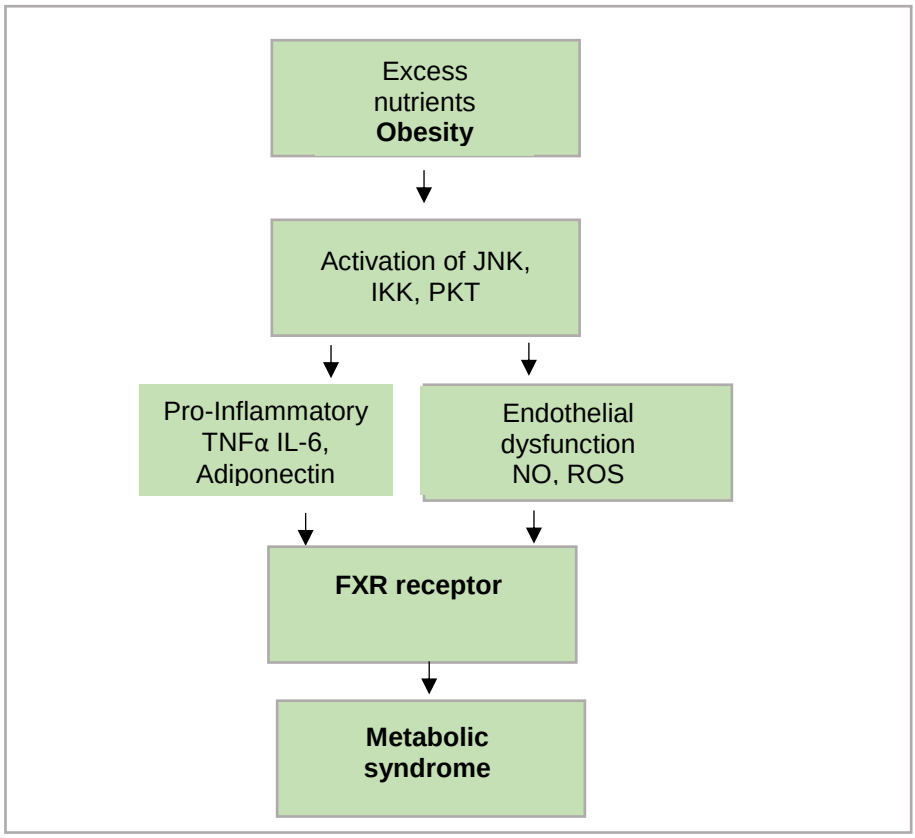

Figure 1.8: Mechanisms linking obesity to inflammation resulting in MS.

Saturated fatty acids have been shown to activate the TLR2 and TLR4 receptors. Activation of TLRs results in a pro-inflammatory state increase in IL-6. The induction of IL-6 and IL-1b results in activation of the farnesoid X receptor (FXR). FXR regulates many genes involved in lipid and lipoprotein metabolism. Activation of FXR results in dysregulation of lipid metabolism genes and endothelial dysfunction. Adapted from (Ellulu et al., 2017).

1.7.3 Tribbles proteins are modulators of inflammatory signalling

Tribbles proteins (Trib) have been described to modulate several components of the inflammatory cell signalling pathways to maintain homeostasis. Early studies have shown the importance of Trib in inflammation. Kiss-Toth et al. have shown that Trib isoforms are able to bind to MAPKKs and modulate their activity (Kiss-Toth et al., 2004a). Furthermore, Trib isoforms can bind to the c-Jun N-terminal kinases (JNKs) and p38 to regulate IL-8 production (Kiss-Toth et al., 2006). Trib have been reported to bind to kinase-dependent proteins like the MAPK and JNK, but they lack kinase activity, hence are called pseudo-kinase proteins (Hegedus et al., 2007, Hegedus et al., 2006).Trib act like scaffold proteins because they balance complex cell signalling pathways. Others have demonstrated that Trib act like allosteric activators. Trib have been shown to compete for binding sites like the MAPK and therefore regulate MAPK signalling (Sung et al., 2007). Additionally, it has been reported that $Trib3^{ko}$ causes increased expression of pro-inflammatory proteins like MCP-1 and TNFα, suggesting that Trib3 is a negative regulator of pro-inflammatory cytokines (Kuo et al., 2012). Knockdown of Trib3 via RNAi significantly induced the production of tumor necrosis factor-α (TNF-α), IL-4, IL-6, and MCP-1.

Trib have an N-terminal domain, central kinase-like domain and C-terminal protein-binding domain. The canonical Trib proteins have an N-terminal domain, which seems to be less conserved, a central domain and a C-terminal which are highly conserved. Trib proteins are part of the pseudokinase family which have a central serine/threonine kinase domain but lack conserved residues, which make them catalytically inactive.

The N domain of Trib, which is known as a PEST region, contains approx. 60–80 amino acids, abundant in proline and serine residues. This makes the half-life of Trib very short as 34 out of the 50 sequences analysed contained predicted PEST regions, making the proteins prone to degradation. This was also demonstrated by Sharova and colleagues (Sharova et al., 2009) where Trib possesses a rapid turnover, less than 1 h. mRNA half-life was measured for nearly 20,000 genes in mouse embryonic stem cells, only 9% of genes had a shorter mRNA half-life than Trib3 (half-life 2.8 hours). 54 genes including Trib3 showed mRNA half-lives less than 1 hour Other studies have suggested this half-life was due to proteasome-dependent degradation, facilitated by E3 ubiquitin ligases (Zhou et al., 2008). The C-terminal domain contains important motifs and binding sites, including COP-1, the Akt and the MAPKK. Trib3 protein structure **(Figure 1.9).**

Figure 1.9: Trib3 protein structure.

Trib have an N-terminal domain, a central pseudokinase domain and the C-terminal. Trib3 is a 358 amino acid protein that contains 4 exons. It has the Akt binding site which is able to inhibit insulin signalling pathway. A MAPKK binding site that is able to bind and modulate MAPKK activity and the COP-1 binding site to direct key target protein to the proteasome for degradation.

1.7.4 Tribbles interacting proteins

Tribbles have been shown to bind and interact with a number of proteins. **Table 1.3** represents a comprehensive list of interacting proteins with biological significance.

Table 1.3 Tribbles have been shown to bind and interact with a number of proteins.

Protein	Tribbles	Biological significance	Citation
COP-1	TRIB1/3	Degradation of target proteins	(Qi et al., 2006)
String (CDC25)	Tribbles (Drosophila)	Inhibition of mitosis and cell cycle	(Grosshans and Wieschaus, 2000)
SIBO	Tribbles (Drosophila)	Regulation of cell migration	(Rørth et al., 2000)
C/EBPα	TRIB1/2	AML induction	(Keeshan et al., 2006, Yamamoto et al., 2007)
C/EBPβ	TRIB1/2	Inhibition of adipocyte differentiation and modification of toll-like receptor signalling	(Keeshan et al., 2006, Yamamoto et al., 2007)
ATF4	TRIB3	Suppression of stress signal upon hypoxia	(Ord and Ord, 2003)
CHOP	TRIB3	Induction of apoptosis upon ER stress	(Ohoka et al., 2005, Qi et al., 2006)
ACC	TRIB3	Suppression of adipogenesis	(Qi et al., 2006)
MEK1	TRIB1/3	Enhancement of ERK phosphorylation and AML induction	(Kiss-Toth et al., 2004b, Yokoyama et al., 2010)
MKK4	TRIB1/3	Suppression of SMC induction	(Yokoyama et al., 2010)
AKT1/2	TRIB1/3	Suppression of adipocytes differentiation, disruption in the insulin signalling pathway	(Du et al., 2003)
MLK3	TRIB/3	Induction of pancreatic B cell death	(Humphrey et al., 2014)
BMPRII	TRIB/3	Promotion of osteogenic differentiation by degradation of smurf1	(Chan et al., 2007)
SMURF1	TRIB/3	Induction of smurf degradation	(Chan et al., 2007)
PPARγ	TRIB/3	Inhibition of adipocyte differentiation by suppressing of PPARγ transcriptional activities	(Takahashi et al., 2008)
P65/RelA	TRIB/2	Apoptotic induction upon TNF and TRAIL stimuli	(Wu et al., 2003)
SIAH1	TRIB/3	Inhibition of TGFβ signalling	(Zhou et al., 2008)

1.7.5 Macrophages

Macrophages are a large phagocytic cells, which are part of the immune system and are involved in detection, phagocytosis and destruction of bacteria and other harmful organisms. In addition, macrophages play a significant role in development, homeostasis antigen presenting and immunomodulation. Macrophages are also involved in chronic inflammatory diseases including atherosclerosis, obesity and non-alcoholic fatty liver disease (NAFLD). Studies have shown that macrophages display remarkable plasticity properties due to be able to respond and adapt to tissue environment. Therefore, the polarisation of macrophages have been traditionally divided into two groups, which are known as M1 and M2. M1 are known to be 'classically' activated macrophages and are induced by Th1 cytokines such as the interferon-γ (IFN-γ) and Tumor necrosis factor- α (TNF-α) and shown to have a pro-inflammatory cytokines secretion profile. Having the release of these molecules play a great part in host defence but overall the mediator and cytokines need to be controlled, as high levels lead to host tissue damage and cause chronic inflammation. Numerous diseases like arthritis and atherosclerosis have been associated with M1 type. M2 macrophages are known as 'alternatively' activated macrophages which have shown to display wound healing properties by releasing cytokines such as IL-4 during the innate immune response. These have shown to have an anti-inflammatory cytokines secretion profile. Although, macrophages have been divided into M1/M2, the heterogeneity of macrophages is far more complex as the cells are highly plastic in different microenvironment. Further macrophage sub groups have emerged and spectrum of macrophages can be displayed which are much more unique (Thomas and Apovian, 2017, Barros et al., 2013, Liu et al., 2014).

1.8 Origin of Tribbles

Trib protein was originally identified in *Drosophila melanogaster* in a developmental study by Grosshans and colleague (Grosshans and Wieschaus, 2000) where a genetic mutation screen had reported Trib to be involved in cell proliferation and migration of mesodermal cells. A mutation in Trib had shown an overproliferation of the mesodermal cells compared with the wild type (WT). Trib was shown to block proliferation of mesodermal cells via degradation of String phosphatase, which prevents it from activating cyclin-dependent kinase 1 (cdc2), important in the cell cycle (Grosshans and Wieschaus, 2000). The highly proliferative behaviour of the mesodermal cells resembles the Tribbles species shown on the Sci-Fi TV show Star Trek, hence the name of this gene.

Furthermore, it was proposed that Trib regulate degradation of CEBPα and cdc25 levels via the ubiquitin-proteasomal pathway. A study by Saka and colleague (Saka and Smith, 2004) had reported that microinjection of the fertilised *Xenopus* embryos with antisense Trib2 had delayed the cell division and led to developmental defects. A distinct phenotype compared with what was shown in the *Drosophila*, which could be due to *Xenopus* having both Trib1 and Trib2 genes compared with *Drosophila* and deleting one could lead to a different phenotype. All of these early studies have highlighted the importance of Trib in the early stages of development as reviewed by Lohan and colleague (Lohan and Keeshan, 2013).

1.9 Lipoproteins are a risk factor for cardiovascular disease

As mentioned before, excessive amounts of nutrients can lead to elevated plasma fatty acids, which further causes insulin resistance. Excessive amounts of lipids have been shown to increase the risk of CVD. Another important event is the influx of LDL into the endothelial cells, which contributes significantly to the pathogenesis of atherosclerosis (Glass and Witztum, 2001).

The liver is the primary organ to regulate cholesterol levels in the body. Lipoprotein molecules allow the transportation of triglyceride and cholesterol throughout the blood vessels. Very low-density lipoproteins (VLDL) are released from the liver which transport triglyceride to the tissues required for energy. In lipid metabolism, there is the endogenous, exogenous and reverse cholesterol pathways (Nguyen et al., 2008).

The exogenous pathway includes consuming an HFD, which contains triglycerides and cholesterol that are broken down by pancreatic, liver and gut enzymes into small non-essential fatty acid chains and glycerol. These are then absorbed by the intestines and are re-esterified into triglyceride that gets combined with the Apolipoprotein B48 (ApoB-48) to form nascent chylomicrons and is transported into the lymphatic system and to the circulation. The nascent chylomicrons mature upon reaching the circulation and then interact with the HDL so it can obtain the Apolipoprotein C (Apo-C) and Apolipoprotein E (ApoE). The Apo-C is a cofactor to activate lipase enzymes in the adipose and skeletal muscle when it is delivered so that it can be broken down and stored as fatty acids. Upon storage and distribution, the chylomicrons reappear in the bloodstream and return the Apo-C to the HDL, but keep the ApoE, which is recognised by the receptor in the liver to be endocytosed and broken down. This is now known as a chylomicron remnant. The endogenous pathway is independent of the intestines. The liver synthesises VLDL that package triglyceride and cholesterol into the bloodstream with the Apo-B100 which deliver them into the tissues, similar to that of the exogenous pathway. Upon arrival at the liver, the receptor ApoE of the remnant VLDL interacts with the liver receptor and is taken up and further hydrolysed by the hepatic lipase to release fatty acids and glycerol, which leaves behind the LDL. The LDL is of high cholesterol and low lipoproteins and is the primary carrier of cholesterol in the bloodstream (Gropper, 2009).

The primary function of the LDL is to transport cholesterol to the tissues that require it. However, the LDL can also migrate into the peripheral tissue and become oxidised, which are taken up by the scavenger receptors leading to steps in atherosclerosis. It is therefore physiologically important that LDL be controlled in the bloodstream. The HDL is secreted primarily by the liver and the gut to remove excess free cholesterol in the bloodstream and peripheral tissue, via the ATP-binding cassette transporter 1 (ABC-A1). This includes macrophages that express the ABC-A1 in its surface. The lecithin–cholesterol acyltransferase (LCAT) converts the cholesterol to cholesteryl esters converting it to mature HDL. The mature HDL returns to the liver for excretion in the bile by scavenger receptors B.

Another method is via cholesteryl ester transfer protein (CETP), which exchanges the ApoB for cholesterol esters and is now able to be taken up by the LDL receptors. This is known as the reverse cholesterol pathway (Fitzgerald et al., 2010). A malfunction in LDL and HDL can lead to an increase in

cholesterol levels, which can lead to hyperlipidaemia and is a significant risk factor to contribute to atherosclerosis and other medical conditions. The current treatment includes statins, which inhibit the enzyme HMG-CoA reductase responsible for cholesterol production. **Figure 1.10** is a schematic diagram of the cholesterol metabolism pathway.

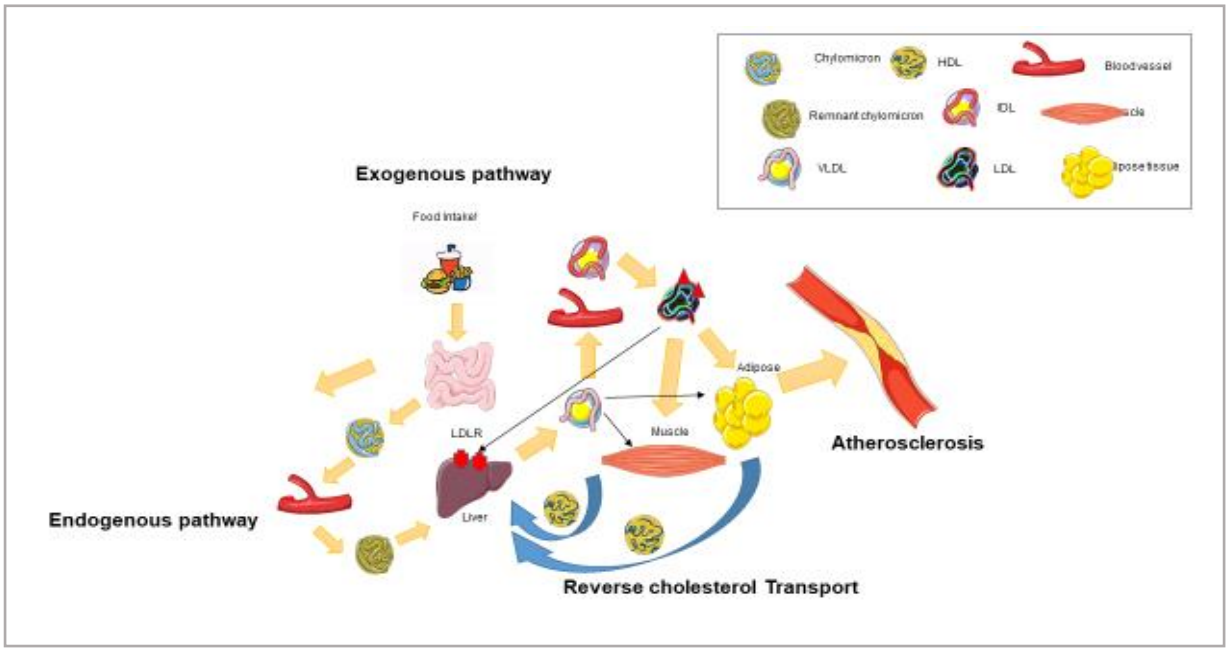

Figure 1.10 Cholesterol metabolism pathway.

The exogenous pathways include consuming a HFD. The triglycerides are broken down by the enzymes into fatty acid chains, which are taken by the chylomicrons and delivered to the tissues and back to the liver. The endogenous pathway is independent of the intestine. The liver produces VLDL for the fatty acids to be transported to the tissues (adipose and muscle) and back to the liver. The reverse cholesterol pathway includes the transportation of cholesterol to the tissues via LDL, however, some of it gets transported to the peripheral tissue and taken up by the scavenger receptor and leads to steps in atherosclerosis.

1.9.1 Structure of the lipoprotein particles

Lipoproteins are particles that are enriched with cholesterol and proteins. Lipoproteins are insoluble in water and are transported via the blood. Lipoproteins are heterogeneous and are classified according to their compositions. These particles include chylomicrons, VLDL, intermediate-density lipoproteins (IDL), LDL and HDL. Ultracentrifugation is a way of separating the particles and provides a better prognosis of CVD. Ion mobility has also been recently used to separate the particles according to charge. The particles are ionised and placed in an electric field, which separates them into different sizes. **Figure 1.11** shows the basic structure of the lipoprotein particle.

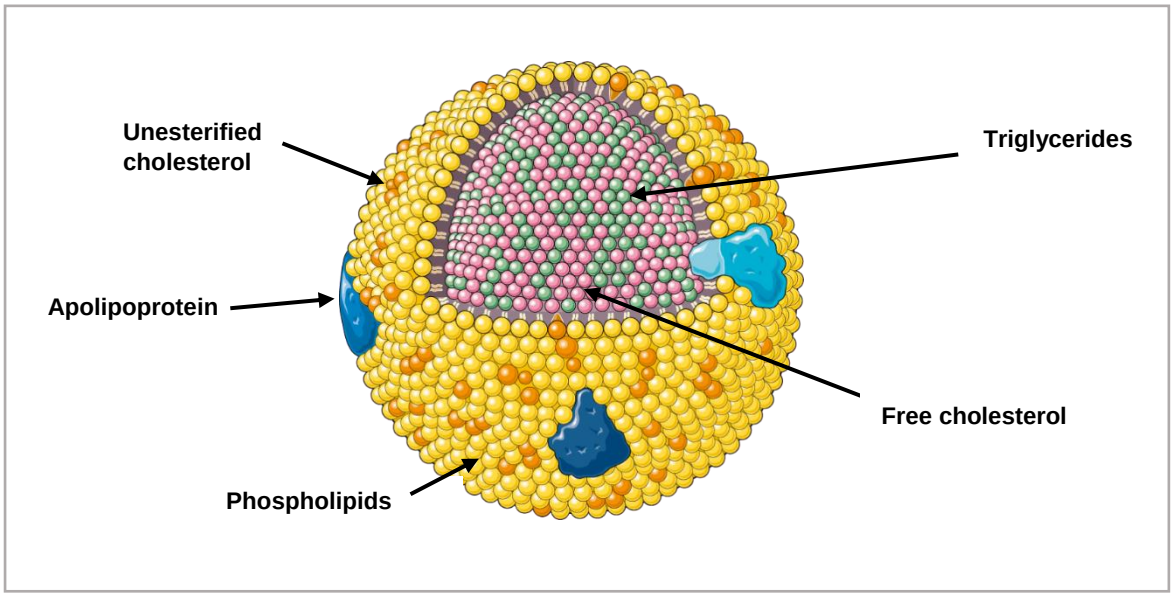

Figure 1.11: Structure of lipoprotein.

A hydrophilic outer core, containing phospholipids, cholesterol and apolipoproteins. The inner hydrophobic core contains triglycerides and free cholesterols. The Apolipoproteins are embedded in the membrane, examples include the plasma lipoprotein particles categorised as HDL, LDL, IDL and VLDL.

1.9.2 Obesity is associated with higher lipid and LDL lipoprotein levels

Dyslipidaemia is a significant comorbidity of obesity which has been reported to have a very high incidence of coronary and vascular events. Many studies have described obese patients as having elevated levels of total and LDL cholesterol and low levels of HDL. These are important risk factors for coronary heart disease and predictors of developing CVD. A study by Szczygielska and colleagues has shown the relationship between BMI and blood lipids. It was revealed the mean total cholesterol and triglyceride concentrations were higher in obese patients than in healthy weights with a reduction in HDL levels (Szczygielska et al., 2003). Furthermore, epidemiological studies have shown elevated cholesterol levels to be a risk factor for CAD (Hajar, 2017). However, due to the function of the lipoprotein being different, LDL is the gold standard measurement for future CAD as well as being a therapeutic target for treating CVD risk (Miller et al., 2005).

1.9.3 VLDL

It has been shown that elevated levels of triglyceride-rich remnant lipoproteins are involved in atherosclerosis development. Many studies have shown an inverse relationship between lipoprotein particle size and atherosclerosis development (Burnett, 2004). Small VLDL particles have been shown to be able to cross the endothelium into the arterial intima. Others like chylomicrons and large VLDL have been shown to not cross the endothelium and are not pro-atherogenic. As mentioned before, the small VLDL and ApoC-III have been shown to be significantly associated with the development of atherosclerosis. Meta-analysis has shown cholesterol, and recurrent events trial indicated that plasma concentration of patients of VLDL and APOC-III are a stronger measure of CAD than plasma triglyceride (Burnett, 2004).

1.9.4 LDL

As mentioned before, LDL levels have been significantly associated with cardiovascular risks. It was reported that an increase in LDL levels is associated with a threefold increase in the risk of CAD (Chan et al., 2004). The key event is the retention and accumulation of cholesterol-rich apoB-containing lipoproteins within the arterial intima at sites of plaque formation. Lipoprotein with a diameter of <70 nm in diameter can easily enter and exit the arterial intima. It has been reported that elevated levels of LDL and lipoproteins less than <70 nm lead to the development of atherosclerotic plaque in a dose-dependent manner (Chan et al., 2004). An autosomal co-dominant disorder known as familial hypercholesterolemia is caused by a mutation in the LDL receptor; LDLR leading to premature atherosclerosis, particularly CAD. Hence LDL is used as a primary target for treatment for CVD. Treatment by statins can reduce LDL levels and the risk of CVD. However, there is still a residual risk of CVD (Libby, 2005). Furthermore, LDL particles vary in composition including size, density, electrical charge and chemistry. Elevated levels of small dense LDL), along with increased triglyceride has been reported to be more associated with obesity and increases with type 2 diabetes (Nikolic et al., 2013, Chan et al., 2004).

1.9.5 HDL

Reduced levels of HDL are increased in obese patients and have been associated with increased risk for the development of CAD. Obesity has an impact on HDL metabolism by increasing CETP activity

due to the increased number of triglyceride (TG)-rich lipoproteins. In brief, the HDL are broken down by the enzyme hepatic lipase, resulting in small HDL particles. These have a decreased affinity for apo A-I, which causes dissociation of apo A-I from HDL. This results in a decreased level of HDL-C and circulating HDL particles causing impairment of the reversed cholesterol transport (Kratzer et al., 2014, Klop et al., 2013). **Table 1.4:** Physical properties of lipoprotein particles.

1.10 Lipogenesis vs. lipolysis

Excessive accumulation of fats leads to lipotoxicity, which affects the metabolic pathways causing cellular dysfunction. This increases the risk of developing metabolic disorders, such as obesity, diabetes, non-alcohol fatty liver disease (NAFLD) and CVDs. Lipotoxicity is not only caused by an HFD but also by alternative sources of lipids, de nova lipogenesis where excess carbohydrates are converted into FFA and triglycerides. These are co-ordinated via enzyme processes and convert citrate to acetyl CoA, which can then be used as energy storage. An excessive amount of nutrients leads to the synthesis and release of VLDL and secreted into the circulation and stored in the peripheral tissue, the adipose tissue is the predominant storage. During starvation, the triglycerides are hydrolysed in the adipose tissue and FFA is released into the circulation, known as lipolysis (Ameer et al., 2014).

Table 1.4: Physical properties of lipoprotein particles.

Lipoprotein	Subclasses	Diameter (nm)	% protein	Major lipids	Apoproteins
VLDL	VLDL-1	330–700	5–10	TG, PL, CE	B100, C ,E
	VLDL-2	300–330			
IDL	IDL-1	285–300	15–20	CE, TG, PL	B100, C, E
	IDL-2	272–285			
LDL	LDL-I	272–285	20–25	CE, PL	B100
	LDL-II	256–272			
	LDL-III	242–256			
	LDL-IV	220–242			
HDL	HDL-1	~120	40–55	PL, CE	A, C, D, E
	HDL-2	103–104			
	HDL-3	73–99			

1.11 Non-coding RNAs

In recent years, non-coding RNAs (ncRNAs) have been shown to play an essential role in disease progression or inhibition. ncRNAs are molecules that are not translated into protein, however, they are important in controlling gene expression. ncRNAs are involved in many cellular processes. Evolutionally these have evolved to protect against foreign organisms by controlling gene expressions and returning to a physiological homeostasis level. **Table 1.5** shows the different small ncRNAs found in mammals.

Table 1.5: Summary of ncRNAs.

Short	Approx length (nt)	Function
MicroRNA (miRNA)	21–23	Post transcription—In animals, involved with the RISC complex and silence target genes.
Small nucleolar RNAs (snoRNA)	60–300	Posttranscriptional—Causes chemical modification via methylation or pseudouridylation of mRNA influencing protein stability and folding.
Small nuclear RNAs (snRNAs)	150	Assist in splicing of introns from the primary genomic transcript.
Silencing RNAs (siRNAs)	21–23	Causes degradation of mRNA via complementary base pairing.
Transcription RNAs (tiRNAs)	13–30	Enriched downstream transcriptional start sites of highly expressed genes.
Piwi-interacting RNAs (piRNAs)	25–30	Causes RNA silencing via RISC specifically transposons.
Transfer RNAs (tRNAs)	76–90	Important in protein translation; interaction between mRNA and protein.
Ribosomal RNAs (rRNAs)	>2000	Essential in protein synthesis
Circular RNAs (circRNAs)	100 to >4000	Have diverse functions, including templates for viral replication

1.12 miRNAs, post-transcriptional regulators of gene expression

miRNA are small non-coding single-stranded RNA nucleotides that post-transcriptionally control the regulation of gene expression by binding to the 3′ or 5′UTR mRNA of the target gene sequence. miRNA are key molecules in the RNA-mediated silencing complex to downregulate a number of genes by translational repression, mRNA cleavage or mRNA deadenylation. The non-coding miRNA was first described as 'junk DNA', but now it is actively shown to be involved in many important cellular processes (Gebert and MacRae, 2018).

Ambros and colleagues initially discovered the first miRNA in 1993 where a genetic screening in the *Caenorhabditis elegans* larval development had identified *Lin 4*, which was shown to be a small RNA ~22-nucleotide long, that was able to bind to the complementary 3′UTR of Lin-14 and cause repressing of the *lin-14* gene. Hence, it was unable to translate lin-14 mRNA into the LIN-14 protein (Lee et al., 1993). This was the first evidence of the regulatory function of RNAs. Since then, there have been a large number of small ncRNAs discovered. High throughput screening has enabled us to discover a high number of novel miRNA with regulatory targets and possible functions. Recent studies have shown computational techniques and bioinformatics algorithms as novel tools for identifying genes regulated by miRNAs (Fehlmann et al., 2017). It has been estimated that more than half of the protein-coding genes in humans are negatively regulated by miRNAs (Cai et al., 2009). With more complex organisms the miRNAs are proportionally more. Each miRNA can target more than one gene and control gene expression. Those genes are important in processes including lipid metabolism, apoptosis and glucose metabolism. Changes in miRNAs expression levels result in diseases and can be used as biomarkers to indicate disease prognosis (Gebert and MacRae, 2018).

1.12.1 Biogenesis of miRNAs in mammals

miRNA has many cellular steps before it can complementarily bind to genes and cause mRNA degradation and/or translation repression. These include 1) Nuclear processing, 2) Transportation by exportin-5, 3) cytoplasmic processing, 4) Argonaute loading and finally 5) mRNA degradation and/or translation repression (Wahid et al., 2010).

miRNAs are non-coding single-stranded RNAs, about 21–25 nucleotides long, which are produced from hairpin-shaped precursors. miRNA has been reported to be mainly transcribed in the introns of their pre-host genes. Other miRNAs have been reported to be pretranscribed within their promoters. Based on miRNA genomic locations, miRNA genes can be classified as intronic miRNAs in coding transcription units (TUs), intronic miRNAs in non-coding TU, exonic miRNAs in coding TU and exonic miRNAs in non-coding TU. Most studies have shown the RNA polymerase II (Pol II) initiates and is responsible for the transcription of the miRNA. This occurs in the nucleus where Pol II or Pol III transcribes the prior-miRNA, which are 60–70 nucleotide long hairpin structures known as precursor miRNA (pre-miRNA). The large precursor RNA is cleaved by Drosha enzyme and binding protein Pasha/DGCR8, which results in the premature hairpin RNA. The Drosha, in combination with either DGCR8 or Pasha, forms a large complex. Mouse models have shown the DGCR8 are conserved within the mammal species and are important genes for developmental processes.

The pre-miRNA is then transported to the cytoplasm by exportin-5 and Ran GTP complex. The transportation occurs via nuclear pore complexes. Studies have shown that hydrolysis of the GTP results in the release of the pre-miRNA. The pri-miRNA is now being processed in the cytoplasm. The endonuclease cytoplasmic RNase III enzyme Dicer creates a mature miRNA. Dicer is a highly conserved protein which exists in all eukaryotic organisms. Other organisms have been shown to have multiple isoforms of Dicer which are required for miRNA maturation. In humans, a Dicer can process the mature miRNA into small double-stranded RNA containing the mature or guide strand and complementary or passenger strand. One strand, normally the weaker and unstable strand, is then transported into the RNA induced silencing complex (RISC complex) to be silenced, and the other is degraded. Dicer, alongside other interacting proteins (TRBP and/or PACT and Ago family proteins, assemble to form RISC also known as RISC loading complex. The Ago protein is critical in the development of the RISC complex. The Ago family proteins are composed of three distinct domains: the PAZ, MID and PIWI domains. The PAZ domains have been shown to bind to the miRNA in a folded structure. The passenger strand is degraded, and the mature strand remains with the Ago proteins to be introduced to the RISC complex and is degraded (Gebert and MacRae, 2018). **Figure 1.12** shows the biogenesis of miRNAs in mammals.

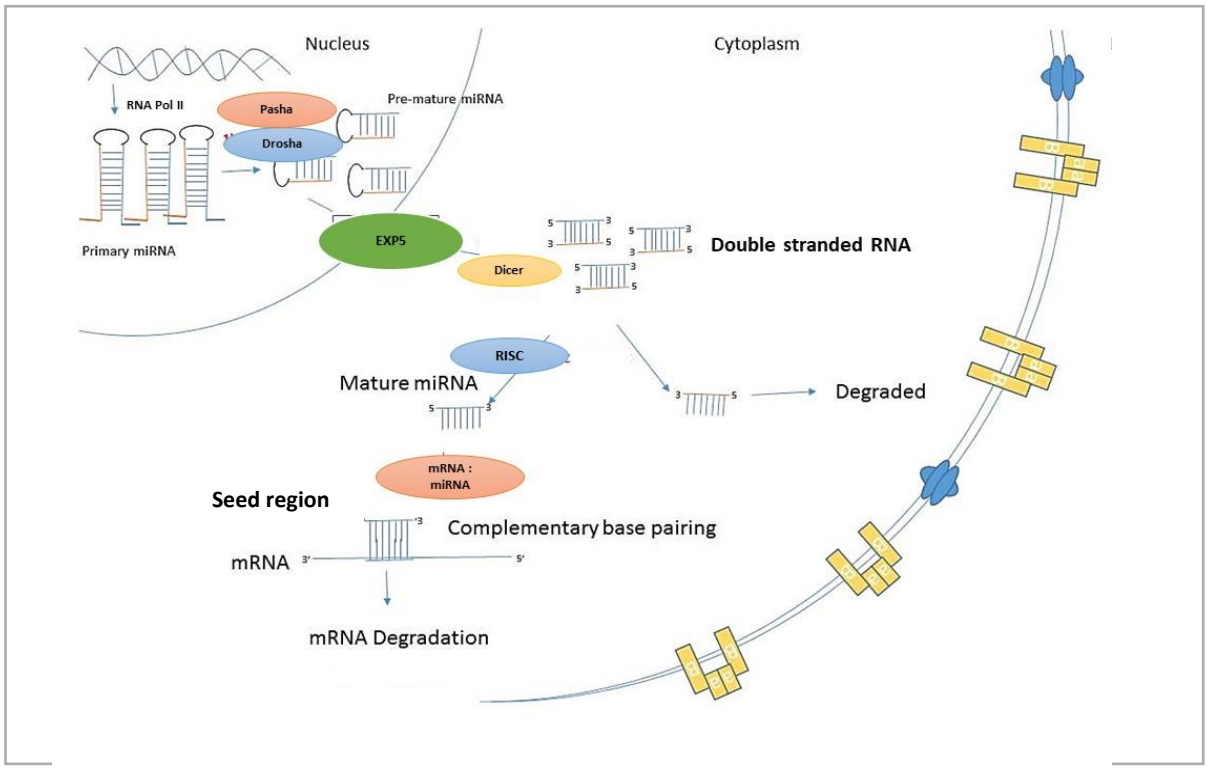

Figure 1.12: Biogenesis of miRNAs in mammals.

miRNA has many cellular steps before it is able to complementary bind to mRNA and cause mRNA degradation or translation repression. These include 1) Nuclear processing, 2) Transportation by exportin-5, 3) cytoplasmic processing, 4) Argonaute loading and finally 5) mRNA degradation and/or translation repression.

1.12.2 miRNA functions in mammals

miRNA has been shown to have distinct roles in the regulation of cellular processes. Over half of our genome is in the control of miRNA, hence this suggests the importance of miRNA in disease development. The mutation of miRNA *Lin-4* and *Lin-7* in *c.elegans* has been shown to cause defects in larval development. Several studies have reported that miRNA is not only able to cause mRNA degradation but also translation repression. However, the exact mechanisms of how translation repression occurs are still unknown. Some studies have proposed mechanisms and shown that Ago can recruit GW182, which interacts with polyadenylate-binding protein, thereby causing mRNA deadenylation by recruiting the poly(A)-nuclease deadenylation complex subunit 2 (Braun et al., 2011). This can cause destabilisation of the target gene before degradation or the protein synthesis inhibition occurring. As mentioned before, the Ago protein is critical for loading the guide strand to the RISC and translation repression. Mammals encode for four Ago proteins. Ago two is highly expressed and can cleave the target full complementary to the guide strand. Furthermore, other studies have shown that inhibition of translation initiation is also caused by the involvement of eukaryotic initiation factor 4 AI (eIF4A-I) and eIF4A-II (Zhong et al., 2018).

There have been previous studies which have reported the extent of complementary base pairing results in either mRNA degradation or protein inhibition. Partial complementary binding of the miRNA to the seed region on mRNA results in protein inhibition and upon miRNA completely binding to the target sequence it has been shown to cause mRNA degradation. The majority of the miRNA have been identified in the 3′UTR. However, there have been several studies that highlight miRNA able to bind to the 5′UTR (Catalanotto et al., 2016).

1.12.3 miRNA in disease and future therapeutics

It has been reported that around 2200 miRNA genes exist in mammals, which regulates many biological processes in cells, including differentiation, metabolism, growth and repair. Up to 50% of miRNAs which are expressed are transcribed from the non-protein-coding genes and the remaining are within the introns of coding genes. Many of the miRNA play a pivotal role in maintaining homeostasis, however, upon dysregulation, they have been linked to many clinical diseases such as CAD autoimmune disease and cancer (Aryal et al., 2017, Ma et al., 2016).

miR-122 has been shown to be predominantly expressed in the liver and can modulate cholesterol levels, shown to be involved in hepatic carcinoma and cancer progression (Hu J et al., 2012). A study by Esau et al. (2006) has also shown inhibition of miR122 to reduce lipogenesis genes and a reduction in plasma cholesterol levels in chow and obese mice. It is evident that the dysregulation of miRNAs has an impact on disease development and progression.

Furthermore, miR-155 and miR-125b have been reported to influence the polarisation of macrophages, which are important in inflammatory responses. miR-155 is upregulated upon TLR activation and has been shown to regulate M1 macrophages in vitro (O'Connell et al., 2007).

Furthermore, miR-33 inhibitors have been shown to reduce atherosclerotic lesions in C57BL6 mice. MiR-33 has been shown to regulate autophagy in macrophages foam cells, which results in a reduction in cholesterol uptake and therefore reduces plaque development (Ouimet, 2013, Ouimet et al., 2017). miR-133 and miR-208 have been shown to be highly expressed in the heart, which reports demonstrating miR133 and miR-208 are important in regulating myocyte differentiation heart development (Ouimet et al., 2017. Downregulation of miR-133 has resulted in heart failure (Ono et al., 2011, Aryal et al., 2017). **Table 1.6** shows miRNA expression associated with disease. This table is adapted from (Ardekani and Naeini, 2010).

Table 1.6: Shows the miRNA associated with disease.

Disease type	miRNA	Up/Down Regulation	References
Cardiac hypertrophy			
	miR-23a, miR-23b, miR-24, miR-195, miR-199a, and miR-214	Up	(Thum et al., 2008)
Down syndrome			
	miR-99a, let-7c, miR-125b-2, miR-155 and miR-802	Up	(Kuhn et al., 2008)
Alzheimer			
	miR-9, miR-128a, miR-125b	Up	(Lukiw, 2007)
Rheumatic arthritis			
	miR-155, miR-146	Up	(Tili et al., 2008)
Systemic lupus erythematosus			
	miR-189, miR-61, miR-78, miR-21, miR-142-3p, miR 342, miR-299-3p, miR-198 and miR-298	Up	(Dai et al., 2007)
	miR-196a, miR-17-5p, miR- 409-3p, miR-141, miR-383, miR- 112, and miR-184	Down	(Dai et al., 2007)

From the evidence above, it can be established that miRNAs play a pivotal role in the development of many cellular processes and disease initiation, therefore, miRNA are the ideal markers to have a great role in diagnosis and treatment of diseases. In the last decade, several techniques such as miRNA silencing, antisense blocking and miRNA modification have been considered for potential therapeutic treatment. Another popular method is Target site blockers, also known as miRNA inhibitors, which have been used to increase the endogenous levels of therapeutic proteins. miR-122 is an LNA-based (locked nucleic acid) antisense molecule against miR-122, which is used for the treatment of hepatitis. Studies have shown miR-122 to affect hepatitis C virus (HCV) replication, phase 2 clinical trials in HCV patients have shown success and in 2017 Santaris Pharma are developing the drug named miravirsen (Bandiera et al., 2015).

1.13 Atherosclerosis

Atherosclerosis is a focal form of CVD and is characterised by chronic inflammation and fatty deposits in the arterial wall. Its underlying mechanism includes endothelial injury, which leads to a cascade of events occurring during disease progression. The endothelial injury can be due to several possible causes, including hyperdyslipidaemia, smoking, hypertension, hyperhomocysteinemia infection and mechanical stress (Wang, 2004).

Recent studies have highlighted the importance of blood flow and its haemodynamics on the different regions of the arteries. Blood flow is generally laminar in the unbranched regions of the arteries with high shear stress. Upregulated levels of atheroprotective genes are found in the region of the endothelium. However, studies have shown an upregulation of pro-atherogenic genes in the disturbed regions of the arteries as reviewed by Chiu and colleague (Chiu and Chien, 2011).

Upon injury, the endothelium transduces the stress into a biochemical signal allowing upregulation of adhesion molecules such as vascular cell adhesion molecule 1 (VCAM-1) which change the cytoskeletal structure of the endothelial cells resulting in cell permeability and allowing the transmigration of leukocytes (Bassiouny, 2012). The endothelium produces a concentration gradient of monocytes that activate the immune system; circulating monocytes transmigrate through the site of injury and differentiate into macrophages. The injury causes the endothelial cells to reduce the production of NO, a vasodilator, releases monocyte chemo-attractant protein-1 (MCP-1) attracting monocyte adhesion and upregulates macrophage colony-stimulating factor (MCSF) expression, thereby promoting monocyte differentiation into macrophages as reviewed by Glass and colleague (Glass and Witztum, 2001).

Lipo-Density-Lipoproteins (LDL) are elevated in the blood vessels which enter the peripheral tissue and become oxidised. The monocytes transmigrate into the endothelium and mature into macrophages and engulf oxidised LDL (oxLDL) via scavenger receptors to become foam cells leading to atherosclerotic lesions (Glass and Witztum, 2001). The macrophages engulf the oxLDL particles which further release inflammatory cytokines, chemokines and matrix metalloproteinase (MMP) which augment the inflammation (Mitchell and Sidawy, 1998). Activated macrophages also produce growth factors which contribute to the migration and proliferation of vascular smooth muscle cells (VSMCs) into the tunica intima, hardening the arteries and causing plaque growth and fibrous cap formation. The lipid content is released from the foam cells which contributes to the necrotic lipid core of the plaque (Tousoulis et al., 2011).

All of these events lead to the restriction of blood flow, which reduces oxygen and nutrients being transported to the tissues. Symptoms of a patient who has atherosclerosis include angina, fatigue, vertigo and nausea. If not treated, the fibrous cap can cause further complications such as thrombosis leading to a stroke or a myocardial infarction. Some of the current treatments include glyceryl trinitrate, a vasodilator, stenting, thrombolysis and surgery depending on the extent of injury and disease progression (Kuroda and Kitazono, 2013) **Figure 1.13:** Pathogenesis of atherosclerosis**.**

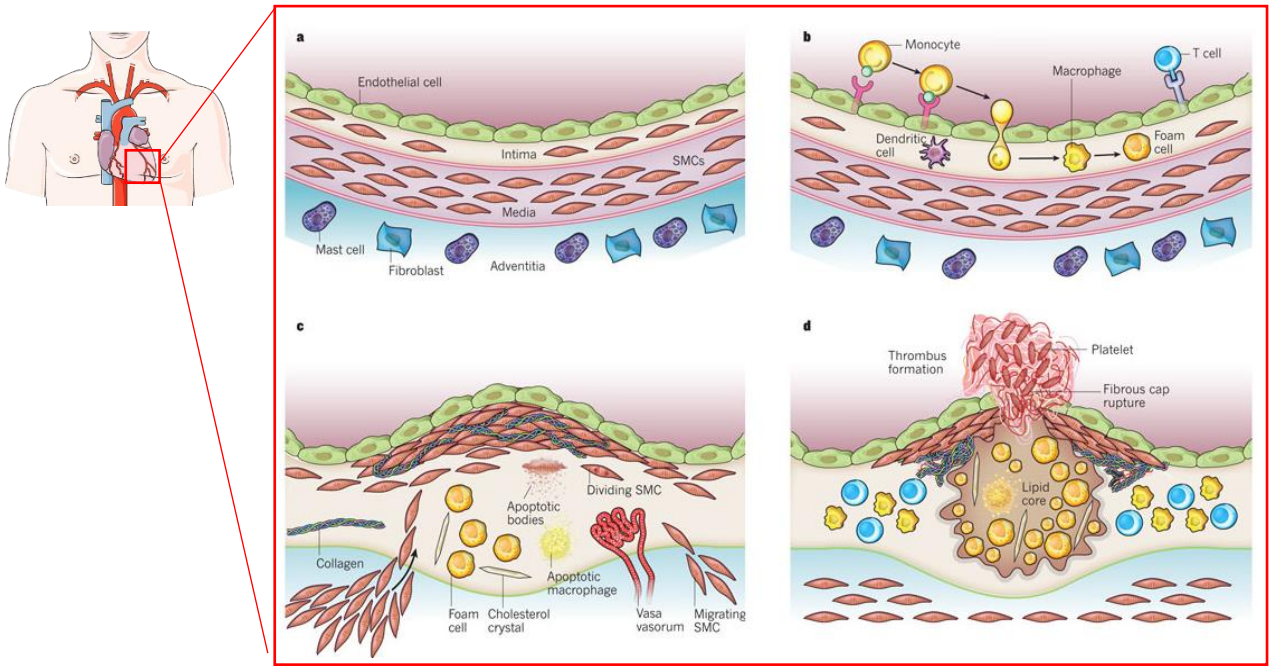

Figure 1.13: Pathogenesis of atherosclerosis.

A) Showing a normal vessel wall, no damage to the endothelium. **B)** Endothelial damage, LDL oxidised, Floating monocytes transmigrate into the tunica intima and differentiate into macrophages, scavenger receptor takes up the oxiLDL, and become foam cells forming the atherosclerotic lesions. **C)** smooth muscle cells proliferate and migrate from the tunica media to the intima, plaque building up on the vessel wall, calcification of the wall and release of MMP, all build up, restricting blood flow and able to cause the plaque to rupture resulting in thrombosis, stroke or a myocardial infarction. Adapted from (Libby et al., 2011).

1.14 TRIB3 is implicated in atherosclerosis and CVD

TRIB3 has been implicated to play a role in many of these metabolic processes that lead to the development of CVD. Human genetic studies have shown a gain of function Q84R polymorphism of TRIB3 to be associated with insulin resistance, carotid atherosclerosis, dyslipidaemia and an increased risk of developing diabetes (Prudente et al., 2005).

There is a reduction in mRNA transcript hepatic and abdominal Trib3 levels in the visceral abdominal fat and the liver of obese patients, additionally, there was a correlation between mRNA levels of Trib3 and plasma insulin levels (Oberkofler et al., 2010). Furthermore, a study has used fibrates to treat hypertriglyceridemia and has shown this had augmented TRIB3 expression levels independent of PPARα. This were done using PPAR alpha knockout (KO) mice treated with and without fibrates (Selim et al., 2007).

Moreover, patients with T2DM were seen to have an elevated level of TRIB3 in the pancreas compared with healthy patients (Liew et al., 2010). Biopsies of islets of Langerhans from patients with T2DM have shown up to fourfold increase in TRIB3 mRNA and a threefold increase in TRIB3 protein levels compared with the control (non-diabetic patients). Insulin resistance is a risk factor for the development of CVD (Freeman and Pennings, 2018).

Amongst 513 unrelated Chinese individuals, Gong and colleagues have found the R84 variant to be associated not only with insulin resistance and metabolic syndromes but also with carotid intima-media thickness (IMT), which is a marker for future cardiovascular events (Gong et al., 2009).

TRIB3 was also implicated in the diabetic atherosclerosis process. Silencing Trib3 in apolipoprotein E (apoE)/LDR receptor (LDLR) double-knockout ($ApoE^{-/-}/LDLR^{-/-}$) mice with diabetes reduced atherosclerotic burden and stabilised the plaque in mice and reduced macrophage apoptosis (Wang et al., 2012). Furthermore, rats with silenced TRIB3 showed an improved insulin resistance and cardiac function (Wang et al., 2012). All the evidence above indicates that Trib3 is an important protein which may contribute towards the development of CVD.

1.15 Trib3 is implicated in lipid metabolism

It has been reported that Trib3 overexpression in 3T3-L1 preadipocytes blocks adipogenesis either directly or through physical interaction via transcriptional factors. Trib3 is able to prevent induction of C/EBPα and PPARγ from trans-activating adipogenic genes or indirectly, in which it inhibits extracellular signal-regulated kinase (ERK) phosphorylation and in turn, activates CEBPβ by phosphorylating its regulatory phospho-acceptor sites (Bezy et al., 2007). Furthermore, the work was confirmed by another group, showing that Trib3 can control the transcriptional activity of PPARγ and therefore suppress adipocytes differentiation and intracellular accumulation of triglycerides (Takahashi et al., 2008).

Trib3 been described as a negative regulator of differentiation of adipocytes but can also control lipid accumulation in mature adipocytes. Fasting has been shown to increase Trib3 levels, which stimulate adipocyte lipolysis and cause inactivation of Acetyl CoA, a key enzyme responsible for fatty acid synthesis via recruiting ubiquitin E3 ligases COP1 and promoted ubiquitin-proteasomal degradation (Qi

et al., 2006). Furthermore, Trib3 overexpressing mice in the adipose tissue are protected from obesity due to an increased rate of fatty acid oxidation via ACC and increased energy expenditure (Prudente et al., 2012). Additionally, it has been reported that Trib3 is upregulated in fatty liver dystrophy (*fld*) mutant mouse which suffers from hypertriglyceridemia and fatty liver in young mice and impaired nerve function in adult mice (Klingenspor et al., 1999). Weismann and colleagues did a study using $Trib3^{ko}$ via antisense oligo in rat livers and showed an elevated weight, improved insulin sensitivity and increase in PPARγ but no changes to Akt activation, suggesting alternative mechanisms (Weismann et al., 2011).

1.16 TRIB3, Akt and insulin resistance

Studies have shown Trib3 to be important in insulin signalling via Akt. Expression levels of Trib3 were induced upon fasting through the induction of PPARα (Selim et al., 2007). It was, therefore, suggested that Trib3 is involved in both lipid and glucose metabolism.

Trib3 has been described as a negative regulator of insulin, mediated via Akt phosphorylation. Another study has shown that overexpression of Trib3 in Hepg2 inhibits Akt activation and therefore affects insulin signalling pathway (Du et al., 2003). Conversely, $Trib3^{ko}$ resulted in induction of phosphorylation in Akt. Similarly, it has been shown in skeletal muscle cells, where overexpression of Trib3 inhibits Akt phosphorylation as well as ERK phosphorylation. This, in turn, affects GLUT4 translocation and glucose transportation (Liu et al., 2010).

It has been reported that Trib3 is elevated upon fasting and overexpression of Trib3 leads to inhibition of insulin via the Akt phosphorylation pathway (Liu et al., 2010). In addition to this, overexpression of Trib3 in mice liver resulted in hyperglycaemia, conversely, $Trib3^{ko}$ in mice liver led to improved insulin and glucose tolerance. Trib3 expression was upregulated in db/db diabetic insulin resistance mice, and overexpression of Trib3 in the control resulted in hyperglycaemia, glucose intolerance and insulin resistance, similar to what was seen in the db/db diabetic insulin resistance mice (Matsushima et al., 2006).

Furthermore, Trib3 is shown to be upregulated in skeletal muscle for type 2 diabetic patients and overexpression of Trib3 in muscle cells blocks insulin-stimulated glucose transport as reviewed by (Angyal and Kiss-Toth, 2012). Trib3 is also able to control muscle differentiation by activating Akt, which in turn increases myogenic differentiation of factor D, a regulator of muscle proliferation. Overexpression of Trib3 leads to inhibition of Akt, a reduction in myogenic differentiation factor D and therefore reduction in myotube formation (Kato and Du, 2007).

Recent studies have questioned Trib3 involvement in the insulin signalling pathway as overexpression of Trib3 in rat liver had no effect on the insulin signalling pathway, suggesting alternative mechanisms (Weismann et al., 2011).

1.17 Trib1 in CVD and inflammation

Although Trib3 is implicated in lipid metabolism and insulin resistance, the isoform Trib1 has also been described as a regulator of inflammatory signalling and lipid metabolism.

A genome-wide association study (GWAS) in a human patient had shown Trib1 to be associated with hyperlipidaemia and an increase in the risk of CAD (Yamamoto et al., 2007). Furthermore, full body $Trib1^{ko}$ in mice had shown an increased level of plasma triglycerides and cholesterol levels due to an increase in VLDL production. Hepatic-specific overexpression of Trib1 using adeno-associated virus serotype eight vector resulted in a decrease in cholesterol and plasma triglycerides (Burkhardt et al., 2010). Trib1 has also been shown to modulate vascular smooth muscle cells (VSMCs) proliferation and migration (Sung et al., 2007).

Trib1 have been described as regulators of pro-inflammatory markers. A study by Sung and colleagues had shown that Trib1 was expressed in resident macrophages of mouse atherosclerotic plaques (Sung et al., 2012). Atherosclerosis in $ApoE^{-/-}IL1R1^{-/-}$ (double knockout) mice models were used. Immunohistochemical analysis has shown a reduction in Trib1 expressing macrophages, compared to the $ApoE^{-/-}$ cohort. Furthermore, it was reported an upregulation of pro-inflammatory IL-12 in Trib1 knockout mice, a characteristic feature of M1 macrophages (Yamamoto et al., 2007). This study has also been validated and was shown that Trib1 is increased in Raw 264.7 cells and overexpression of Trib1 leads to a reduction in IL-6 and IL-12 levels (Sung et al., 2012).

Furthermore, it has been reported that Trib1 is critical for differentiation of M2 macrophages. $Trib1^{ko}$ resulted in a reduction of M2-macrophages in various organs, including bone marrow, spleen, lung and adipose tissues. The above studies demonstrate that Trib1 is important in the polarisation of macrophages towards an M2 phenotype. However, more *in vivo* studies are required to validate this in an atherosclerosis context (Satoh et al., 2013).

1.18 Tribbles in cancer

Tribs have been shown to be expressed in many cancerous cell lines, including human lung, colon, oesophageal and breast tumours (Xu et al., 2007). Trib1 has been reported to accelerate the degradation of CEBPα in acute myeloid leukaemia (AML) cells, and this is done via MAPKK dependence (Yamamoto et al., 2007). Additionally, Keeshan and colleagues have shown that overexpression of Trib2 in mice leads to AML (Keeshan et al., 2010). Furthermore, a study conducted a transcriptomic analysis of over 200 human blood samples from AML patients and demonstrated the contrary with a reduction in levels of Trib2 in AML patients compared with healthy volunteers (Gilby et al., 2010). Both studies could be correct and it could be possible that dysregulation of both Trib1 and Trib2 levels could lead to a disease state. Other possibilities include Trib could be working as heterodimers and work in a compensatory manner as reviewed in (Liang et al., 2013, Kiss-Toth, 2011).

Both Trib1 and Trib2 have also been shown to interact and co-operate with HOXA9 to accelerate the onset of AML (Keeshan et al., 2008). There is an increase in evidence that Trib1 and Trib2 have a role in oncogenesis and the development of AML. However, understanding the details of the mechanism by which it regulates this is of importance to developing future therapeutics.

1.19 Summary

From the review, it can be shown that obesity is a significant risk factor for many facets of metabolic diseases including diabetes, hypertension and CVD. Trib3 has been implicated to play a role in these

metabolic processes including the insulin signalling and lipid metabolism. While several tissue-specific transgenic and knockdown experiments have been published recently, our unpublished knockout studies are the first to address this question at the level of the whole mouse. So far, it is clear that the various organs may be affected differently and that the interplay between these changes may lead to the obese phenotype. Our insight into the role of Trib3 in various organs remains limited. This study aims to use a systemic approach, for the first time on a whole body Trib3^{ko} mice to decipher a role for Trib3 in metabolic dysfunction.

1.20 Hypothesis

Based on current knowledge, Trib3 is hypothesised to have a tissue-specific function in different metabolic tissues and is an important regulator of metabolic homeostasis.

1.21 Aims

The project aims to:

Chapter 3

- Characterise the anatomy and lipid profile of the full body Trib3^{ko} in mice, alongside MRI images to localise fat distribution.
- Characterise the energy consumption, food and water intake and other metabolic activities of the full Trib3^{ko} mice.
- Conduct a glucose tolerance test (GTT) and Insulin tolerance test (ITT) to characterise if the full body Trib3^{ko} in mice become insulin resistance.

Chapter 4

- Characterise tissue-specific consequences, i.e. assess the morphology of the metabolic tissues of the male Trib3^{ko} compared with WT littermates.
- Characterise Trib3 dependent, tissue-specific regulatory mechanisms of metabolic tissues in male Trib3^{ko} compared with WT littermates by microarray and validate key findings using standard molecular biology techniques.

Chapter 5

- Identify miRNAs that can bind to the Trib1 3′UTR using bioinformatics databases.
- Test and characterise the impact of miRNAs on Tribbles expression levels via dual luciferase assay and qRT-PCR and western blots.
- Determine the impact of miRNA on tribbles on high fat diet (HFD) and chronic inflammatory settings.
- Use a target site blocker (TSB) to increase Hepatic Trib1 levels and test for plasma lipid profile and triglyceride in the liver.

Chapter 2—Materials and Methods

2.1 Animals

2.1.1 Licensing

All experiments were in accordance with the UK legislation under the 1986 Animals (Scientific Procedures Act). All animal experiments were approved by the University of Sheffield Project Review Committee and carried out under a UK Home Office project license holder (PPL, 70/77992 Professor S.E. Francis by personal licence holder (procedure individual licence; PIL) J. Johnston 40/10901.). Animal experiments were carried out by myself after culling and Dr Jessica Johnston.

2.1.2 Husbandry

All mice were housed in a controlled environment with a 12 h light and dark cycle at around 22 °C room temperature. All mice were fed *ad libitum* on standard chow diet (Harlan 18% rodent diet unless otherwise stated). Where possible, littermates were housed together at no more than 6 mice per cage.

2.1.3 Generation of Trib3^{ko} mice

The Trib3^{ko} mice strain were created using the gene-trap system.Trib3 heterozygous mice were back-crossed with C57BL6 mice for 10 generations before intercrossing to produce Trib3^{ko} mice. This was carried out in Madrid, in Prof Guillermo Velasco's lab. Full detail of the breeding can be found in (Salazar et al., 2014). **Figure 2.1** illustrates the principle pf generating the Trib3^{ko} mice using the gene-trap system.

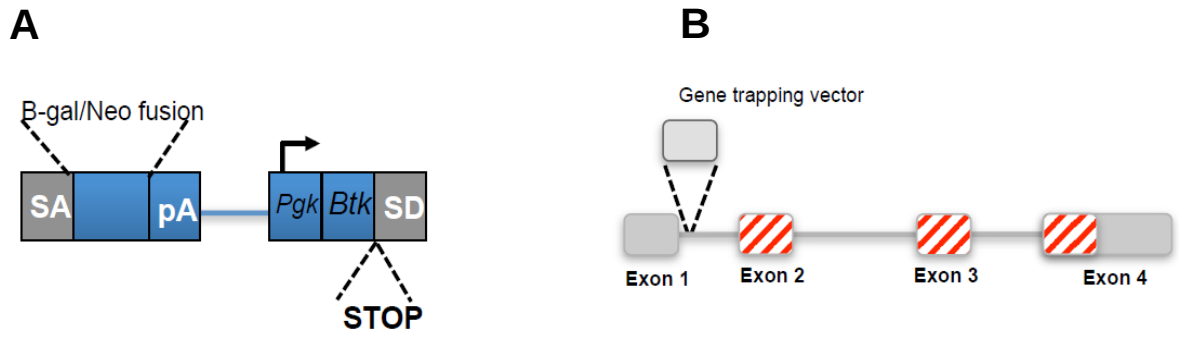

Figure 2.1: Generation of Trib3^{ko} mice using the gene-trap system.
(**A**) The gene trap vector used to inactivate the Trib3 allele included two expression cassettes. (**B**) Schematic showing the Trib3 allele, which was targeted in the first intron using the gene-trap vector. Adapted from (Salazar et al., 2014).

2.1.4 Genotyping Analysis

The Genotyping was carried out by Mark Arians, a technician in the core faculty of the University of Sheffield. WT and Trib3^{ko} were weaned and genotyped at 3 weeks of age. Mice were anaesthetised, and ears were clipped approximately 2 × 2 mm^2 that was then digested in 300 μl of lysis buffer containing Tris-HCl, 100 nM EDTA, 0.5% sodium dodecyl sulfate (SDS), 0.1 mg/ml Proteinase K (Promega, Madison, WI, USA), and 0.2 mg/ml RNase A (Qiagen, Germantown, MD, USA), at 56 °C in agitation for 30 min. The lysates were centrifuged at 12,000*g* at room temperature for 5 min and to precipitate the isolated DNA, 500 μl of isopropanol was slowly added to the supernatant followed by 1 ml of ice-cold 70% ethanol. The tubes were then repeatedly inverted until the DNA had completely flocculated.

Precipitated products were centrifuged at 12,000*g* for 5 min and the pellets were air dried at room temperature before suspended in 200 μl of water at 65 °C in agitation for 5 min.

Mice were genotyped by a multiplex polymerase chain reaction (PCR) assay. Specific details of the PCR reaction can be found in **Appendix II**.

2.1.5 End of procedure

Mice were weighed and culled via a pharmacological overdose of 0.2 ml sodium pentobarbital (200 mg/ml) given into the peritoneal cavity. Blood for plasma was taken directly from the heart through the chest wall into a heparinised syringe following the loss of pedal reflex. Blood was centrifuged at 2000*g* for 5 min at room temperature. Plasma was immediately frozen and stored at –80 °C.

2.2 MRI scans of Trib3^{ko} and WT littermates

MRI images were carried out by Steven Reynolds in the Radiography department of the University of Sheffield. MRI images were obtained using a 9.4 Tesla, Bruker Avance III MRI scanner (Bruker Biospin MRI GmbH, Ettlingen, Germany) with a 25 mm ^{1}H volume coil. The mice were placed in the coil so that the centre of their abdomen was aligned with the centre of the coil. The mice were oriented in the scanner so that their hips were at the top of the image. Structural MRI scans were performed using an MSME spin echo sequence (FOV 3.0 cm × 3.0 cm, 512 × 512 matrix, TE/TR 16 ms/1000 ms). 34–36 1 mm slices were used for each mouse, creating a pack extent of 35 ± 1 slices. The images produced were processed using Bruker paravision 5.1 software. The slice package of MRI images was segmented and analysed for fat content using a custom MATLAB program (MathsWorks Inc, Natick, MA).

A common image reference point was used to compare different mice. This was defined by using the location of the hips; the mid-slice between the first slice with hips visible and the last slice with visible hips was chosen as a standardised reference point for each mouse. For image processing in each mouse, the package of image slices was first normalised. A binary mask was created by thresholding each image between 10–95%, at 5% intervals, of image intensity. All image voxels above the threshold intensity were selected and summed to give the fat volume in each image. Images were inspected at the 50% threshold to confirm fat identification.

2.3 Metabolic measurements

Metabolic cage studies were performed by Zoe Bichler from the animal facility at NTU. 12-week-old mice (n = 6 per genotype) were conducted in a Comprehensive Laboratory Animal Monitoring System (8-chamber CLAMS, Columbus Instruments, Columbus, OH, USA). The mice were adapted to powdered food for 24 h before they were introduced into the metabolic cages, where a 48-h acclimation preceded the 24-h recording time. Metabolic parameters, including food and water consumption, O_2 consumption, CO_2 emission, metabolic rate and physical activity, were recorded for 24 h from the beginning of a light cycle until the end of a dark cycle. Metabolic rate was derived from the heat production by assessment of the exchange of O_2 and CO_2 during the metabolic process.

Physical activity was determined by dual axis detection of animal motion. Horizontal movements (Xamb) and rearing movements (Ztot) were measured by counting the number of horizontal and vertical infrared beam breaks. Respiratory exchange ratio (RER) was calculated by VO_2/VCO_2 to reveal the fuel consumption preference. Oxygen and carbon dioxide sensors were calibrated using calibration gas mixtures. High-precision weighing stations in combination with leak- and spill-proof containers accurately recorded the body weight, food and water intake (in grams). Spontaneous activity was recorded with two levels of infrared light beam frames surrounding each cage. Raw data can be found in **Appendix III**.

2.4 Histology

Frozen tissue samples from the adipose and liver were either paraffin embedded or cryo-sectioned. Oil red O staining and haematoxylin and eosin (H&E) was used to assess tissue morphology and look

at lipid content. Images were captured using a Nikon Eclipse E600 microscope with either 20×, 50× or 100× magnification. The histological detail protocol can be seen below:

Staining:

- Dewax slides for 10 minutes in xylene and rehydrate through graded alcohols (100%, 90%, 70 and 50% (v/v) ethanol), finishing in water
- Stain with Carazzi's haematoxylin for 2 minutes, rinse in water
- Stain with eosin (1% (w/v)) for 30 seconds
- Rinse in water and quickly dehydrate through graded alcohols for 30 seconds in each, beginning at 90% (v/v) ethanol, ending in xylene
- Mount with coverslips using DPX mountant

Interpretation:

- Nuclei — Purple/blue
- Cytoplasm — Pink
- Muscle fibres — Deep red
- RBCs — Orange/red
- Fibrin — Deep pink

Oil red O staining:

Solution:

- Add Oil Red O powder to 99% (v/v) isopropanol until it becomes saturated
- Filter the solution using Whatmann grade 1 filter paper
- The stock stain can be kept at room temperature
- Dilute to 60% (v/v) fresh using distilled water on day of staining

Staining:

- Tissues should be stained in individual 1.5ml eppendorf tubes
- Rinse tissues in distilled water followed by 60% (v/v) isopropanol for 2 minutes
- Immerse in 60% (v/v) Oil Red O for 10-15 minutes
- Rinse in 60% (v/v) isopropanol for 2 minutes followed by distilled water.
- Stained tissue can be stored at 4°C until pinning out.

2.4.1 Tissue processing

Metabolic tissues; adipose, liver and skeletal muscle tissues were dissected and placed in 10% (v/v) formalin or snap frozen in liquid nitrogen. The tissues were embedded in paraffin wax for histology examinations. The three main steps include clearing, dehydration and infiltration. After paraffin embedding tissues, the wax was placed on cold ice for 1 h before being sectioned. The blocks were trimmed until the desired tissue thickness and area were reached. Around 2–10 μm was sectioned using a microtome. The sections were mounted onto a glass microscopic slide and dried at room temperature before being placed on 37 °C overnight.

2.5 Blood biochemistry

Samples were sent to Royal Hallamshire Hospital, Sheffield to measure total cholesterol, HDL-C, triglycerides and glucose levels were measured from plasma from the mice on a Roche Cobas 8000 modular analyser. LDL-C was estimated using the Friedewald equation. LDL-chol] = [Total chol] - [HDL-chol] - ([TG]/2.2) where all concentrations are given in mmol/L.

2.5.1 Lipid profiling

Blood taken from the mice was stored at –80 °C. The samples were sent to Royal Hallamshire Hospital at the Department of Clinical Chemistry. A full-blood lipid profile was measured, which included triglycerides, cholesterols levels, major lipoproteins (HDL, LDL) and glucose level (Roche Cobas 8000 modular series).

2.6 Triglyceride quantification in the liver

Lipids were extracted from tissues using the Folch extraction method. Fatty acid and triglyceride concentrations were measured using a fatty acid and glycerol kit (Wako pure chemical industries, Osaka, Japan). Reading was measured using a spectrometer and plotted. Data were normalized against the tissue weight.

2.7 Microarray gene analysis

RNA yield quantity and quality were assessed using a NanoDrop Spectrophotometer (NanoDrop Products, Thermo Fisher Scientific, Inc., Wilmington, DE, USA) and Agilent Bioanalyzer (Agilent Technology, Santa Clara, CA, USA). Samples were considered acceptable for testing when 28S and 18S rRNA bands resolved into two discrete bands that had no significant smearing below each band. Double-stranded cDNA was generated from the RNA sample using the GeneChip® WT PLUS Reagent Kit according to the manufacturer's protocol. Fragmentation and end-terminus labelling of cDNAs were performed using the same kit according to the manufacturer's protocol. The samples were then hybridized to GeneChip® Mouse Transcriptome Array 1.0 at 45 °C for 16 h overnight, following the manufacturer's procedures. GeneChips post-processing was done on the AFX Fluidics 450 Station, according to all AFX protocols and procedures defined for the Mouse Transcriptome Array 1.0 (FS450_0001), as outlined in the kit manual. GeneChips were scanned on the GC3000 G7 Scanner.

2.7.1 Bioinformatics software used to analyse the microarray:

Data were extracted and processed using Partek® Genomics Suite™ (Partek Incorporated, St. Louis, MO, USA) and IPA (intuitive pathway analysis) PCA, gene list of P-value of <0.05 and a fold difference of <–2.5 and >2.5 were used to create hierarchical clustering heatmap, gene ontology and a Pathway network analysis.

2.8 Measurements of FFA and glucose uptake in HepG2

HepG2 cells were seeded in a 12-well plate and siTrib-3 was transfected using lipofectamine 3000 (Dharmacon) alongside an NTC. Media were removed after 24 h and washed with PBS. 10 μM of FFA dye was added to the cells for 30 min. Cells were lysed using trypsin and a flow cytometer was used to detect the uptake via FITC.

2.9 Glucose tolerance test (GTT) and insulin tolerance test (ITT)

The GTT and ITT experiments were carried out by Jihan AlGhamdi, a previous PhD student at EKT lab. Mice were fed on chow or 60% HFD for 8 weeks and then fasted overnight. Fasting mice were weighed and blood was collected from the tail. A 20% glucose solution was prepared and filtered through 0.2-μm filter. For GTT, mice were fed with 2 mg glucose/g of body weight. Blood was collected at different intervals, 0, 30, 60, 90 and 120 min after glucose challenge by the tail sampling method. For ITT, mice were fasted for 2–3 h and then weighed. They were then intraperitoneally injected with 0.75 mU insulin/g of body weight using an insulin syringe. Blood glucose was determined at 0, 20, 40 and 60 minutes.

2.10 Western blotting

Relative protein expression was measured using the western blotting method. The tissue was lysed using the RIPA lysis buffer (50 mM HEPES, 100 mM NaF, 10 mM EDTA, 10 mM sodium pyrophosphate, 1% Triton v/v X-100, 10% v/v glycerol.) Protease inhibitors (1:7, Roche) and phosphatase inhibitors (1:10, Roche) were also added to the solution. Cells were then sonicated for ~20 s to complete the lysis step. Cell lysates were centrifuged at 15,000*g* for 15 min at 4 °C and the supernatant was transferred into a separate Eppendorf tube and the pellet discarded. Proteins were quantified using the Bradford method and kept at –80 °C until required. The proteins were mixed 2× lamellae buffer (1:7, 4% SDS (w/v), bromophenol blue 0.0004% (w/v), 2-mercaptoethanol, 20% glycerol, 0.125 M Tris-HCl, pH 6.8) The samples were then boiled for 5 min at 95 °C. Proteins were loaded onto NuPAGE 4–12% Bis-Tris SDS-PAGE gel (Novex) with a pre-stained protein ladder (Thermofisher), to mark the size of the bands. Electrophoresis allows the bands to separate according to size and charge. MES-SDS running buffer (50 mM MES, 0.1% SDS, 50 mM Tris-Base, 1 mM EDTA, pH 7.3) were also added in the tank, alongside the gel for 45 min at 100 V. Upon separation of the protein, the proteins were transferred to a nitrocellulose membrane at 35 V for 1 h with a transfer buffer (5% 20× Transfer buffer, 20% methanol and 0.1% antioxidant). Ponceau Red was added to the nitrocellulose membrane to validate bands and washed off with 5% Marvel TBST (20 mM Tris pH 7.5, 150 mM NaCl, 0.1% Tween20). The nitrocellulose membrane was blocked in 5% Marvel TBST for 1 h at room temperature on a shaker. The membrane was then washed with TBST 3× for 15 min. Primary

and secondary antibodies were added and specific protein bands were detected upon addition of a chemo-luminescent substrate (ECL prime western blotting detection reagent, GE Healthcare) and its exposure was detected by the Biorad imager or Licor machine. **Table 2.1** represents the antibodies used and its dilutions.

Table 2.1 represents the antibodies used and its dilutions.

Antibody	Company	Dilutions
mPPARα	Santa Cruz Biotechnology, Inc. USA	1:1000 in 5% milk
mPPARγ	Santa Cruz Biotechnology, Inc. USA	1:1000 in 5% milk
mPPARβ	Santa Cruz Biotechnology, Inc. USA	1:1000 in 5% milk
mpAKT	Cell Signalling Technology (CST)	1:2000 in 5% BSA
mTAKT	Cell Signalling Technology (CST)	1:2000 in 5% BSA
mGlut4	Santa Cruz Biotechnology, Inc. USA	1:2000 in 5% milk
mGlut2	Santa Cruz Biotechnology, Inc. USA	1:2000 in 5% milk
mCebpβ	Santa Cruz Biotechnology, Inc. USA	1:2000 in 5% milk
mCebpα	Cell Signalling Technology (CST)	1:2000 in 5% milk
mPCNA	Santa Cruz Biotechnology, Inc. USA	1:2000 in 5% milk
mTrib3	Abcam	1:3000 in 5% milk
Trib1	Abcam	1:3000 in 5% milk
Tubulin	Santa Cruz Biotechnology, Inc. USA	1:5000 in 5% milk or BSA
GAPDH	Cell Signalling Technology (CST)	1:5000 in 5% milk or BSA

2.11 qRT-PCR

Total RNA of adipose, liver and muscle was isolated using the RNAeasy Mini Plus Kit (#74134, Qiagen) kit and according to the manufacturer's guidelines. RNA was reverse transcribed into cDNA using iScript cDNA synthesis kit (#1708890, Bio-Rad). Assays were performed using either TaqMan (Invitrogen) or SYBR green (Precision PLUS, Primer Design, UK) to detect the mRNA levels of the genes of interest. qRT-PCR reactions were run using the Bio-rad system C3779 machine. Values were normalised using either Tubulin or GAPDH. Fold changes were calculated using the DDCT method. **Table 2.2** shows the primer sequences for the qRT-PCR

Table 2.2- The primer sequences for the mRNA expression.

Gene	Forward sequence (sense) 5′→-3′	Reverse sequence (Antisense) 5′→-3′
mPPARα	AGAGCCCCATCTGTCCTCTC	ACTGGTAGTCTGCAAAACCAAA
mPPARγ	TCGCTGATGCACTGCCTATG	GAGAGGTCCACAGAGCTGATT
mPPARβ	TCCATCGTCAACAAAGACGGG	ACTTGGGCTCAATGATGTCAC
mpAKT	CCTCCACGACATCGCACTG	TCACAAAGAGCCCTCCATTATCA
mGlut4	GATTCTGCTGCCCTTCTGTC	ATTGGACGCTCTCTCTCCAA
mGlut2	GCTGTCTCTGTGCTGCTTGT	CGTAACTCATCCAGGCGAAT
mCebpβ	TTAAGCGTAACTGGCGGAAACC	CAGTAAGATTTGTTGCACATCAGC
mCebpα	CAAGAACAGCAACGAGTACCG	GTCACTGGTCAACTCCAGCAC
mPCNA	GGCCGAAGATAACGCGGATAC	GGCATATACGTGCAAATTCACCA
mTrib3	TCGACTGGGGCCTTATATCCTT	CAGGTGTACTCTGTGCCTGTG
mAPOE	CTGACAGGATGCCTAGCCG	CGCAGGTAATCCCAGAAGC
mFabp4	AAGGTGAAGAGCATCATAACCCT	TCACGCCTTTCATAACACATTCC
mLDLR	TCCCTGGGAACAACTTCACC	CACTCTTGTCGAAGCAGTCAG
mAngptl8	CTGACCCTGCTCTTTCACGG	GCTCTGTCATAGAGGCCCAG
mTubulin	GTTCACTGGTCAGTCAGAACC	TCCGAACACTGGAAAGAATCTTG
mGAPDH	TGGATTTGGACGCATTGGTC	TTTGCACTGGTACGTGTTGAT

RT-PCR was performed with the following:

- 2 µl of cDNA
- 0.5 µl Primer mix
- 5 µl of Taqman RT-PCR mix (2×)
- 2.5 µl of H_2O

All of the above mixtures were added and mixed into sterile Eppendorf tubes with a total end volume of 10 µl. It was then transferred into the 384-well plates and placed in the PCR machine. The thermal cycling parameters are as follows:

- Step 1 – 94 °C for 1 minute
- Step 2 – 35 cycles at 94 °C - (Denaturation) for 30 s, 55 °C – (Annealing) for 30 s, 72 °C – (Extension) for 1 minute.
- Step 3 – 72 °C for 5 minutes
- Step 4 – 4 °C on Hold

2.12 Dual luciferase assay

The Dual Luciferase Reporter (DLR) Assay System (Promega) was used to create Trib1 plasmids fused to the Renilla luciferase. The activities of firefly luciferase (Photinus pyralis) and Renilla luciferase (Renilla reniformis) were measured sequentially from a single sample. Firefly luciferase was expressed constitutively as a housekeeping gene and Renilla luciferase was an indirect measure of the WT or mutant TRIB1 activity. HepG2 cells were seeded in a 96-well plate and transfected with the luciferase plasmids and a miRNA (Ambion). They were left overnight in the incubator and then washed with PBS and lysed using Lysis buffer 1:4 supplied with the kit (Promega). The substrates were added to the lysates and chemiluminescence light was detected by the plate reader. For more information, refer to the standard Promega Dual luciferase assay standard manual.

2.13 Flow cytometry

An LSR flow cytometry machine was used to look at percentage GFP and siGlow transfection using different transfection reagents. Furthermore, free fatty acid uptake and glucose uptake were analysed using flow cytometry in HepG2s.

2.14 Cell culture of HepG2 cells

The human hepatocellular carcinoma cells (HepG2) were maintained in Dulbecco's Modified Eagle Medium (DMEM) (Invitrogen) supplemented with L-glutamine (Invitrogen), 25 mM HEPES, 10% inactivated foetal bovine serum (FBS), 1% streptomycin/penicillin and kept at 37 °C in a 5% CO_2 incubator overnight.

Mycoplasma testing was done every 3 months to look at whether the cells were infected. The haemocytometer was used to count the cell numbers and Trypan blue was used to test for cell viability before experiments.

2.15 Statistical Analysis

All statistical analyses were performed with GraphPad Prism. The relevant tests are stated in the figure legend of each graph. One-way ANOVA and Student's *t* test were mainly used. P-value was labelled as significant if the value was <0.05. Results are presented as Mean ± SEM unless stated otherwise. The number of repeats are also stated in the figure legends.

Chapter 3—Results

Trib3 deficiency leads to male-specific obesity, dyslipidaemia and altered energy homeostasis

3.1 Introduction

Obesity is a systemic disease that involves the dysregulated communication amongst different organs, contributing to the development of metabolic processes that can lead to chronic diseases, including coronary artery disease (CAD), diabetes and cancer. Tribbles-3 (TRIB3) has been implicated in many of these metabolic processes. Human genetic studies have shown a Q84R polymorphism of TRIB3 to be associated with insulin resistance, dyslipidaemia and an increased risk of developing diabetes (Prudente et al., 2005). Furthermore, patients with T2DM were seen to have an elevated level of TRIB3 in the pancreas compared with healthy patients (Liew et al., 2010). Biopsies of islets of Langerhans from patients with T2DM have shown up to fourfold increase in TRIB3 mRNA and a threefold increase in TRIB3 protein levels compared with the control (non-diabetic patients) (Liew et al., 2010). Insulin resistance is a risk factor for the development of CVD (Freeman and Pennings, 2018). Additionally it was reported that Trib3 is upregulated in fatty liver dystrophy (*fld*) mutant mice which suffers from hypertriglyceridemia and fatty liver in young mice and impaired nerve function in adult mice (Klingenspor et al., 1999). Furthermore, in 513 unrelated Chinese individuals, Gong and colleagues have found the R84 variant to be associated not only with insulin resistance and metabolic syndromes but also with carotid IMT, which is a marker for future cardiovascular events (Prudente et al., 2005). TRIB3 was also implicated in the diabetic atherosclerosis process. Silencing Trib3 in apolipoprotein E (apoE)/LDR receptor (LDLR) double-knockout ($ApoE^{-/-}/LDLR^{-/-}$) mice with diabetes reduced atherosclerotic burden and stabilised the plaque in mice (Wang et al., 2012). All the evidence above indicates that Trib3 is an important regulator in insulin resistance and CVD.

Over the years, there have been many mouse models developed to investigate the consequences of Trib3 tissue-specific overexpression or knockout mice. Adipose-specific overexpression of Trib3 has shown reduced weight gain, reduced WAT and these animals were protected from diet-induced obesity (Qi et al., 2006). Another study has shown that skeletal muscle-specific overexpression of Trib3 mice led to an increased proportion of oxidative muscle fibres but no change in glucose homeostasis (An et al., 2014). In addition, PPARα expression levels and miR208b and miR499 were both increased. Both miR208b and miR499 have been shown to be significantly elevated in acute myocardial infarction patients in a Greek population, hence used as biomarkers for CVD in Greek populations (Agiannitopoulos K et al., 2018).

Together, these observations suggest that Trib3 plays a tissue-specific role and that it may be involved in the communication amongst different organs, including adipocyte differentiation and insulin signalling, to maintain lipid homeostasis.

A knockdown of Trib3 in hepatic with antisense oligonucleotides was shown to increase the mass of WAT by 70% and enhanced expression of PPARγ (Weismann et al., 2011). Furthermore, a study by Okamoto and colleagues have shown a genetic deletion of Trib3 with no difference in hepatic glucose production, lipid levels and energy metabolism in the liver (Okamoto et al., 2007). Thus, the global loss of Trib3 in this model does not appear to affect glucose homeostasis in mice maintained in standard conditions. However, our insight into the role of Trib3 in various insulin-sensitive organs remains limited. In this study, full body Trib3^{ko} mice were used to characterise a role for Trib3 in metabolic dysfunction via a systematic analysis of lipid and glucose homeostasis and transcriptomic alterations in key metabolic tissues. In this chapter, the phenotype of a full body Trib3^{ko} alongside metabolic changes will be characterised.

3.2 Hypothesis

TRIB3 is an essential regulator of lipid metabolism and insulin signalling and may display an obese phenotype in a full body Trib3^{ko} mouse model.

3.3 Aims

- Characterise the anatomy and lipid profile of the full body Trib3^{ko} in mice, alongside MRI images to localise fat distribution.
- Characterise the energy consumption, food and water intake and other metabolic activities of the full body Trib3^{ko} mice.
- Conduct a glucose tolerance test (GTT) and Insulin tolerance test (ITT) to characterise if the full body Trib3^{ko} in mice become insulin resistance.

3.4 Results

Full body Trib3^{ko} mice were created using the gene-trap system. Trib3 heterozygous mice were back-crossed with C57BL6 mice for 10 generations before intercrossing to produce Trib3 mice. The details of the generation of the Trib3^{ko} mice have been described in (Salazar et al., 2014).

3.4.1 Trib3^{ko} mice lead to male obesity

Although many models have been used to study Trib3, this study is the first to address the question at the level of a whole body Trib3^{ko} mouse. A study by (Qi et al., 2006) has shown that adipose-specific overexpression of Trib3 reduced weight gain, reduced white adipose tissue (WAT) and protected from diet-induced obesity. **Figure 3.1A** shows an elevated body weight of the Trib3^{ko} compared with WT littermates (WT) at 13 weeks of age.Trib3^{ko} weighed an average of 29.8g compared to 25.6g of WT littermates. Furthermore, **Figure 3.1B** shows no significant difference in the weights of female mice.

3.4.2 Male Trib3^{ko} mice lead to an increase in subcutaneous fat

Upon dissection of a mouse, it has appeared that male Trib3^{ko} mice had an increased amount of subcutaneous fat compared with WT littermates. Signs of adipose hypertrophy was shown (arrows). **Figure 3.1C** shows representative images of the gross anatomy of male Trib3^{ko} mice compared with WT littermates.

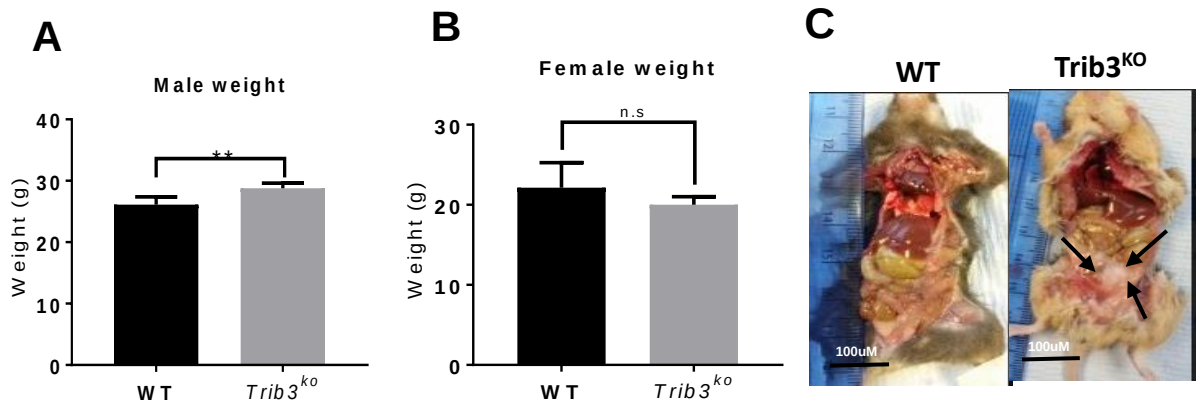

Figure 3.1: Male Trib3^{ko} lead to male obesity with an increase in subcutaneous fat.

(A) Male Trib3^{ko} mice have an increased body weight at 13 weeks of age, compared with WT littermates however **(B)** female Trib3^{ko} mice did not show any significant difference in weight, compared with WT littermates. **(C)** Representative images of male Trib3^{ko} and WT littermates mice. Results are presented as Mean ± SEM N=5-8. Unpaired T-test. P value: (*$p \leq 0.05$. **$p \leq 0.01$. ***$p \leq 0.001$. ****$p \leq 0.0001$, N.S. = Not significant)

3.4.3 Male Trib3^{ko} leads to an increase in abdominal fat as detected by MRI

To characterise the fat composition of Trib3^{ko} and WT littermates further, MRI scans were taken for both Trib3^{ko} and WT littermates. **Figure 3.2A, B** show an increase in fat volume for the Trib3^{ko} male mice and the area under the curve shows a statistically significant increase compared with the WT littermates. Interestingly, the females show an opposite change (**Figure 3.2D, E**), with a reduction in fat volume and area under the curve, suggesting the female are becoming leaner. **Figure 3.2C, F** shows representative MRI images from the male Trib3^{ko} and WT littermates, showing you an increase in fat depot around the abdominal region for the Trib3^{ko} **Figure 3.2G** shows the overall fat ratio for the male Trib3^{ko} compared with the WT littermates. The hipline was used as the reference point. It can be seen MRI slices between 28–35 show an statistical significant increase in fat volume for the male Trib3^{ko} compared with WT littermates.

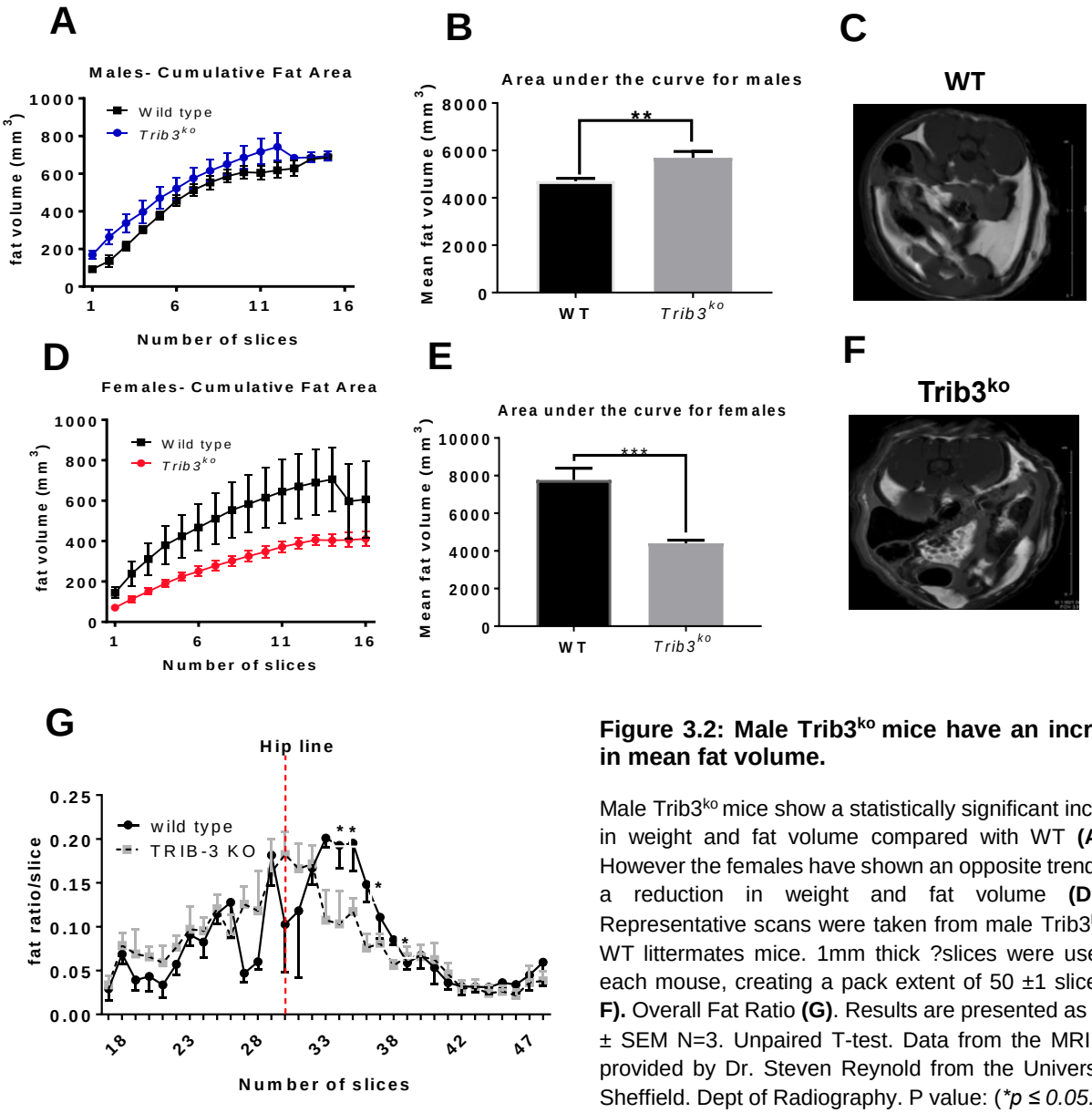

Figure 3.2: Male Trib3^{ko} mice have an increase in mean fat volume.

Male Trib3^{ko} mice show a statistically significant increase in weight and fat volume compared with WT **(A, B)**. However the females have shown an opposite trend, with a reduction in weight and fat volume **(D, E)**. Representative scans were taken from male Trib3^{ko} and WT littermates mice. 1mm thick ?slices were used for each mouse, creating a pack extent of 50 ±1 slices **(C, F).** Overall Fat Ratio **(G)**. Results are presented as Mean ± SEM N=3. Unpaired T-test. Data from the MRI were provided by Dr. Steven Reynold from the University of Sheffield. Dept of Radiography. P value: (**p ≤ 0.05. **p ≤ 0.01. ***p ≤ 0.001. ****p ≤ 0.0001, N.S= Not significant)*

3.4.4 Male Trib3^{ko} mice alter plasma cholesterol homeostasis

Having observed that male Trib3^{ko} mice become obese, further characterisation the plasma lipid profile of the mice were carried out. **Figure 3.3A, B** shows a statistically significant increase in total cholesterol levels, with an increase in HDL levels in the Trib3^{ko} compared with WT littermates. However, there was no difference in triglyceride levels as shown in **Figure 3.3C**. In collaboration with Prof. Ronald Krauss (Berkeley), the fractions of HDL were further looked at, and no difference was observed between the fractions of HDL between Trib3^{ko} compared with WT littermates (**Figure 3.3D**). Next, the LDL fractions were characterised, and **Figure 3.3E** shows Trib3^{ko} to have a reduction in VLDL. However, there was an increase in lgVLDL. Different fractions of LDL interact differently with the extracellular matrix. Small, dense LDL particles are more likely to bind to proteoglycans than large LDL particles. There is an increased risk of heart disease with elevated levels of LDL particles shown in prospective epidemiologic studies (Maranhao et al., 2014).

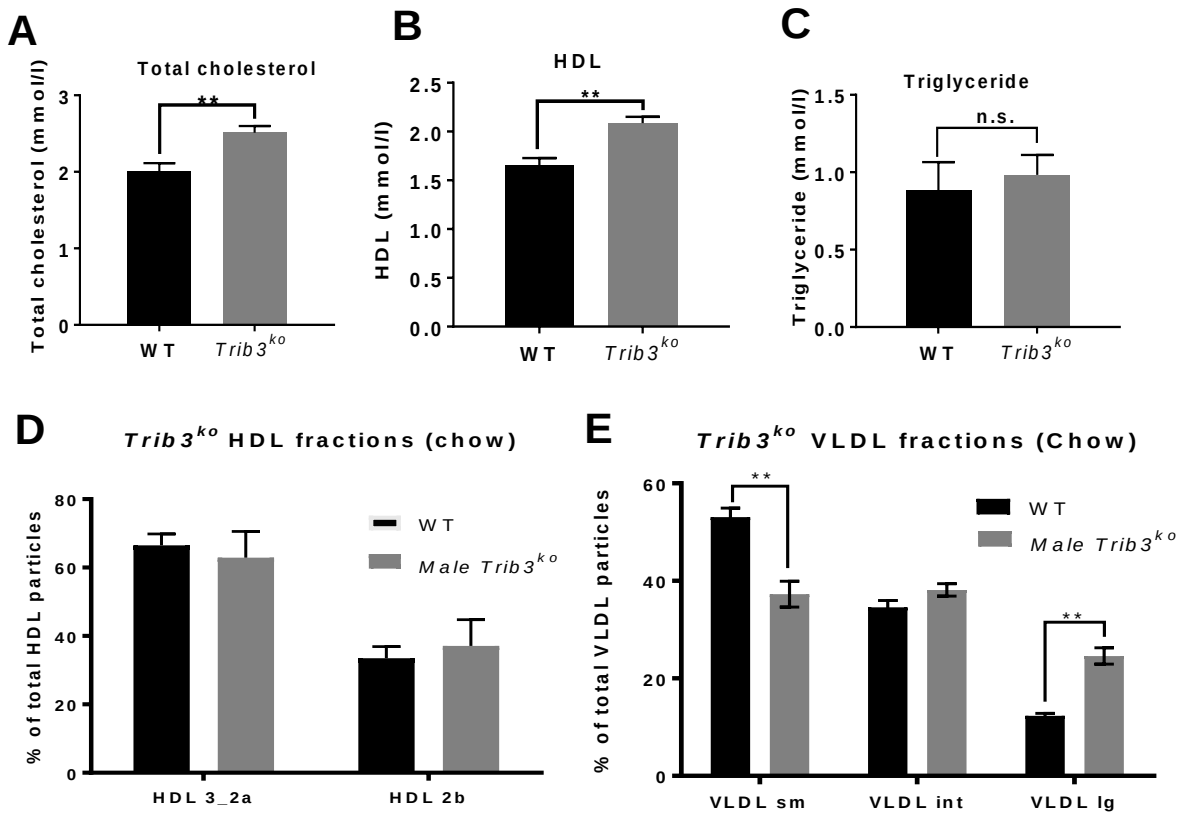

Figure 3.3: Male Trib3^{ko} mice alters plasma cholesterol homeostasis

Blood was isolated from male Trib3^{ko} and WT mice at 13 weeks age and the lipid profile were measured by ion mobility analysis. (**A**) There is an increase in total cholesterol levels and an increase in **(B)** HDL plasma levels of the male Trib3^{ko} compared with WT littermates. **(C)** There was no significant difference in the plasma triglyceride levels between male Trib3^{ko} compared with WT littermates. **(E)** There was no significant difference in HDL Fractions. **(F)** Upon VLDL fractions, you can see a statistical reduction in smVLDL and an increase in lgVLDL. Results are presented as Mean ± SEM N=5-8. Unpaired T-test. P value: (**p ≤ 0.05. **p ≤ 0.01. ***p ≤ 0.001. ****p ≤ 0.0001, N.S= Not significant).* The above data were provided by Dr. Jihan-al Ghamdi, a previous PhD student in Endre-Kiss-Toths lab.

3.5 Male Trib3^{ko} has an altered physiology

After establishing that full body Trib3 deficiency alters plasma lipid and adipose homeostasis, leading to obesity in male animals, the metabolic activity of male Trib3^{ko} vs. WT littermates were characterised, in collaboration with the animal facility at Nanyang Technological University in Singapore. The mice were 38 weeks old and fed on a standard chow diet. The mice were kept habituated three full days in the calorimetric cages in the testing room before being kept inside the climate chamber for seven days at a constant temperature of 22 °C and humidity of 45%. The light cycle was between 7 am and 7 pm. The calorimetric chamber measured oxygen consumption and carbon dioxide production. Recording began from the first entry in the chamber and measures were considered only from the third day in the chamber, which made a habituation phase of a total of 6 days. All measurements were taken every 15 min and hourly averages are presented.

3.5.1 Male Trib3^{ko} mice have a reduced exchange respiratory ratio

Male Trib3^{ko} require a higher level of oxygen consumption (**Figure 3.4A**), during the dark phase with a reduced amount of CO_2 produced (**Figure 3.4B**). This is reflected in the **Figure 3.4C, D.** The RER, which is the ratio between CO_2 and O_2 showed a reading between 0.7 and 0.8 for the male Trib3^{ko} mice (**Figure 3.4E**). The RER ratio can be used for estimating the respiratory quotient (RQ), which is an indicator for measuring which fuel type is being oxidised (carbohydrate or fat) to supply energy to the body. In brief, a RER value of 0.7 indicates that fat is the predominant fuel source, a RER of 0.85 suggests a mix of fat and carbohydrates, and a value of 1.00 or above is indicative of carbohydrate being the predominant fuel source. It seems that Trib3^{ko} use fat as the predominant fuel source to supply energy to the body. This will be discussed more at the end of the chapter.

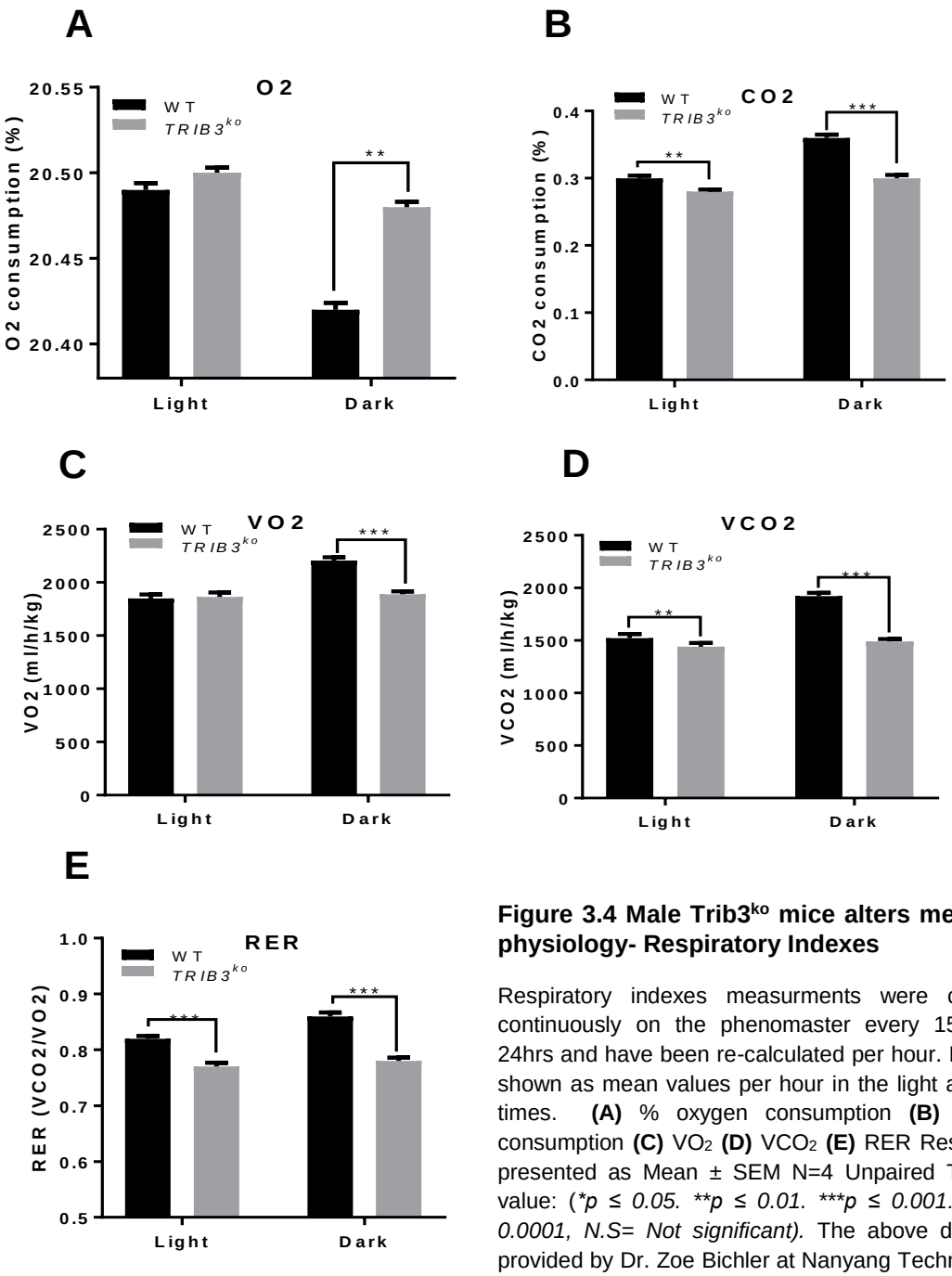

Figure 3.4 Male Trib3^{ko} mice alters metabolic physiology- Respiratory Indexes

Respiratory indexes measurments were collected continuously on the phenomaster every 15min for 24hrs and have been re-calculated per hour. Data are shown as mean values per hour in the light and dark times. **(A)** % oxygen consumption **(B)** % CO_2 consumption **(C)** VO_2 **(D)** VCO_2 **(E)** RER Results are presented as Mean ± SEM N=4 Unpaired T-test. P value: (**p ≤ 0.05. **p ≤ 0.01. ***p ≤ 0.001. ****p ≤ 0.0001, N.S= Not significant).* The above data was provided by Dr. Zoe Bichler at Nanyang Technological University.

3.5.2 Male Trib3^{ko} mice require less energy than WT littermates

(Figure 3.5A) shows in the dark phase, male Trib3^{ko} mice show reduced movement compared with WT littermates. There is no difference during the light phase. The male Trib3^{ko} mice use less energy than WT littermates (**Figure 3.5B**). The daily energy expenditure is expressed in kcal/h/kg , it is the average individual heat production over 24 h. The baseline of male Trib3^{ko} is the same as WT littermates, at least from the beginning of the experiment (**Figure 3.6**). Interestingly, daily energy expenditure (DEE) decreases with time in Trib3^{ko} mice, but not in WT. **Figure 3.5C, D** shows that Trib3^{ko} mice have a reduced food and drink intake compared with WT littermates.

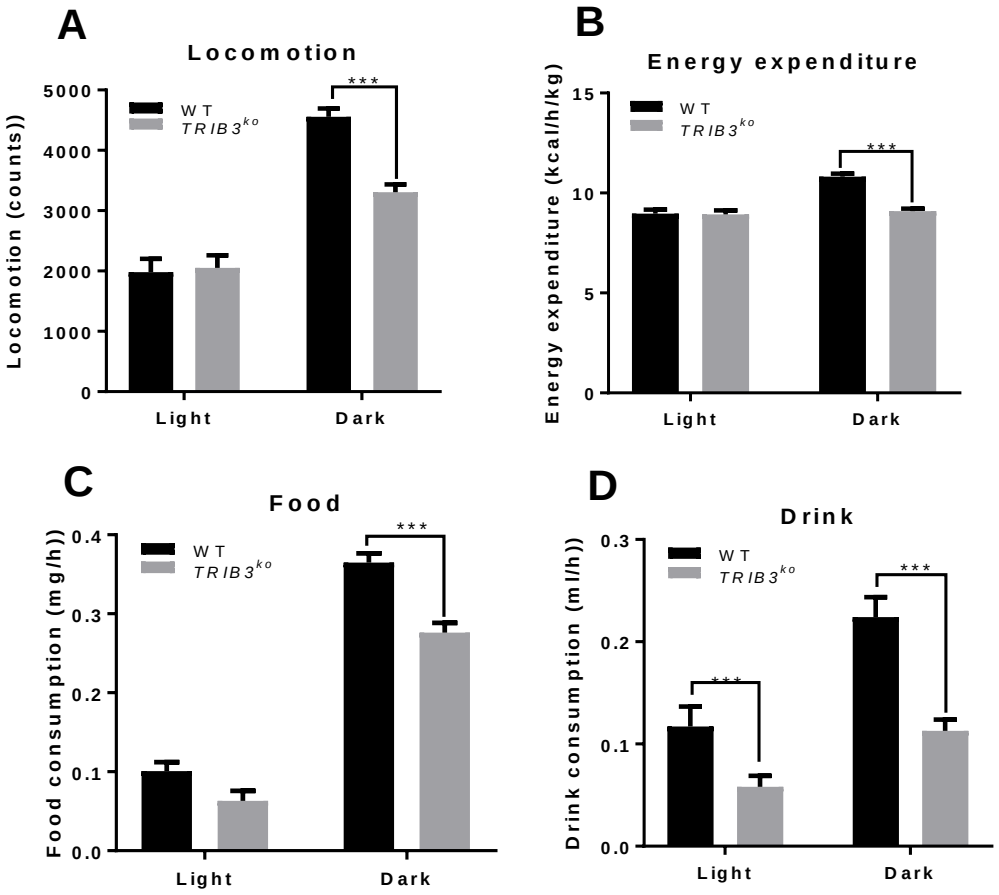

Figure 3.5: male Trib3^{ko} mice alters metabolic physiology- Energy homeostasis.

Phenomaster measurements were collected continuously every 15 min for 24hrs and have been re-calculated per hour. Data are shown mean values per hour. **(A)** Locomotor activity (counts) (**B)** Energy expenditure consumption **(C)** Food consumption **(D)** Drink consumption. Results are presented as Mean ± SEM N=4. P value: (**p ≤ 0.05. **p ≤ 0.01. ***p ≤ 0.001. ****p ≤ 0.0001, N.S= Not significant)* Unpaired T-test. The above data was provided by Dr. Zoe Bichler at Nanyang Technological University.

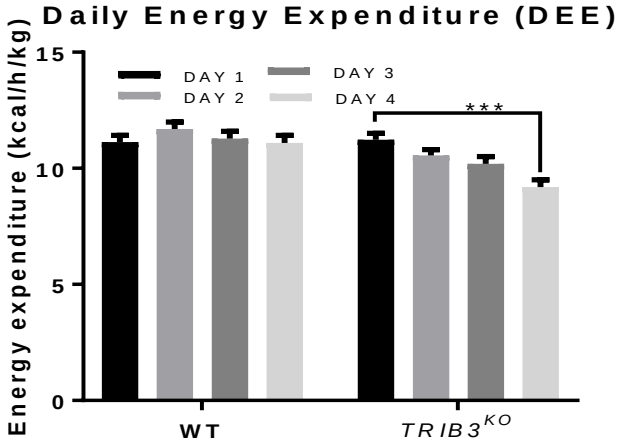

Figure 3.6: Male Trib3^{ko} mice alters metabolic physiology- Daily energy expenditure.

Phenomaster measurement were collected continuously every 15 min for 24hrs and have been re-calculated per hour. Data are shown mean values per hour. Data are shown mean values per hour. **(A)** Energy expenditure consumption per day. Results are presented as Mean ± SEM N=4 ONE WAY ANOVE. P value: (**p ≤ 0.05. **p ≤ 0.01. ***p ≤ 0.001. ****p ≤ 0.0001, N.S= Not significant).* The above data was provided by Dr. Zoe Bichler at Nanyang Technological University.

3.6 Altered plasma glucose homeostasis

Next, Jihan Al Ghamdi conducted a GTT and an ITT on Trib3^{ko} compared to WT littermates. Trib3 deficient mice on a chow diet have been shown to have impaired glucose transport. From **Figure 3.7A**, it can be seen that the GTT had shown male Trib3^{ko} mice to be able to release glucose at a much faster rate than WT littermates. **Figure 3.7B** Upon ITT, it was revealed that the uptake of glucose is normal and there is an impairment in the release of glucose. Furthermore, **Figure 3.7C** there was no difference in the fasting glucose between male Trib3^{ko} mice vs. WT littermates

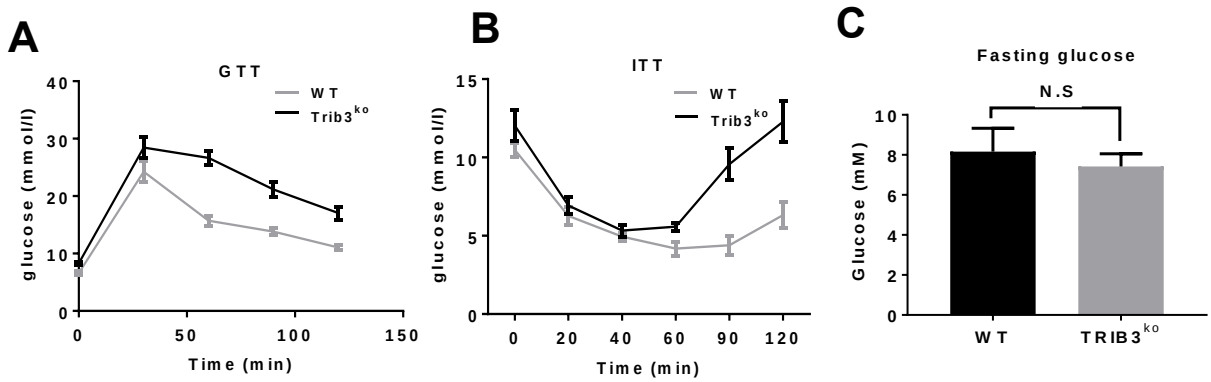

Figure 3.7 Altered plasma glucose homeostasis.

10 ul/g BW (20% D-glucose was injected in mice and blood levels were measured in 30 min intervals. **(A)** Insulin was injected and blood glucose levels were measured. Trib3^{KO} mice shown impaired recovery of plasma glucose levels **(B).** Trib3^{KO} did not show any significant difference on fasting glucose levels, compared with wild type littermates. Unpaired T-test (**p ≤ 0.05. **p ≤ 0.01. ***p ≤ 0.001. ****p ≤ 0.0001, N.S= Not significant)*

The work in this chapter characterises a full body Trib3^{ko} in males and females at 13 weeks of age and defines a new role for TRIB3 in male mice. It can be concluded from these data that TRIB3 is a critical protein that contributes towards obesity and metabolic dysfunction. The observations made here provide a firm association with TRIB3 and altered energy homeostasis.

3.7 Summary

- Male Trib3^{ko} leads to an obese phenotype. However, female Trib3^{ko} do not show any significant weight gain.
- There is an increase in cumulative fat volume for the male Trib3^{ko} mice compared with WT littermates. However, the females become leaner.
- Male Trib3^{ko} mice show an increase in abdominal subcutaneous fat compared with WT littermates.
- There is an altered plasma cholesterol profile for the Trib3^{ko} male mice. Increase in HDL, no difference in HDL fractions, no difference in triglyceride content, but we see an increase in smVLDL and lgLDL fractions.
- Male Trib3^{ko} are significantly less active in the dark phase: they eat and drink significantly less than the WT littermates. Male Trib3^{ko} have an RER that is decreased night and day as compared with WT littermates. However, male Trib3^{ko} have a higher per cent oxygen consumption during the dark phase compared with WT littermates.
- Male Trib3^{ko} mice also have a reduced food and drink intake compared with WT littermates.
- The baseline for the DEE of Trib3^{ko} male is the same as the WT. Interestingly, DEE decreases with time for the male Trib3^{ko} mice, but not in the WT littermates.

3.8 Discussion

Although many models have been used to assess the role of Trib3 in different tissues, the lipid profile and metabolic profile of the Trib3 knockout mice remains mostly unexplored. There have been some studies that have used tissue-specific Trib3^{ko} mouse models and depending on the studies have reported different phenotypes. It was reported that an adipose tissue-specific overexpression of Trib3 reduced WAT, slowed weight gain with a concurrent increase in dietary intake (Qi et al., 2006). This study highlights the importance of Trib3 in the differentiation of adipocytes. Furthermore, it was shown that Trib3 overexpression in 3T3-L1 preadipocytes blocks adipogenesis by degradation of CEBPβ and PPARγ (Bezy et al., 2007). Trib3 acts as a negative regulator of adipocytes differentiation and can also control lipid accumulation in mature adipocytes. Additionally, Takashashi and colleague have shown that Trib3 is also able to control the transcriptional activity of PPARγ and therefore suppress adipocytes differentiation (Takahashi et al., 2008). In contrast, studies by Weismann and colleagues have shown a knockdown of Trib3 with antisense oligonucleotides in the liver had shown an increase in the mass of WAT by 70% and enhanced expression of PPARγ (Weismann et al., 2011). This has therefore raised questions on Trib3 phenotype and alternative mechanisms. From this study, It can be seen male Trib3^{ko} mice have an increase subcutaneous tissue compared with WT littermates. Furthermore, MRI scans

show male Trib3^{ko} have a higher fat volume compared with females. All the above evidence indicates that Trib3 is an essential regulator in contributing to lipid metabolism and obesity. Human genetic studies have also shown a genetic Q84R polymorphism of TRIB3 to be associated with insulin resistance**,** hyperlipidaemia and increase in the risk of developing diabetes which are all risk factors contributing towards CVD (Prudente et al., 2005).

Obesity is a systemic disease that involves dysregulated communication amongst different organs, contributing to the development of many metabolic processes, so a full body Trib3^{ko} mouse model was generated to analyse Trib3 function in different organs simultaneously and our knockout studies show an elevated body weight for the Trib3^{ko} compared with WT littermates at 13 weeks of age. The difference in male and female weights is an interesting observation and can be explained by a number of mechanisms, including hormonal influences. Unpublished studies from our lab have shown there is a platelet defect in the female Trib3 knockout mice compared with the males. Furthermore, it was identified by our group that the Trib1 promoter site has a putative androgen binding site, which in turn affects testosterone production. However, whether testosterone or oestrogen has an impact on Trib3 levels and the mechanism as to how it occurs is still unknown.

Upon dissection, it can be observed that the male Trib3^{ko} mice have an increase in subcutaneous adipose tissue compared with the WT. MRI scans show an increase in body fat volume for the male Trib3^{ko} mice over WT littermates. The female Trib3^{ko} mice, in contrast, become leaner. The anatomical fat position was shown to be around the abdominal region of the male Trib3^{ko} mice. The increased weight in the Trib3^{ko} mice could be due to an increase in the volume of adipose tissue alongside the liver. The muscle is also a dense organ, so it would be interesting to look at the morphology of the different metabolic organs including triglyceride levels. A study has reported that Trib3 is a negative regulator in insulin and its effect is mediated via Akt phosphorylation. Furthermore, overexpression of Trib3 in HepG2 cells inhibits Akt activation and therefore affects insulin signalling pathway (Du et al., 2003). The increase in sensitivity to insulin would lead to an increase in adipogenesis as excess glucose is converted into fatty acids, in a process known as lipogenesis (Avramoglu et al., 2006). In **Chapter 4**, a microarray will be conducted for the different metabolic organs to identify the dysregulated genes that contribute to obesity in the male Trib3^{ko} mice.

Having observed obese male Trib3^{ko} mice with an increase in fat volume compared with the females, the lipid profile of these mice was of interest. Interestingly, male Trib3^{ko} have been seen to show elevated levels of plasma cholesterol with an increase in HDL levels. However, no difference in triglyceride levels were detected. Having an altered lipid profile suggests the mishandling of lipids. Mice and rats are naturally deficient in CETP activity, although the reason behind the deficiency in activity is still unknown. The enzyme CETP is responsible for moving cholesterol esters and transfer of triglycerides between different fractions of lipoproteins. Low levels of CETP are associated with a decreased risk of atherosclerosis because it promotes HDL and the reverse cholesterol pathway. The mouse genome databases has shown sequences could not code for a functional CETP (Hogarth et al., 2003).

To understand further the dynamics and physiology of the male Trib3^{ko} compared with WT littermates, a metabolic cage experiment was provided to us by our collaborators. It measured the respiratory indexes, including sleeping, motion and energy expenditure of the mice. The male Trib3^{ko} mice have a precise circadian rhythm similar to the WT littermates. The male Trib3^{ko} mice eat and drink significantly less than the WT littermates and are much less active, with a decreased RER. When the respiratory function is reduced, the Trib3^{ko} mice need to use more oxygen and produce more carbon dioxide, for an activity that decreased overall as compared with the WT littermates hence an increase in oxygen levels for the male Trib3^{ko} mice can be observed. Furthermore, the male Trib3^{ko} mouse have a lower RER corresponding to a predominance of fat metabolism versus carbohydrates or mixed use of a source of energy. The Trib3^{ko} seem to lack switching their metabolic strategy from fat to carbohydrate depending on the circadian rhythm and their overall activity level. The male Trib3^{ko} are using more energy than the WT littermates. Having a reduced movement, with reduced food intake and using more energy could suggest that the male Trib3^{ko} mice are using the energy from the stored fats or glucose (Nisoli et al., 2007).

From the respiratory indexes, the value of the RER stands between 0.7 and 1, which is reflecting a healthy standard exchange ratio. However, the male Trib3^{ko} are closer to the lower values (0.75), which suggest that the male Trib3^{ko} mice have an increase in fat metabolism compared with the WT littermates, and fat is their predominant source of fuel, as opposed to WT mice, which use predominantly carbohydrates (when RER is closer to 1, mainly during the dark/active phase) or a mix of both (in lower RER values of about 0.8, mainly during the light/less active phase). Interestingly, the male Trib3^{ko} do not seem to change their metabolism according to the circadian cycle; they always use the same source of fuel, independent of their activity. Accordingly, they also do not consume more food or water during the active phase as compared with WT littermates, and their consumption is not cyclic even though they are still more active in the dark phase.

Furthermore, some studies have shown the temperatures in mice to be between 27 °C and 30 °C, which makes the temperature chosen for this experiment (22 °C) dramatically below the standards. It is possible that the male Trib3^{ko} mice are sensitive to thermal stress and hence utilise the energy more than the WT littermates. Alternatively, it has been reported that genetically modified mice develop more weight at warmer temperatures but not at colder temperatures (Feldmann et al., 2009).

In summary, the male Trib3^{ko} have a lower RER corresponding to a predominance in fat metabolism versus carbohydrates or mixed use of a source of fuel. Male Trib3^{ko} seem to lack switching their metabolic strategy from fat to carbohydrate depending on the circadian phenomena, which is not seen in humans (a low RER at rest may predict a high peak fat oxidation during exercise and a healthy metabolic phenotype in moderately overweight people (Rosenkilde et al., 2010). Although the data are interesting, they cannot be used to explain the obesity observed in the male Trib3^{ko} mice because of the difference in age. The male Trib3^{ko} mice and WT littermates were studied at 38 weeks of age. The male Trib3^{ko} mice become obese by 13 weeks of age. As altered physiology can be seen at 38 weeks of age, a future experiment could be to conduct a metabolic cage experiment for the male Trib3^{ko} mice at 13 weeks of age and compare metabolic activity between different age groups.

Finally, a GTT and ITT were carried out to see if the male Trib3^{ko} mice become glucose tolerant and insulin resistance. It can be seen that the male Trib3^{ko} mice are able to release glucose at a much faster rate than WT littermates, suggesting glucose tolerance. Upon ITT, it was revealed that the uptake of glucose is normal and there is an impairment in the release of glucose. Furthermore, there was no difference in the fasting glucose between male Trib3^{ko} mice vs. WT littermates.

Chapter 4–Results

Male-specific Trib3 deficiency leads to key metabolic changes in the liver, adipose and skeletal muscle

4.1 Introduction

In **Chapter 3**, it was shown that male Trib3^{ko} mice have an increased body weight compared with WT littermates at 13 weeks of age. In contrast, the females did not show any statistical difference in weight or fat volume. Chapter4, will investigate the molecular mechanisms that contribute towards male Trib3^{ko} obesity by conducting transcriptome analyses of various organs with a focus on key metabolic changes and validate those using standard molecular biology techniques.

From previous literature, TRIB3 was shown to be an essential regulator of adipocyte differentiation (Takahashi et al., 2008), lipid metabolism (Qi et al., 2006) and insulin signalling (Du et al., 2003). However, our insight into the molecular roles of TRIB3 in various insulin-sensitive organs remains limited. A study in skeletal muscle supports the notion that TRIB3 is important in insulin signalling (Liu et al., 2008). TRIB3 is upregulated in the skeletal muscle of patients with Type II diabetes. Overexpression of Trib3 in the muscle cells blocks insulin-stimulated glucose transport and impair phosphorylation of Akt, including ERK, and insulin receptor substrate-1 (IRS1) (Liu et al., 2008). Trib3 expression in the pancreas is also upregulated in (db/db) diabetic insulin resistance mice (Matsushima et al., 2006). Overexpression of Trib3 in the non-diabetic (control) mice resulted in hyperglycaemia, glucose intolerance and insulin resistance, similar to what was seen in the (db/db) diabetic insulin resistance mice (Matsushima et al., 2006). All of the evidence so far suggests Trib3 overexpression impairs insulin signalling, thus one would hope that reducing Trib3 levels may be beneficial to insulin sensitivity. A study by Okamoto and colleagues performed a genetic deletion of hepatic Trib3 and measured Akt and downstream signalling pathway in the liver which did not change (Okamoto et al., 2007), suggesting possible alternative mechanisms for Trib3 action.

Additionally, it was reported that Trib3 overexpression in 3T3-L1 preadipocytes blocks adipogenesis by degradation of CEBPβ and PPARγ. Trib3 acts as a negative regulator of differentiation of adipocytes but can also control lipid accumulation in mature adipocytes (Bezy et al., 2007). Furthermore, it was shown Trib3 is also able to directly control the transcriptional activity of PPARγ and therefore suppress adipocyte differentiation (Takahashi et al., 2008). In the contrary, a study by Weismann and colleagues have shown that Trib3^{ko} in rats increased body weight, PPARγ activity and improved insulin sensitivity, with no notable changes in Akt activity (Weismann et al., 2011). Trib3 was also shown to induce inactivation of Acetyl CoA, a key enzyme responsible for fatty acid synthesis via recruiting ubiquitin E3 ligases and promote its ubiquitin-proteasomal degradation. This was shown in transgenic mice expressing TRIB3 in adipose tissue (Qi et al., 2006).

Furthermore, overexpression of Trib3 in the liver completely blocks insulin action through inhibition of Akt phosphorylation, suggesting Trib3 promotes glucose output from the liver under fasting conditions

and that its abnormal expression may contribute to insulin resistance and thereby promote hyperglycaemia. Further, liver-specific overexpression of Trib3 resulted in hyperglycaemia. Conversely, liver-specific Trib3^{ko} leads to improved insulin sensitivity and glucose tolerance (Du et al., 2003).

A study has reported that Trib3 is upregulated in fatty liver dystrophy (fld) mutant mouse which suffers from hypertriglyceridemia and fatty liver in young mice and impaired nerve function in adult mice (Klingenspor et al., 1999). Another study has shown a knockdown of PGC1, a PPARc co-activator, in the liver induced fasting hypoglycaemia and decreased expression of Trib3 (Koo et al., 2004). From the literature, Trib3 seems to be involved in gluconeogenesis in the liver. However, the exact mechanism is still unclear.

In this chapter, a full body Trib3^{ko} mouse will be used to use a systematic approach to decipher a mechanistic role for Trib3 in metabolic dysfunction in primary metabolic tissues; liver, subcutaneous adipose tissue and skeletal muscle tissue. Key Trib3 effectors involved in the dysregulation between the tissues and contributing to obesity will be identified. Furthermore, the anatomical position of the adipose tissue will be assessed and the morphology of the different metabolic tissues analysed.

4.2 Hypothesis

From the literature and Chapter 3, it is hypothesised that TRIB3 is involved in the interplay communication between the different metabolic organs which contribute towards an obese phenotype in a full body male Trib3^{ko} mouse model. In this chapter, the systemic consequences of a full body Trib3^{ko} mice and further identify key genes that may contribute towards the obesity observed in **Chapter 3.**

4.3 Aims

- Characterise tissue-specific consequences, i.e. assess the morphology of the metabolic tissues of the male Trib3^{ko} compared with WT littermates,
- Characterise Trib3 dependent, tissue-specific regulatory mechanisms of metabolic tissues in male Trib3^{ko} compared with WT littermates by microarray and validate key findings using standard molecular biology techniques.

4.4 Microarray for metabolic tissues; Liver, subcutaneous adipose tissue and skeletal muscle

Liver, subcutaneous adipose tissue and skeletal muscle were chosen as primary metabolic tissues which are involved in regulating glucose and lipid metabolism. The chosen metabolic tissues are predicted to be dysregulated in male Trib3^{ko} mice and contribute towards obesity (Cornier et al., 2008).

4.4.1 Quality control for 13-weeks male Trib3^{ko} and WT mice; liver tissue

Liver tissue was homogenised and RNA was extracted and sent to Denova Limited for the microarray analysis. Mouse Transcriptome Array 1.0 (FS450_0001) Agilent chip was used. Four male Trib3^{ko} and 3 WT littermates liver tissue was sequenced. Microarray data were analysed using Partek and Ingenuity Pathway Analysis (IPA) software packages. **Figure 4.1A** shows hierarchical clustering, assigning genes from the microarray into groups between the different samples. **Figure 4.1B** shows principal component analysis (PCA), which shows the variability between different samples. From **Figure 4.1B**, male Trib3^{ko} mice and WT littermate samples were shown to be close together. Furthermore, Liver tissues taken from the male Trib3^{ko} and WT littermates were analysed to confirm Trib3 mRNA expression levels. Trib3^{ko} has shown to have a statistically significant reduction for Trib3 compared with WT littermates shown in **Appendix VII.** 23,435 genes were dysregulated and 2342 genes were created using the Partek software; with a P-value of <0.05 and a fold difference of >2, <–2.

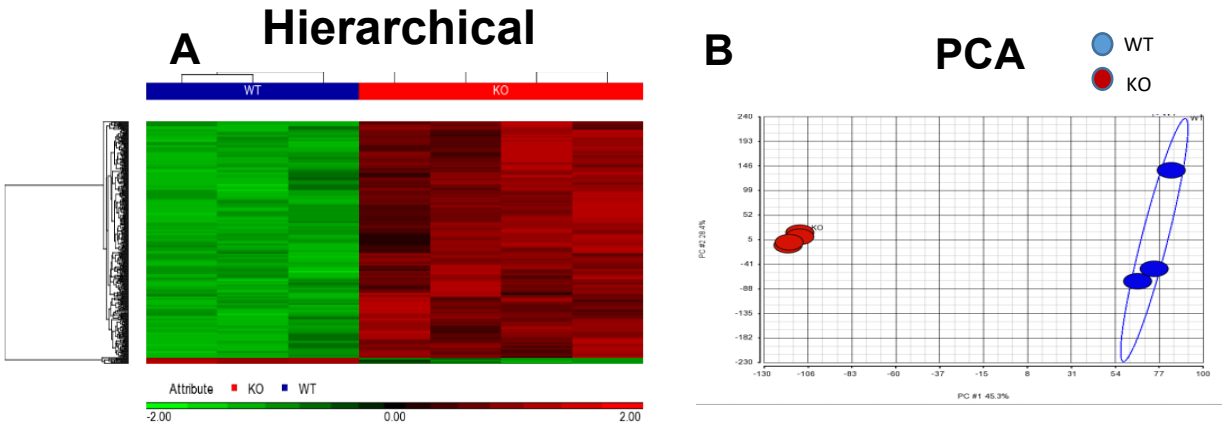

Figure 4.1: Quality control for 13 weeks male Trib3^{ko} and WT mice; liver tissue.

(A) Shows hierarchical clustering, to assign the genes from the microarray into groups between the different samples. **(B)** Principle component analysis (PCA) is used to determine the variability between different data sets. Results are presented as Mean ± SD N=3-4 (**p ≤ 0.05. **p ≤ 0.01. ***p ≤ 0.001. ****p ≤ 0.0001, N.S= Not significant).*

4.4.2 Gene ontology for the liver

IPA software was used to create gene ontology and pathway analysis for the gene lists created in Partek. **Table 4.1A** shows 56 genes were associated with the CVD pathway with a P-value of 4.91×10^{-2}. **Table 4.1B** shows the genes highlighted for the molecular and cellular function. Significant genes were selected based on pathways.

A

Disease and disorder	Number of genes	P-Value
Cancer	182	4.73×10^{-02} - 1.11×10^{-13}
Organismal injury and abnormalities	278	4.93×10^{-02} - 1.11×10^{-13}
Tumour morphology	59	4.93×10^{-02} - 1.11×10^{-13}
Cardiovascular disease	56	4.91×10^{-02} - 1.267×10^{-04}
Haematological disease	48	4.93×10^{-02} - 1.26×10^{-03}

B

Molecular and cellular function	Number of genes	P-Value
cell death and survival	32	3.17×10^{-08}-2.17×10^{-29}
Cell morphology	45	3.53×10^{-09}-7.601×10^{-24}
Gene expression	41	1.95×10^{-09}- 7.01×10^{-24}
Cellular function and maintenance	39	2.98×10^{-08}- 7.71×10^{-18}
Cellular development	78	4.46×10^{-02}-6.1×10^{-11}

Table 4.4: Gene ontology for liver

(A) For the disease and disorder, 56 genes were associated with cardiovascular disease with a P value of 4.91×10^{-2} **(B)** shows the number of genes involved in the molecular and cellular function (*$p \leq 0.05$. **$p \leq 0.01$. ***$p \leq 0.001$. ****$p \leq 0.0001$, N.S= Not significant).

4.4.3 Validation of microarray genes

Selected genes involved in the cardiovascular pathway were used to create a network analysis. **Figure 4.2A** shows a heat map of the list of genes from the cardiovascular pathway. **Figure 4.2B** shows the microarray genes validated by qRT-PCR and **Figure 4.2C** western blots. A reduction in CEBPα protein levels was observed; a gene which has been previously reported to be involved in the proliferation and lipogenesis of hepatic Trib1 (Bauer et al., 2015).

Of particular interest, reduced expression of PPARα was detected, an important lipid sensor gene, in the male Trib3^{ko} liver tissue compared with its WT littermates. PPARα is involved in fatty acid metabolism pathways and is involved in mitochondrial β-oxidation of the liver and regulation have shown to impact plasma lipoprotein metabolism during nutritional deficit, and inflammatory response (Takahashi and Sakai, 2006, Seedorf and Assmann, 2001, Kaplan et al., 2001). Furthermore, there is a decrease in ANGPT8, an important glyco-protein involved in the lipid metabolism pathway. ANGPT8 have shown to be associated with liver steatosis and ANGP4, an isoform of ANGPT8 have shown to be involved in the breakdown of fatty acids in the liver (Wang et al., 2017, Kadomatsu et al., 2011).

Furthermore, a reduction in ApoE, which is a key component of lipoprotein particles, suggested a decrease in cholesterol transport of LDL cholesterol leading to an influx of cholesterol and its build up in the liver. ApoE is produced in the liver and is an important gene involved in cholesterol metabolism pathway. APOC was decreased, which another important protein is found in triglyceride-rich lipoproteins. LDLR was also shown to increase, which is an important receptor in the uptake of LDL involved in transporting fatty acids to the peripheral tissues and back to the liver (Au et al., 2017). This suggests, Trib3 is able to uptake an increase levels of cholesterol but unable to break it down, building up in the liver.

Additionally, pAKT and GLUT2 expression was increased in male Trib3^{ko} suggesting an increase in glucose uptake in the male Trib3^{ko} mice. Both AKT and GLUT2 are part of the insulin signalling pathway. Insulin is secreted to the bloodstream in response to high glucose levels in the blood. This then triggers the uptake of glucose to the main metabolic organs, like the liver, adipose and skeletal muscle to promote storage. This suggests, a dysregulation in glucose homeostasis and Trib3 to be involved in the uptake of glucose.

Additionally, from the microarray, expression levels of the canonical inflammatory transcription factor, RelA nuclear factor kappa-light-chain-enhancer of activated B cells (p65 NF-κB) was also increased in the liver, suggesting hepatic inflammation. All the genes highlighted in the microarray of the liver suggest that male Trib3^{ko} is involved in fatty acid oxidation, lipogenesis and inflammation.

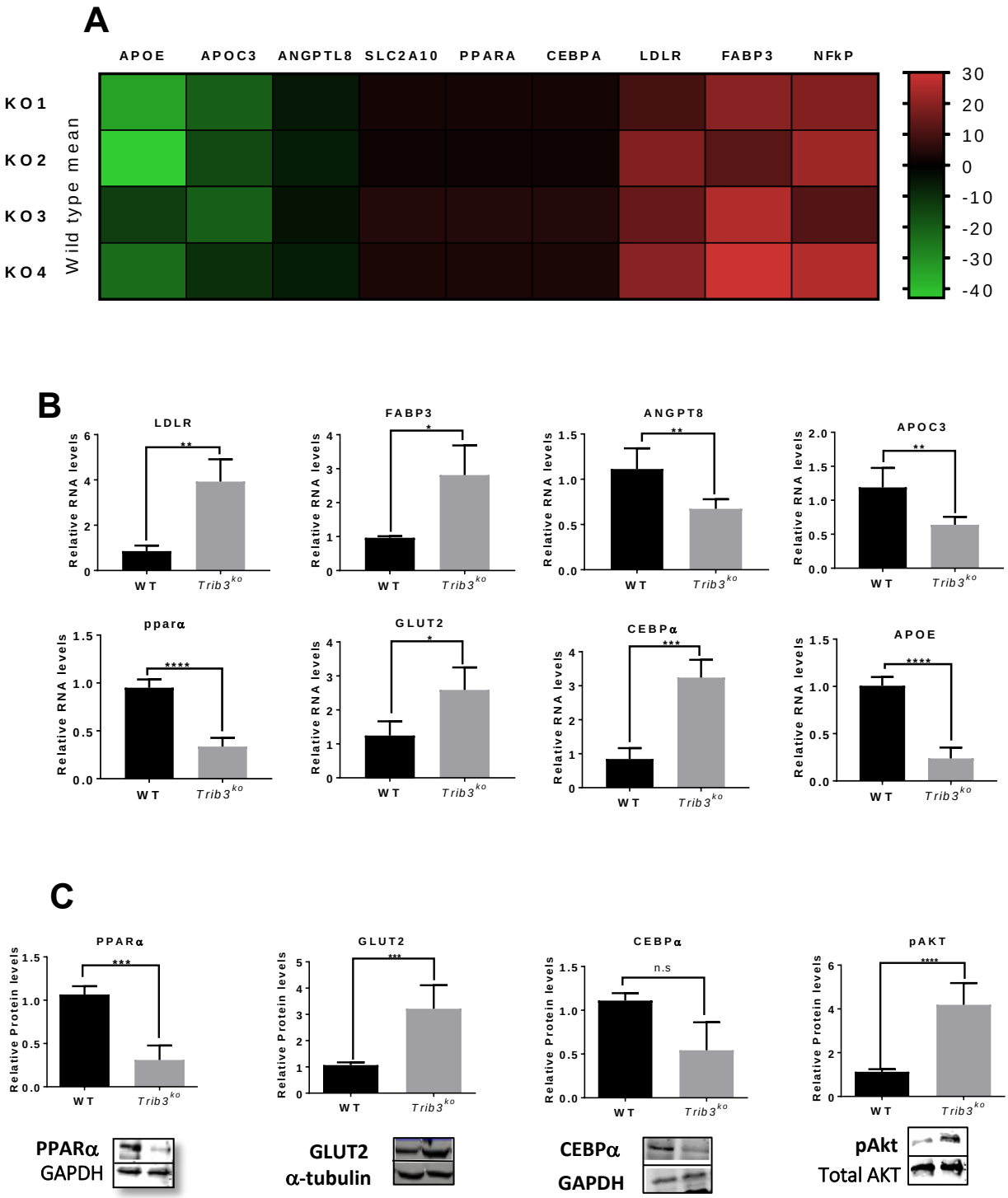

Figure 4.2: Validation of microarray genes- Liver.

Microarray analysis was performed on the liver male Trib3^{ko} mice vs WT littermates' mice. Partek and IPA software packages were used for bioinformatics analysis of the data. **(A)** Heatmap created with the highlighted genes; Green is downregulated, Red is upregulated. KO represents the Trib3^{ko} samples. **(B)** qPCR normalized against B-actin housekeeping gene and **(C)** Western blotting were performed and shown for genes that show a statistical significance. Further analysis using ImageJ densitometry were used. Results are presented as Mean ± SEM N=6-8. Unpaired T-test. P value (*$p \leq 0.05$. **$p \leq 0.01$. ***$p \leq 0.001$. ****$p \leq 0.0001$, N.S= Not significant).

4.4.4 Increase in lipid accumulation in the liver tissue

So far, from the microarray of the male Trib3^{ko} liver samples compared with the WT, there is a reduction in PPARα levels, an important gene involved in the oxidation of FFA. An increase in mRNA LDL mRNA, which has been shown to be important in FFA uptake. This suggests FFA are unable to be broken down with an increase in FFA uptake leading to accumulation of lipids in the liver. Thus, the lipid content of the liver needed to be characterised. Liver tissue were sectioned using cryo-sectioning, and Oil red O staining was performed for the male Trib3^{ko} samples compared with WT littermates. From **Figure 4.3A**,**B** it can be visibly seen that there is an increase in Oil red O staining in the male Trib3^{ko} samples compared with the WT littermates suggesting an increase in lipid content for the male Trib3^{ko} samples. A triglyceride detection kit was used quantify the FFA levels. **Figure 4.3C** shows a significant increase in triglyceride levels in the male Trib3^{ko} compared with WT littermates.

4.4.5 Increase in free fatty acid (FFA) uptake in the HepG2 cells

Having observed an increase in Ldlr mRNA in our microarray, it was important to confirm if there is an increased uptake of FFA in Trib3-deficient cells. HepG2 cells were incubated with FFA attached to a fluorescent probe to measure the amount of FFA uptake. Flow cytometry was used to quantify FFA uptake. **Figure 4.3D** shows an increase in FFA uptake in the Trib3 knockdown samples compared with controls, suggesting an increase in the uptake and build-up of lipids which in turn are not broken down. **Figure 4.3D** showing fluorescence peaks of the different conditions, alongside **Figure 4.3E** showing you a histogram of the mean fluorescence uptake of the different conditions.

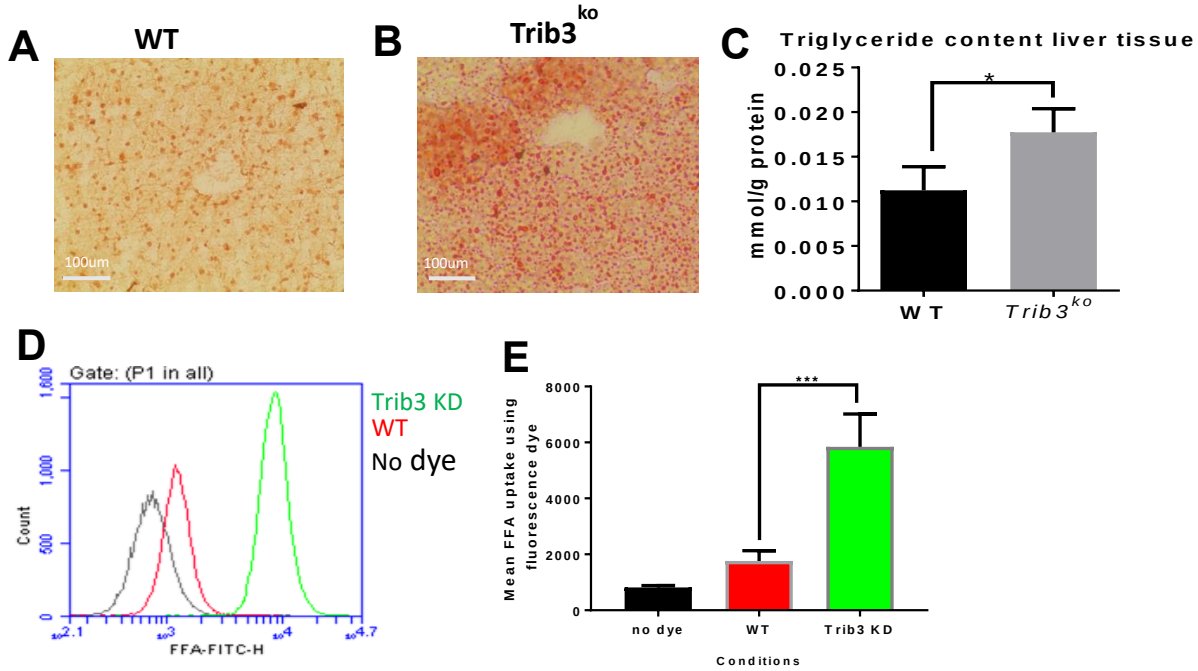

Figure 4.3: Increase in lipids accumulation in Trib3^{ko} mice compared with WT littermates, alongside increase in Free Fatty acid (FFA) uptake in the HepG2 cells.

(A, B) Oil-O stain (red/orange) was performed on cryo-sectioned liver samples and have shown an increase in oil droplets for the Trib3^{ko}mice compared with WT **(C**) Triglyceride was measured in the liver tissue using the Folsch lipid extraction method. There is an increase in triglyceride content in the male Trib3^{ko}compared with the WT mice of the liver tissue**. (D)** Flow cytometry was used to look at Fatty acid uptake in HepG2 cells. Trib3 knockdown compared with Vehicle control. Fluorescence showing an increase in fatty acid uptake in Trib3 knockdown cells alongside the **(E)** histogram. Results are presented as Mean ± SD N=4-6. (**p ≤ 0.05. **p ≤ 0.01. ***p ≤ 0.001. ****p ≤ 0.0001, N.S= Not significant)*

4.5 Quality control for 13 weeks male Trib3^{ko} and WT mice; Adipose tissue

Adipose tissue was homogenised, RNA was extracted and sent to Denova Limited for the microarray analysis. Mouse Transcriptome Array 1.0 (FS450_0001) Agilent chip was used. Four male Trib3^{ko} and three WT littermates was sequenced. Microarray data were analysed using Partek and IPA software packages. **Figure 4.4A** shows hierarchical clustering, assigning genes from the microarray into groups between the different samples. **Figure 4.4B** shows the PCA, which shows the variability between different samples. From **Figure 4.4B**, both male Trib3^{ko} and WT littermate's samples were shown to be close together. Furthermore, adipose tissues taken from the male Trib3^{ko} and WT littermates was analysed to confirm Trib3 mRNA expression levels. Trib3^{ko} has shown to have a statistically significant reduction for Trib3 mRNA compared with WT littermates shown in **Appendix VII**. 26,234 genes were dysregulated and 3276 genes were created using the Partek software; with a P-value of <0.05 and a fold difference of >2, <–2.

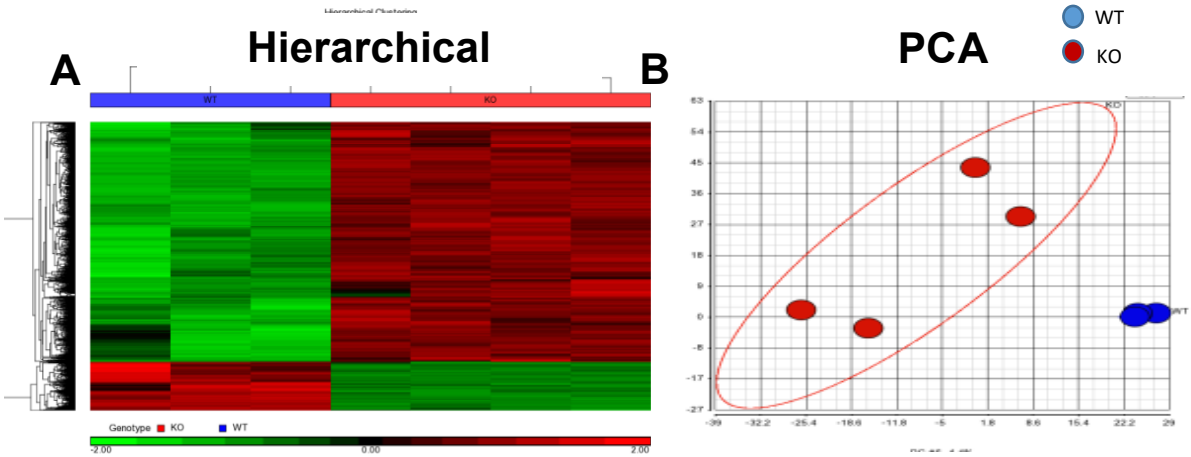

Figure 4.4: Quality control for 13 weeks male Trib3^{ko} and WT mice; Adipose tissue.

(A) Shows hierarchical clustering, to assign the genes from the microarray into groups between the different samples. **(B)** Principle component analysis (PCA) is used to determine the variability between different data sets. Results are presented as Mean ± SD N=3-4 (**p ≤ 0.05. **p ≤ 0.01. ***p ≤ 0.001. ****p ≤ 0.0001, N.S= Not significant).*

4.5.1 Gene ontology for adipose samples

IPA software was used to create gene ontology and pathway analysis for the gene list created in Partek for the adipose samples. **Table 4.2** shows 48 genes associated with the inflammatory response with a P-value of 1.62×10^{-2}. Lipid metabolisms genes were selected for the molecular and cellular functions highlighted. Significant genes were selected based on pathways.

A

Disease and disorder	Number of genes	P-Value
Tumour morphology	13	4.36×10^{-02} - 1.13×10^{-04}
hypersensitivity response	9	1.62×10^{-02} - 4.33×10^{-05}
Organismal injury and abnormalities	99	1.62×10^{-02} - 433×10^{-05}
Cancer	47	1.62×10^{-02} - 3.01×10^{-05}
Inflammatory response	48	1.62×10^{-02} - 1.81×10^{-05}

B

Molecular and cellular function	Number of genes	P-Value
protein synthesis	32	1.62×10^{-02}-2.96×10^{-05}
cell to cell signalling and interaction	45	1.62×10^{-02}-1.81×10^{-05}
small molecule biochemistry	41	1.62×10^{-02}-4.06×10^{-06}
lipid metabolism	39	1.62×10^{-02}-1.81×10^{-06}
cell death and survival	78	1.62×10^{-02}-1.02×10^{-07}

Table 4.5: Gene ontology for adipose

A) for the disease and disorder, 48 genes were associated with the inflammatory response with a P value of 1.62×10^{-2}. **(B)** For the molecular and cellular function, lipid metabolism and cell death and survival was the top hit (**p ≤ 0.05. **p ≤ 0.01. ***p ≤ 0.001. ****p ≤ 0.0001, N.S= Not significant).*

4.5.2 Validation of microarray genes

Genes involved in the inflammatory response pathway which have been shown to be the most significant were selected and a network analysis created. **Figure 4.5A** shows a heat map from the microarray for the samples. **Figure 4.5B** shows the selected microarray genes validated by qRT-PCR and **Figure 4.5C** western blots. Gene ontology analysis revealed an enrichment of differentially expressed genes involved in cellular proliferation, lipid metabolism and inflammation (**Table 4.3**).

Amongst the genes, it is confirmed the upregulation of proliferative and adipogenesis genes, such as PCNA and CEBPβ, respectively, at both the mRNA and protein levels. The nuclear receptor PPARγ is a master regulator of adipogenesis and has shown that the formation of WAT is dependent on the presence of PPARγ and CEBPα (Farmer et al., 2015). *In vitro* studies in 3t3-L1 cells have shown that Trib3 can block adipogenesis via inhibiting CEBPβ (Bezy et al., 2007), whose expression was also elevated in Trib3 knockout mice. Together with these observations, it is plausible to hypothesise that male Trib3^{ko} have an increased preadipocyte proliferation leading to an increase in adipogenesis.

Furthermore, the fatty acid-binding proteins (FABPs) which are a group of molecules that coordinate lipid responses in cells. These are known as the chaperones of the cell. FABPs have shown to facilitate the transport of lipids to different places of the cell, such as to the lipid droplet for storage. A study overexpressing fatty acid binding protein 3 has shown to promotes remodeling after myocardial infarction by inducing apoptosis. overexpression of FABP3 in rat promoted drastically death and apoptosis of neonatal rat ventricular cardiomyocyte's (Zhuang et al., 2019).

Additionally, pAKT expression was reduced in male Trib3^{ko} suggesting a decrease in glucose uptake in the male Trib3^{ko} mice of the adipose tissue. AKT is part of the insulin signalling pathway. In the liver of the Trib3^{ko} mice there was an increased in pAKT levels compared with Trib3^{ko} adipose tissue, suggesting liver is the primary organ taking up glucose. The uptake of glucose is mainly occurs in the liver and skeletal muscle to promote storage. Again, this suggests, a dysregulation in glucose homeostasis in Trib3^{ko} mice (Qin et al., 2011).

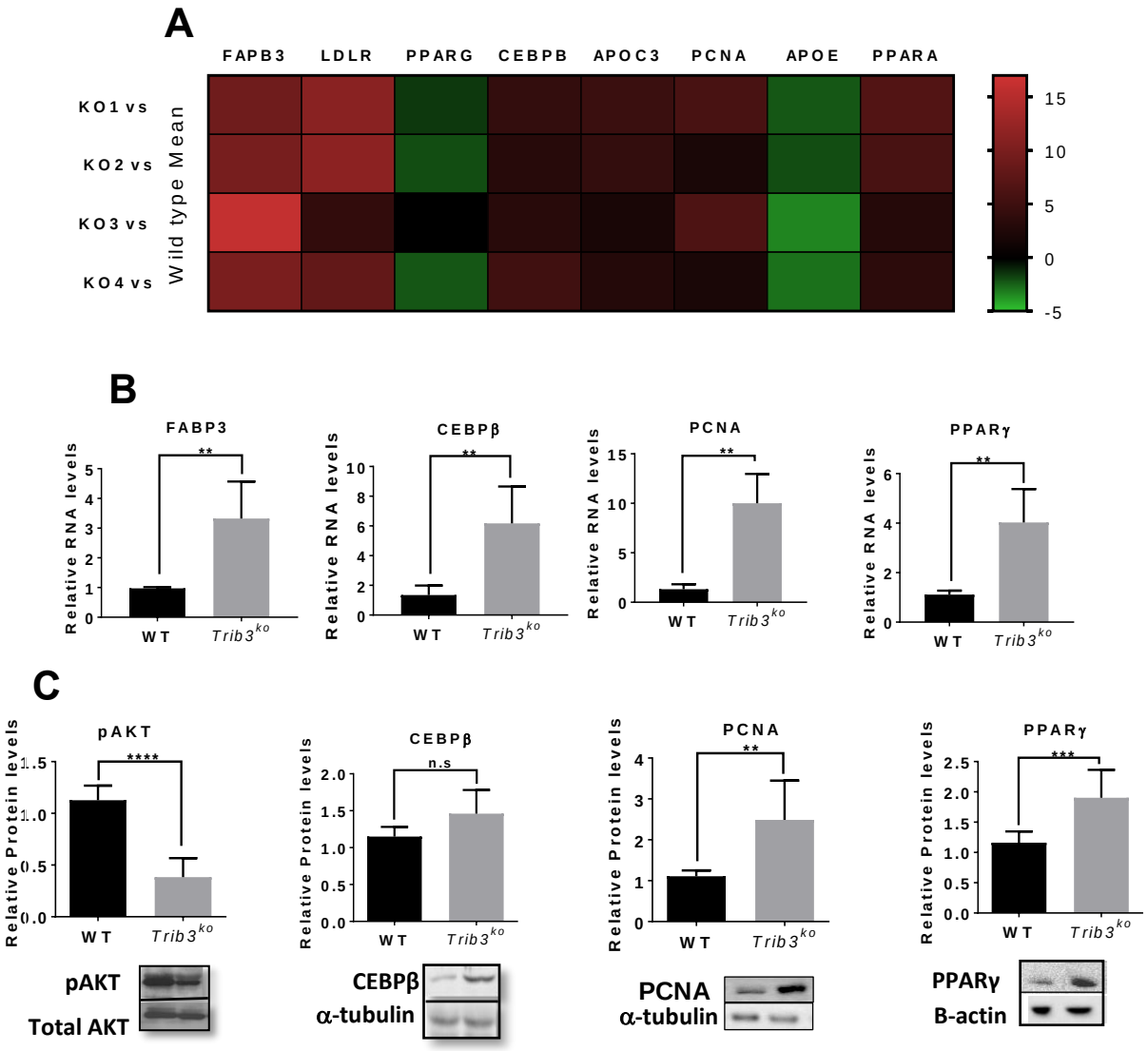

Figure 4.5: Validation of microarray genes-Adipose.

Microarray analysis was performed on the adipose male Trib3^{ko} vs WT littermates' mice. Partek and IPA software packages were used for bioinformatics analysis of the data. **(A)** Heatmap created with the highlighted genes; Green is downregulated, Red is upregulated. KO represents the Trib3^{ko} samples. **(B)** qPCR normalized against B-actin housekeeping gene and **(C)** Western blotting were performed and shown for genes that show a statistical significance. Further analysis using ImageJ densitometry were used. Results are presented as Mean ± SEM N=6-8. Unpaired T-test. P value (*$p \leq 0.05$. **$p \leq 0.01$. ***$p \leq 0.001$. ****$p \leq 0.0001$, N.S= Not significant).

4.5.3 Increase in adipocytes in the Trib3^{ko} adipose tissue

The MRI analysis shown in **Chapter 3,** revealed that male Trib3^{ko} have an increase in fat volume compared with WT littermates. PPARγ and PCNA genes show statistically significant upregulation in the microarray analysis, suggesting that adipogenesis and proliferation are affected by Trib3. Histological examination of subcutaneous adipose tissue has shown no difference in the adipocyte size between male Trib3^{ko} and its WT littermates (**Figure 4.6A, B**) suggesting adipocyte hyperplasia as a consequence of Trib3 deficiency. This was expected as it was seen an increase in proliferative genes such as PPARγ and PCNA. Trib3 have shown to be able to bind to PPARγ and suppress adipocyte differentiation in 3T3-L1 adipocytes. Furthermore, Trib3 expression in 3T3-L1 cells decreased the mRNA levels of PPARγ and the intracellular triglyceride levels (Takahashi et al., 2008). **Figure 4.6C** shows the densitometry measurements of the male Trib3^{ko} compared with WT littermates.

4.5.4 Increase in macrophage influx

Having seen an increase in the expression of inflammatory response genes in the microarray, the expression of macrophage marker F4/80 in the adipose tissue was quantified. **Figure 4.6D** shows an increase in F4/80 positive nuclei, probably due to macrophage influx in the male Trib3^{ko} compared with WT littermates. Macrophages display plasticity due to their ability to alter their physiology upon a change of environmental signals. The impact of Trib3 deficiency on macrophage polarisation is unknown. Future studies would be to show the polarisation and function of the macrophages and therefore understand the interplay between macrophage and adipocytes.

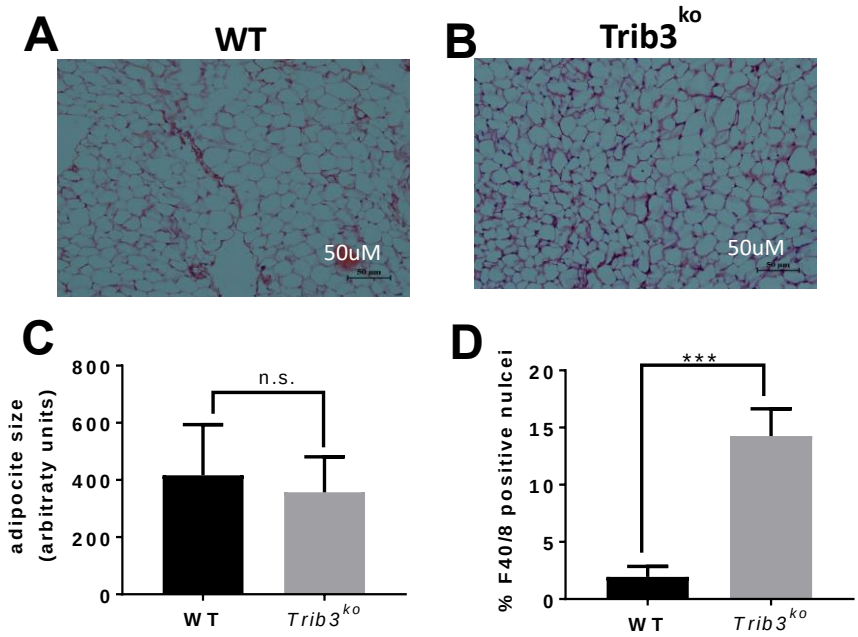

Figure 4.6 Increase in macrophage influx in the male Trib3^{ko} adipose tissue with no change in adipocyte size.

(A, B) Representative histology graphs showing male Trib3^{ko} vs WT littermates adipocyte size. There was no difference in size **(C),** densitometry **(D)** however we did see an increase in F4/80 positive nuclei (**p ≤ 0.05. **p ≤ 0.01. ***p ≤ 0.001. ****p ≤ 0.0001, N.S= Not significant).*

Microarray muscle

4.6 Quality control for 13-week male Trib3^{ko} and WT mice; Muscle tissue

Muscle tissue was homogenised and RNA was extracted and sent to Denova Limited for the microarray analysis. Mouse Transcriptome Array 1.0 (FS450_0001) Agilent chip was used. Four male Trib3^{ko} and 3 WT littermates liver tissue was sequenced. Microarray data were analysed using Partek and Ingenuity Pathway Analysis (IPA) software packages. **Figure 4.7A** shows hierarchical clustering, assigning genes from the microarray into groups between the different samples. **Figure 4.7B** shows principal component analysis (PCA), which shows the variability between different samples. From **Figure 4.7B**, both male Trib3^{ko} and WT littermate samples were shown to be close together. Furthermore, muscle tissues taken from the male Trib3^{ko} and WT littermates was analysed to confirm Trib3 mRNA expression levels. Trib3^{ko} has shown to have a statistically significant reduction for Trib3 mRNA compared with WT littermates shown in **Appendix VII.** 14,324 genes were dysregulated and 732 genes were created using the Partek software; with a P-value of <0.05 and a fold difference of >2, <–2.

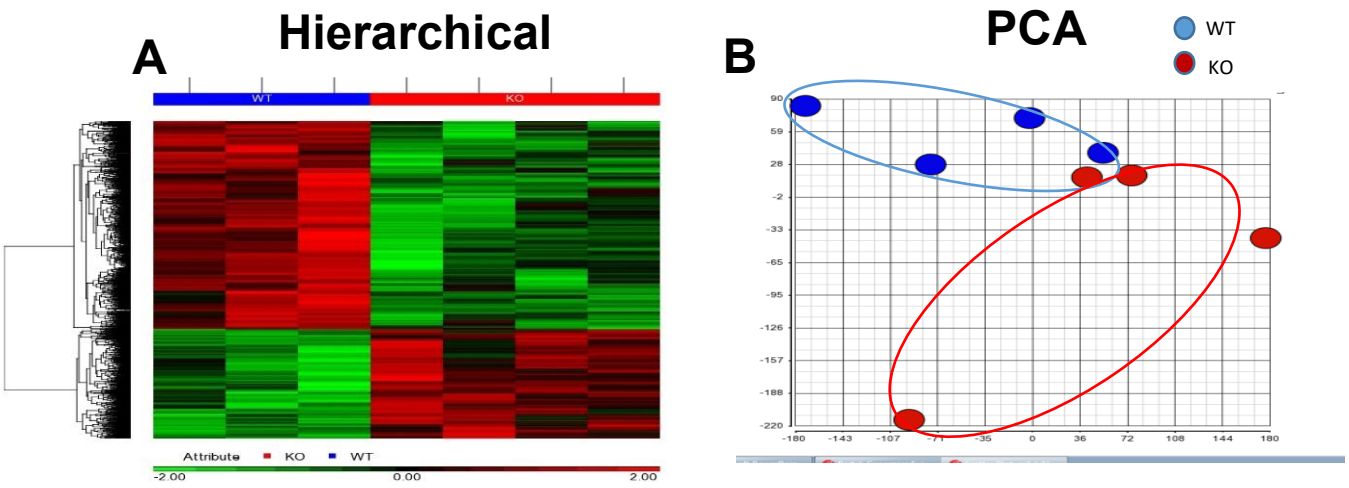

Figure 4.7: Quality control for 13 weeks male Trib3^{ko} and WT mice; Muscle tissue.

(A) Shows hierarchical clustering, to assign the genes from the microarray into groups between the different samples. **(B)** Principled complement analysis (PCA) is used to determine the variability between different data sets. Results are presented as Mean ± SD N=3-4 (**p ≤ 0.05. **p ≤ 0.01. ***p ≤ 0.001. ****p ≤ 0.0001, N.S= Not significant).*

4.6.1 Gene ontology for muscle

IPA software was used to create gene ontology and pathways analysis for the gene list created in Partek for the muscle samples. **Table 4.3A** shows that 73 genes were associated with endocrine system disorder with a P-value of 3.53×10^{-2}. **Table 4.3B** shows the genes highlighted for the molecular and cellular function. Significant genes were selected based pathways.

A

Disease and disorder	Number of genes	P-Value
Endocrine system disorder	73	3.53×10^{-02} - 3.34×10^{-04}
Hepatic system disease	34	3.53×10^{-02} - 3.34×10^{-04}
Metabolic disease	67	4.11×10^{-02} - 3.34×10^{-04}
Organismal injury and abnormalities	254	4.11×10^{-02} - 3.34×10^{-04}
Developmental disorder	65	4.11×10^{-02} - 3.34×10^{-04}

B

Molecular and cellular function	Number of genes	P-Value
cell-to cell signalling and interaction	232	3.53×10^{-02}-7.95×10^{-05}
cell signalling	54	2.66×10^{-03}-2.37×10^{-04}
post-translation modification	58	4.11×10^{-02}-2.37×10^{-04}
cellular compromise	24	$2.66\text{-}02 \times^{-10}$ -05.20×10^{-04}
Cellular function and maintenance	138	3.09×10^{-02}.- 6.9610×10^{-04}

Table 4.6: Gene ontology for muscle

(A) For the disease and disorder, 73 genes were assigned to be play a part in endocrine system disorder with a P value of 3.53×10^{-2}.(**B)** shows the molecular and cellular function that cellular function and maintenance was the top hit. (**p ≤ 0.05. **p ≤ 0.01. ***p ≤ 0.001. ****p ≤ 0.0001, N.S= Not significant).*

4.6.2 Validation of microarray genes

Genes involved in the endocrine disorder pathway which have been shown to be significant were selected and a network analysis created. **Figure 4.8A** shows a heat map from the selected microarray genes, showing an increase in insulin receptor 2 (IRS2), important in the insulin signalling pathway. lipoprotein lipase (LPL) part of the fatty acid pathway, has shown to break down fat in the form of triglycerides. **Figure 4.8B** shows the selected microarray genes validated by qRT-PCR and **Figure 4.8C** western blots. As can be seen, GLUT4, pAKT expression was increased in maleTrib3^{ko} suggesting an increase in glucose uptake in the skeletal muscle. PPARδ has shown an increase in mRNA expression levels between male Trib3^{ko} and WT littermates, however it did not show significant at the protein levels suggesting post-translational modification.

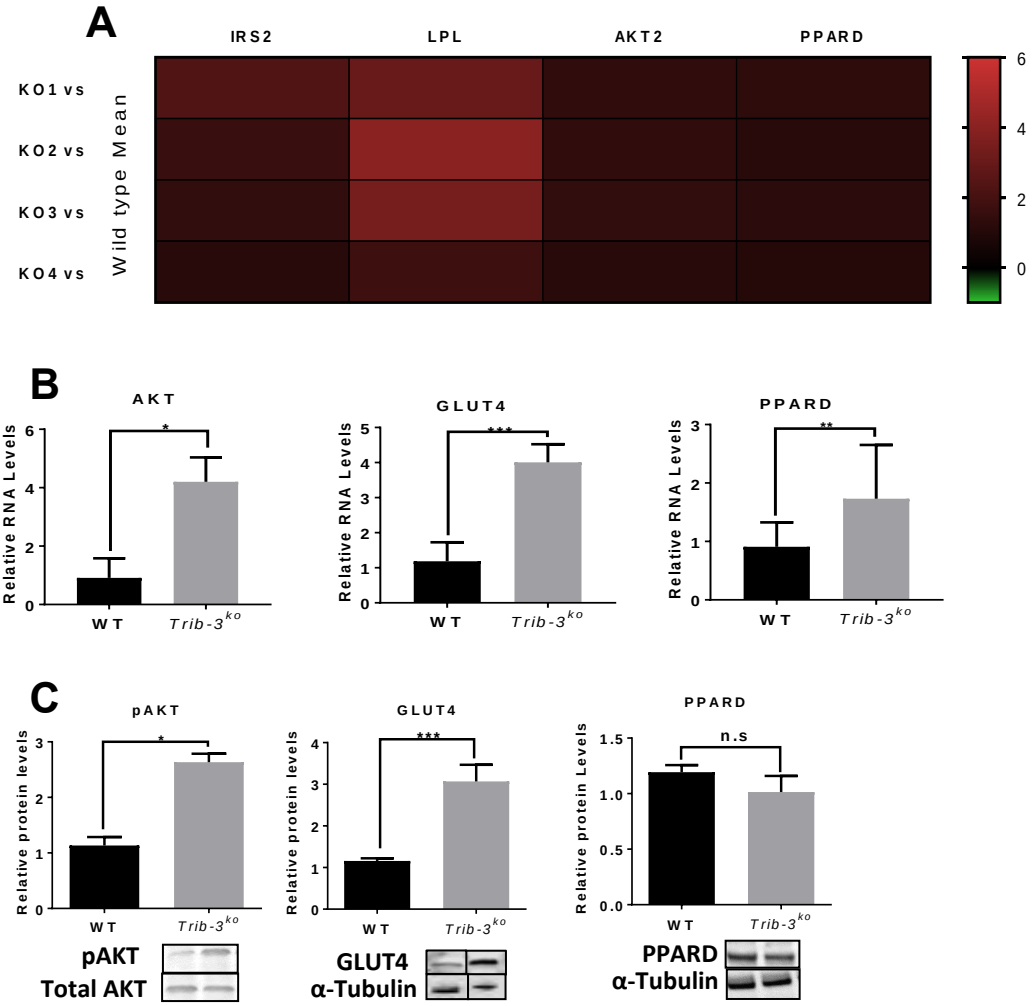

Figure 4.8 Validation of microarray genes- Muscle.

Microarray analysis was performed on the muscle male Trib3^{ko} vs WT littermates' mice. Partek and IPA software packages were used for bioinformatics analysis of the data. **(A)** Heatmap created with the highlighted genes; Green is downregulated, Red is upregulated. KO represents the Trib3^{ko} samples. **(B**) qPCR normalized against B-actin housekeeping gene and **(C)** Western blotting were performed and shown for genes that show a statistical significance. Further analysis using ImageJ densitometry were used. Results are presented as Mean ± SEM N=6-8. Unpaired T-test. P value (**p ≤ 0.05. **p ≤ 0.01. ***p ≤ 0.001. ****p ≤ 0.0001, N.S= Not significant).*

4.6.3 Increase in glucose uptake in the HepG2 cells

Having observed an increase in pAKT in our microarray, it was important to see if there is an increased uptake of glucose in the Trib3-deficient cells. HepG2 cells were used and glucose attached to a fluorescent probe to measure the amount of glucose uptake. Flow cytometry was used to measure glucose uptake. **Figure 4.9A** shows an increase in glucose uptake in the Trib3 knockdown samples compared with controls, suggesting an increase in glucose uptake and storage. Alongside, **Figure 4.9B** is the histogram; showing the fluorescence of the different conditions.

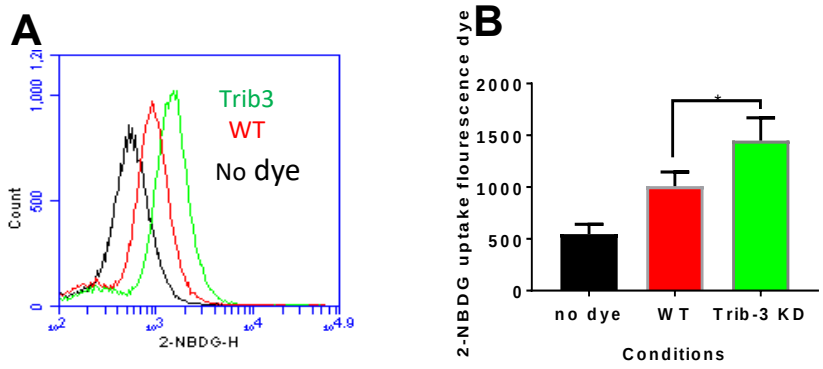

Figure 4.9 Altered glucose uptake in HepG2s.

(A) Flow cytometry was used to look at glucose uptake in Trib3 knockdown compared with Vehicle control. **(B)** Densitometry showing an increase in glucose uptake in Trib3 knockdown cells. One-way ANOVA T-Test used to test for statistical significance (**p ≤ 0.05. **p ≤ 0.01. ***p ≤ 0.001. ****p ≤ 0.0001, N.S= Not significant).*

4.7 Changes in adiponectin levels in male Trib3^{ko} mice compared with WT littermates

Next, the adiponectin levels for the Trib3^{ko} were examined, as it has shown to be important cytokine to regulate a number of metabolic processes, including glucose regulation and fatty acid oxidation. Obese patients have been shown to have reduced adiponectin levels compared with healthy individuals. This increases the risk of developing insulin resistance and CVD (Bruckert, 2008, Matsuzawa, 2005, Lacquemant et al., 2005, Matsuzawa et al., 2004, Whitehead et al., 2006). Leptin and adiponectin were downregulated in the microarray however were not significant. From **Figure 4.10,** although not significant, there is a slight reduction in adiponectin in the Trib3^{ko} plasma compared with WT littermates, suggesting a dysregulation of metabolism.

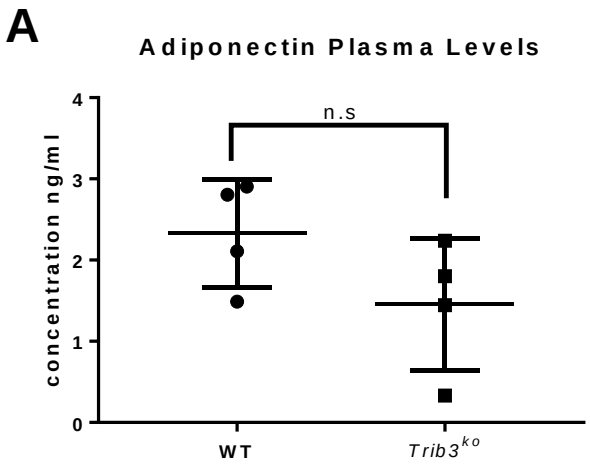

Figure 4.10 Changes in adiponectin levels in Trib3^{ko} plasma compared with WT littermates.

(A) Adiponectin levels measured using ELISA. Graphs showing male Trib3^{ko} vs WT has a reduced adipokine levels compared with WT littermates, however was not statistically significant. Unpaired T test. N=4 (**p ≤ 0.05. **p ≤ 0.01. ***p ≤ 0.001. ****p ≤ 0.0001, N.S= Not significant).*

4.8 Summary

Liver

- Gene ontology confirms dysregulation of CVD genes.
- Reduction of PPARα and pAKT with an increase in LDLR genes involved in lipid metabolism and insulin signalling.
- Increase in lipid droplets in the male Trib3^{ko} liver tissue compared with WT littermates with an increase in triglyceride content.
- *In vitro* experiments show an increase in FFA and glucose uptake of the Trib3 knockdown HepG2 cells compared with control.

Adipose

- Gene ontology confirms dysregulation of inflammatory and lipid metabolism genes.
- Increase in PCNA, PPARγ and pAKT genes involved in lipid metabolism.
- No differences in adipocyte size in the male Trib3^{ko} adipose tissue compared with WT littermates with an increase in F4/80+, macrophage influx.

Muscle

- Gene ontology confirms dysregulation of metabolic and lipid metabolism genes.
- The increase of pAKT and GLUT4 genes involved in glucose metabolism.
- Male Trib3^{ko} mice showed impaired recovery of plasma glucose levels compared with WT littermates.

4.9 Discussion

In this chapter, the systemic effects of Trib3^{ko} in male mice were investigated. The liver, adipose and muscle were chosen as the primary metabolic organs. From **Chapter 3**, an obese phenotype in male Trib3^{ko} mice compared with WT littermates at 13-weeks of age was known. Elevated cholesterol levels were observed with no difference in triglyceride. It was hypothesised that TRIB3 was an important regulator of lipid metabolism and insulin signalling and may contribute towards an obese phenotype in a full body male Trib3^{ko} mouse model.

The liver is one of the main metabolic organs involved in fat metabolism and breakdown and storage of triglycerides for energy. The liver is also involved in carbohydrate metabolism and allows the glucose levels in our blood to remain constant. A fatty liver is generally associated with patients who are obese a nd ordinarily diabetic. There are many stages of development of liver disease, which are 1) non-alcoholic fatty liver disease (NAFLD) 2) non-alcoholic steatohepatitis, 3) fibrosis and 4) cirrhosis (Antunes and Bhimji, 2018).

The male Trib3^{ko} mice have shown a fatty liver phenotype. A triglyceride assay was performed for the liver, which had shown elevated triglyceride levels in male Trib3^{ko} mice compared with WT littermates

(Freeman and Pennings, 2018). A study have shown Trib3 to be upregulated in fatty liver dystrophy (fld) mutant mouse which suffers from hypertriglyceridemia and fatty liver in young mice and impaired nerve function in adult mice (Klingenspor et al., 1999). Furthermore, a study by Wang and colleagues analysed three groups of Sprague Dawley rats including controls, NAFLD fed on HFD for eight weeks, and NAFLD fed for 16 weeks on HFD. The expression level of Trib3 mRNA was significantly higher in the NAFLD fed for 8 weeks compared with controls. A significantly lower expression level of Akt and pAKT compared with the control groups was also seen in this study. The animals models here was fed on HFD compared to our models. It would be interesting to further investigate the impacts of $Trib3^{ko}$ on HFD (Wang et al., 2009).

Trib3 has been shown to play an essential role in insulin signalling. Previous studies suggest that Trib3 is a negative regulator of insulin, mediated via Akt phosphorylation. It was reported that overexpression of Trib3 in Hepg2 inhibits Akt activation and therefore affects the insulin signalling pathway. Conversely, a Trib3 knockdown in HepG2s resulted in induction of phosphorylation in Akt (Du et al., 2003).

Furthermore, patients with NAFLD, more than 95% of are insulin resistant, so there is a possibility that insulin resistance plays a vital role in the development or inducing of NAFLD. It can, therefore, be possible that Trib3, may not only be a cause of insulin resistance but also an important factor in inducing or development of NAFLD (Chitturi and Farrell, 2001). Other studies implicate activation of peroxisome proliferator-activated receptor alpha (PPARα) as a leading cause of NAFLD. $Pparα^{ko}$ mice in HepG2 cells were treated with and without fenofibrate at different doses. Fibrates activate Pparα. Hepatic steatosis was detected through oil red O staining. It was shown that the fenofibrate-treated mice, hepatic triglyceride content was increased in a dose-dependent manner (Tanaka et al., 2017, Yan et al., 2014). The microarray analysis of the liver and validation of both mRNA and protein levels has shown a decrease in PPARα with a concurrent increase in Akt phosphorylation. PPARα is a member of the nuclear receptor family, which was shown to be a significant regulator of lipid metabolism. It is predominantly expressed in the liver and is a major activator of fatty acid oxidation. Knockdown studies of PPARα have shown induced hypoglycaemia and reduction in hepatic glucose levels, demonstrating its importance in glucose homeostasis (Sanders et al., 2014). Additionally, it was shown that Trib3 to be induced by fasting through the induction of PPARα, which suggests that Trib3 is involved in lipid and glucose metabolism (Koo et al., 2004).

The male $Trib3^{ko}$ has an increase in liver LDLR expression, a receptor for upregulation of lipids. Alongside, with a reduction in PPARα, a potential mechanism could be Trib3 can regulate PPARα levels which have an impact on lipid disposition and therefore, contribute to the development of fatty liver. Whether there is any direct or indirect interaction between Trib3 and PPARα, is unknown. An increase in uptake of free fatty acids *in vitro* was confirmed. An increase in fatty acid uptake in Hepg2' cells after Trib3 knockdown was seen, alongside an increase in glucose uptake. The above experiments alongside previous literature indicate that Trib3 is involved in regulating hepatic lipid levels and can be a potential therapeutic target in the future for NAFLD. There was also a reduction of GLUT2 and pAKT levels in the liver; involved in the insulin signalling pathway and have been highlighted in our microarray, suggesting Trib3 is involved in the glucose handling. A study by Lie and colleagues has also shown that Trib3 is elevated upon fasting and overexpression of Trib3 leading to inhibition of insulin via Akt

phosphorylation pathway in mouse (Liu et al., 2010). In addition to this, overexpression of Trib3 in mouse liver resulted in hyperglycaemia.

Conversely, liver-specific deletion of Trib3 in mice leads to improved insulin and glucose tolerance (Prudente et al., 2012). A similar phenotype was observed in our male Trib3^{ko} model. Upon a GTT and ITT, male Trib3^{ko} mice show a quicker recovery of plasma glucose levels, suggesting male Trib3^{ko} become insulin sensitive. In the muscle, there is an increase in GLUT4 protein and pAKT suggesting an increase in glucose uptake, which correlates with the microarray data.

Another gene highlighted in the microarray analysis for the adipose tissue is peroxisome proliferator-activated receptor-γ (PPARγ). PPARγ is an essential regulator for adipogenesis. There are two different isoforms, known as PPARγ1 and PPARγ2. PPARγ2 is expressed predominantly in the adipose tissue, whereas PPARγ1 is ubiquitously expressed. Others include the members of the CCAAT/enhancer-binding protein (C/EBP) family of transcription factors, which also play an essential role in promoting adipocyte differentiation. It was shown that CEBPα^{ko} mice to lack WAT, suggesting a key regulatory contribution to adipocyte differentiation (Siersbaek R, 2010). Another study by Spiegelman and colleagues has shown PPARγ can induce adipogenesis in CEBPα^{ko} in MEFs. However, CEBPα is unable to induce adipogenesis in PPARγ^{ko} mice (Sharma AM1, 2007). TRIB3 is an essential regulator of adipocytes and has a role not only in adipocyte differentiation via C/EBPβ and PPARγ but also lipid metabolism and homeostasis (Prudente et al., 2012). TRIB3 inhibits ERK and prevents the phosphorylation and activation of C/EBPβ, which in turn induces PPARγ, both essential proteins for adipocyte function. An increase in PCNA and PPARγ was observed, suggesting an increase in adipocyte differentiation and contribution to the obese phenotype observed in the male Trib3^{ko} mice. The previous study by Bezy and colleagues has shown Trib3 overexpression in 3T3-L1 preadipocytes blocks adipogenesis by degradation of CEBPβ and PPARγ (Bezy et al., 2007). Trib3 acts as a negative regulator of differentiation of adipocytes but also can control lipid accumulation in mature adipocytes. The Takahashi group has shown that Trib3 is also able to control the transcriptional activity of PPARγ and therefore suppress adipocytes differentiation (Takahashi et al., 2008). From the microarray, inflammatory genes were also observed, so histology was performed in adipose sections for F4/80, a marker for macrophages. An increase in F4/80 was observed, suggesting an increase in macrophage influx in the adipose tissue. Upon male Trib3^{ko} there is a proliferation of adipocytes and an increase in macrophages, whether the macrophages are behaving like M1 or M2, is still unexplored. All experiments in this project focussed on subcutaneous tissue. Unpublished studies from our lab have suggested an increase in adipocyte size and a reduction in macrophages in the visceral tissue, the opposite of what was shown in the subcutaneous tissue. This is an interesting observation because different adipose tissues are linked differently to disease progression. Another tissue that is unexplored is the BAT. Male Trib3^{ko} have a tissue-specific impact, and from this study, it seems that there is a spillover of lipids from the adipose into the liver, and maybe into the muscle. Adiponectin levels show a slight reduction in the Trib3^{ko} compared with WT littermates. Further cytokine analysis would have revealed more information in regard to the communication between different tissues.

Chapter 5—Results

miR202 is a novel regulator of endogenous TRIB1 protein expression

5.1 Introduction

During my PhD, work was done in profiling miRNAs that bind and modulate Trib1 levels. This chapter would therefore be focusing on Trib1, rather than the isoform, Trib3.

Trib1 has been shown to play an important role in lipid haemostasis and atherosclerosis. A GWAS conducted in healthy controls and human coronary artery disease (CAD) patients showed genetic variants near the TRIB1 locus to be associated with hyperlipidaemia and increased the risk of developing CAD (Kathiresan et al., 2008). Furthermore, a study by Burkhardt and colleagues demonstrated that $Trib1^{ko}$ in mice increases plasma TG and cholesterol levels with an increase in VLDL production, thus assigning a protective function to this protein in hepatocytes. Additionally, overexpression of Trib1 in hepatic cells had shown opposite effects, it reduces cholesterol and TG levels, with a reduction in VLDL production. Trib1 is also critical for macrophage polarisation. A study by Satoh and colleagues has shown that Trib1 is a critical regulator for differentiation of anti-inflammatory, M2 macrophages. A $Trib1^{ko}$ resulted in a reduction of M2 macrophages in various organs, including bone marrow, spleen, lung and adipose tissues. Trib1 was shown to be an important negative regulator in controlling inflammation and acts to lower plasma lipid levels (Satoh et al., 2013).

While our understanding of the TRIB1 function is becoming clearer, the regulation of TRIB1 remains unexplored. The half-life of TRIB1 mRNA is <1 hour, so the aim is to find ways to stabilise Trib1 mRNA levels which would, therefore, have beneficial effects on lipogenesis. The liver is the primary organ to modulate systemic cholesterol levels, so we aim to stabilise TRIB1 levels in the liver.

Furthermore, all the Tribbles mammalian family members have a long and conserved 3′ untranslated region (UTR), which suggests post-transcription modification via miRNAs. The Trib1 miRNA transcript contains a 1948 bp long 3′UTR, making it ideal for miRNA cleavage. An example of this is miR122, which regulates multiple target genes which have been associated with the metabolism of hepatic fatty acids. Forty-five targets of miR122 were highlighted including Trib1 (Yang et al., 2015). In this study, novel miRNA that are able to regulate hepatic TRIB1 levels and therefore control inflammation and lipid levels will be demonstrated.

5.2 Hypothesis

In this chapter, bioinformatics databases will be used to search for miRNA that controls Trib1 expression levels. I believe that TRIB1 proteins are important negative regulators in controlling inflammation and

act to lower plasma lipid levels and lipid homeostasis, so increasing levels of TRIB1 protein would, therefore, have beneficial effects on the atheroma.

5.3 Aims

- Identify miRNA's that can bind to the trib1 3′UTR using bioinformatics databases.
- Test and characterise the impact of miRNAs on Tribbles expression levels via Dual luciferase assay and qRT-PCR and western blots.
- Determine the impact of miRNA on Tribbles on HFD and chronic inflammatory settings.
- Use TSB to increase hepatic Trib1 levels and test for plasma lipid profile and triglyceride in the liver.

5.4 miR202 predicted to bind to Trib1 3′UTR

miRTarget is an online database made by the algorithm to predict miRNA binding (Wong et al., 2015, Wang et al., 2016). The program was used to search for miRNAs that can bind and interact with Trib1. miR202 was highlighted as the most significant with a pairing score of more than 150 and energy score <–7. Furthermore, it has a mirSVR cut off of ≤–1.2. Over 500 miRNA hits were observed from 12/03/2018. **Table 5.1** shows the top 3 predicted miRNAs that are able to bind and modulate Trib1 levels. Alongside are the miRNA sequence and binding site position. **Figure 5.1** shows the constructed Renilla Luciferase plasmid created by a Vera, a technician in Endre-Kiss-Toth group, with the different lengths of the Trib1 3′UTR site.**3**.

Table 5.1 showing the top two hits of miRNA able to bind and modulate Tribbles. The initial bioinformatics analysis was performed by a PhD student in our group; Chiara Niespolo.

Target gene	Species	MiRNA	Sequence	Seed location
TRIB1	**Human**	**miR202-3p**	**AGAGGUAUAGGGCAUGGGAA**	**1517**
TRIB1	Human	miR129-2-3P	AAGCCCUUACCCCAAAAAGCAU	1467
TRIB1	Human	miR-888-5p	UACUCAAAAAGCUGUCAGUCA	368,780

5.5 Plasmids—Renilla luciferase fused with Trib1 UTRs

Renilla Luciferase plasmids were created with different lengths of the Trib1 3′UTR site. **Figure 5.1**shows the different plasmids used in the experiment. Different plasmids were created and tested for mRNA stability. A dual luciferase assay was used to transfect Trib1 3′UTR vs. control in HepG2 cells transfected in a 96-well plate. **Figure 5.1D** shows the 3′UTR region of the Trib1 is destabilising the mRNA level and it is the truncated 3′UTR responsible for this.

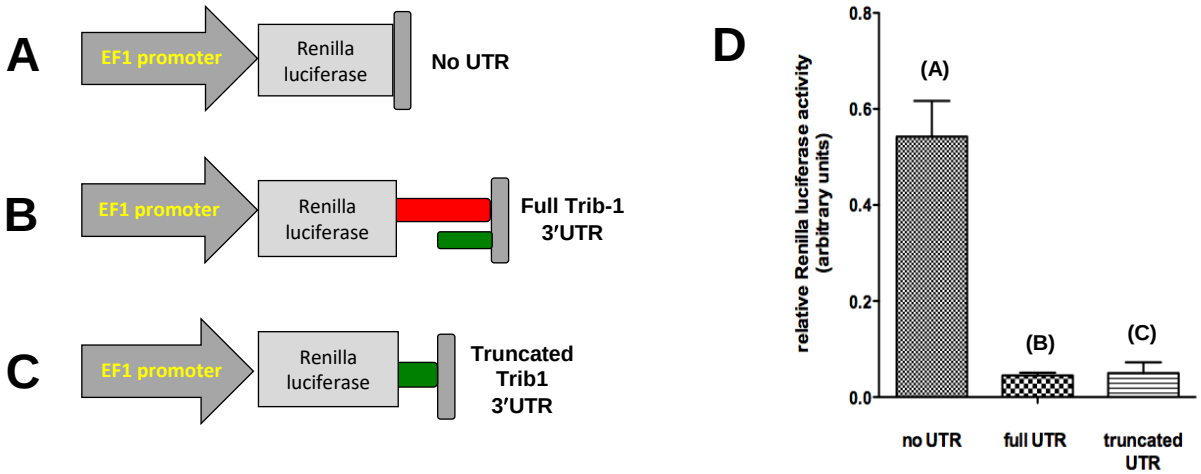

Figure 5.1: Plasmids- Renilla luciferase fused with Trib1 UTRs.

A,B,C) Structures of the transcriptional reporters, to test the impact of Trib1 3′UTR on mRNA stability. Red represents the Full UTR. Green represents Truncated UTR. D) Transiently transfected HeLa cells with the reporters shown and measured Renilla luciferase and Firefly luciferase activity using a spectrophometer. Unpaired T test. N=4 (**p ≤ 0.05. **p ≤ 0.01. ***p ≤ 0.001. ****p ≤ 0.0001, N.S= Not significant).*

5.6 miR202 modulate TRIB1 levels

miR202 was selected because it was a top hit in the bioinformatics screen; it has also been shown in a previous study to be an essential regulator in human hepatocyte metabolism. miR202 was also identified in an RNA screen to identify upstream regulators of TRIB1 in HepG2 cells. TRIB1 suppression in HepG2 resulted in impairment of lipid metabolism and liver function genes like CEBPα and ApoB (Soubeyrand et al., 2016).

Dual luciferase constructs were made, and co-transfected with miR202 mimics (50nM) and miR202 (100nM) inhibitors which was purchased from Exicon, alongside with Renilla luciferase fused with truncated Trib1-3′UTR. A Renilla luciferase with no Trib1-3′UTR was used as a negative control. **Figure 5.2A** shows no significant change upon addition of miR202 mimic or miR202 inhibitor alongside the negative control. However, **Figure 5.2B, C** shows upon the addition of miR202mimic, a sharp reduction in Trib1-3′UTR levels and an increase in Trib1-3′UTR levels upon addition of the miR202 inhibitor. This suggests miR202 is able to bind and modulate the Trib1-3-‘UTR levels. Cell viability were measured using trypan blue and it showed no significance difference in cell death between miR202mimic and miR202 inhibitor. Renilla luciferase and firefly luciferase were measured suing a spectrometer.

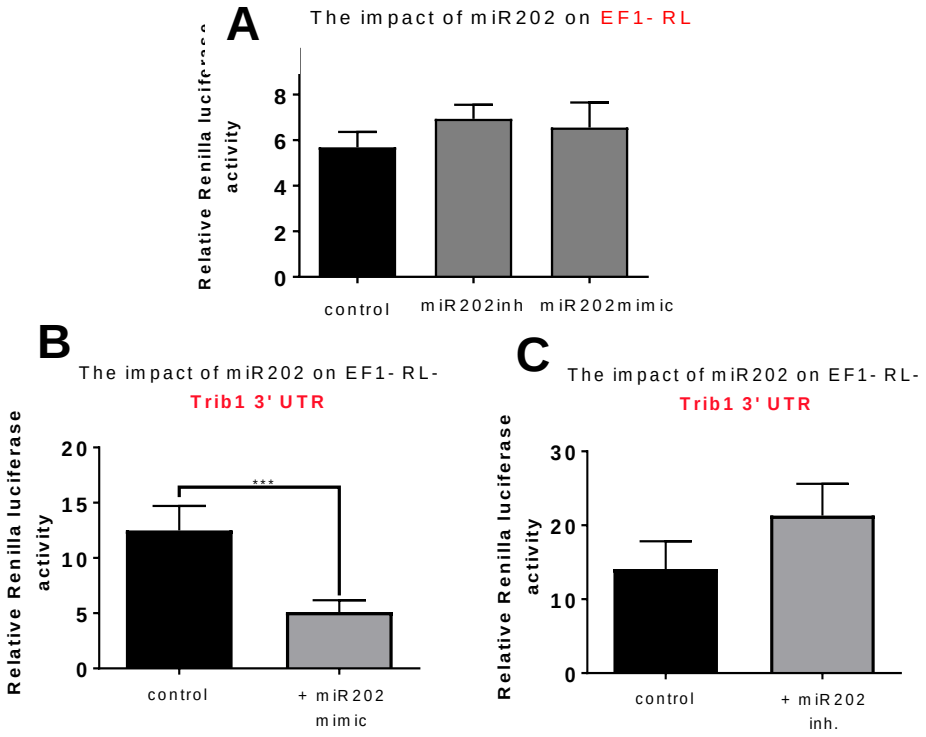

Figure 5.2: miR202 is a binding site for TRIB1 3′UTR in HepG2 cells.

A) Co-transfection of EF1 promoter driven Renilla luciferase only with mimic and inhibitor as a negative control (Mean ± SEM, No statistical significance One-way ANOVA with Bonferroni post test) **B)** Co-transfection of EF1 promoter driven Renilla Luciferase containing the 3′UTR of TRIB1 and mimic and **C**) inhibitor. (Mean ± SEM, * P<0.05, *** P<0.001 T-test with Bonferroni post test, N=6).

5.7 No changes in mutant Trib1-3′UTR levels upon miR202

The impact of miR202 on Trib1-3′UTR was further validated by using a mutant Trib1-3′UTR which has a mutated site where miR202 binds to and the effect of miR202 mimic was observed. The mutant were generated by Vera, a technician in EKT group. The construct formation can be found in the method section. **Figure 5.3** had shown no significant effect on Trib1-3′UTR levels upon addition of miR202 mimic, however, from the non-mutated site, there is a statistically significant reduction in Trib1 3′UTR levels.

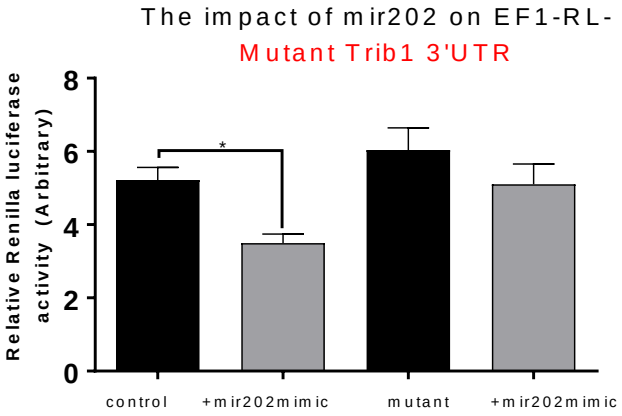

Figure 5.3: No changes in mutant Trib1-3′UTR levels upon miR202.

A) Co-transfection of EF1 promoter driven Renilla Luciferase containing the 3′UTR of Trib1, with the miRNA202 binding site mutated, and mimic and inhibitor (Not statistically significant Mean ± SEM, * P<0.05, *** P<0.001 T-test with Bonferroni post test, N=6), to validate miR202 binding to TRIB1.

5.8 miR202 is important in maintaining the double hairpin structure

So far, it has been shown that miR202 can bind and modulate Trib1 3′UTR levels, with a mutant Trib1 this binding is abolished. Next, the mutational analysis of miR202 was looked at to look for polymorphism sites. miR202 is conserved within the mammalian species and has been shown to be in expressed in most of the human and mouse tissues. However, it is abundantly expressed in the liver. Collaborative studies with Dr Clint Millar have shown 2D mutational analysis of TRIB1 3′UTR around miR-202 site, showing miR202 to be important in maintenance of the double hairpin structure. **Figure 5.4A** shows a mutational analysis of TRIB1 3′UTR around the miR-202 site. Mutating a nucleotide and mapping chemical accessibility reveals interactions in the three-dimensional structure of the RNA. This has been done to see the miR202 binding and its accessibility site. **Figure 5.4B** shows the hairpin structure of TRIB1 and the location of miR202 binding site, showing it is more accessible and located around the hairpin structure. The miR202 site is also very critical and polymorphic variants have been shown at the miR202 position. This bioinformatics data is important as it deepens our understanding in the location of the miR202 binding site, therefore suggesting us to visualize its accessibility.

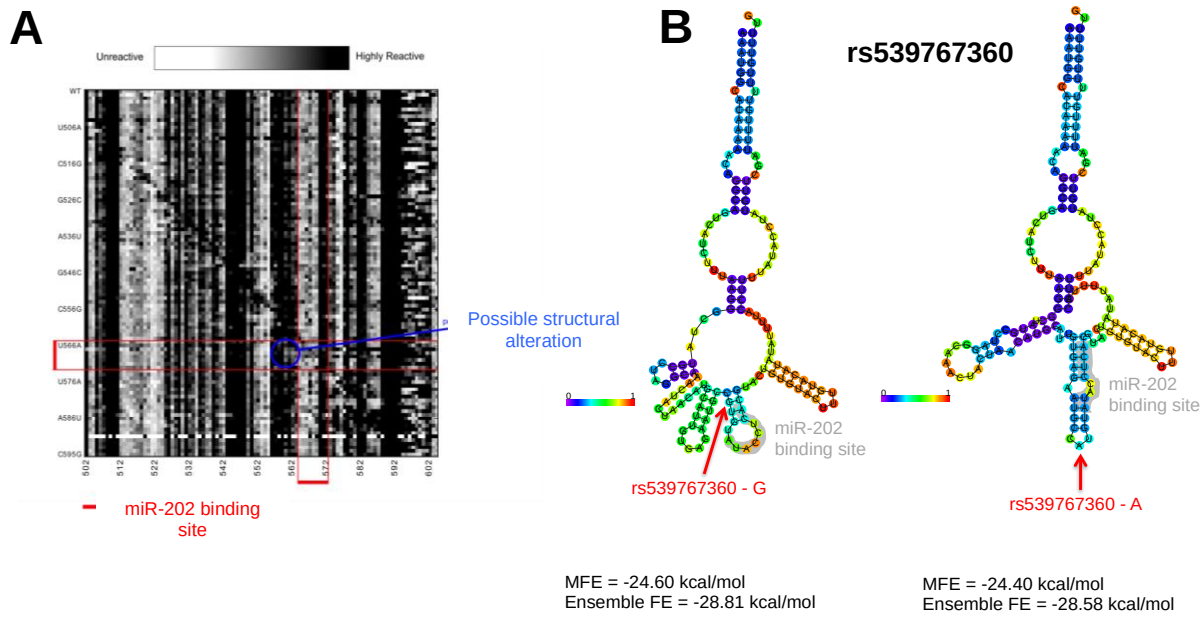

Figure 5.4: Mutational analysis of TRIB1 3′UTR around miR-202 site.

The data above was provided by Dr Clint Miller, Stanford University USA. **A)** Developed a shape seq. This has been done to see the miR202 binding and its accessibility site. Mutating a nucleotide and mapping chemical accessibility reveals interactions in the three-dimensional structure of the RNA. More info refer to (Kladwang et al., 2011) **B)** Showing the hairpin structure of TRIB1 and the location of miR202 binding site, showing it is more accessible and located around the hairpin structure. The miR202 site is also very critical and polymorphic variants have been shown at the miR202 position. Z-score key showing (number of standard deviations from mean at each residue).

5.9 Mir202 can modulate endogenous Trib1 mRNA and protein levels in HepG2s

Next, it was tested if Trib1 is expressed endogenously in HepG2 cells and if this is regulated upon miR202 mimic and miR0202 inhibitor. qPCR was used to measure Trib1 mRNA levels and normalised against B-actin, which acted as a housekeeping gene. **Figure 5.5 (A, B)** shows miR202 is expressed in HepG2's and can bind and modulate endogenous Trib1 levels Furthermore. **Figure 5.5 (C, D)** shows miR202 is expressed in HepG2's and can bind and modulate TRIB1 protein levels.

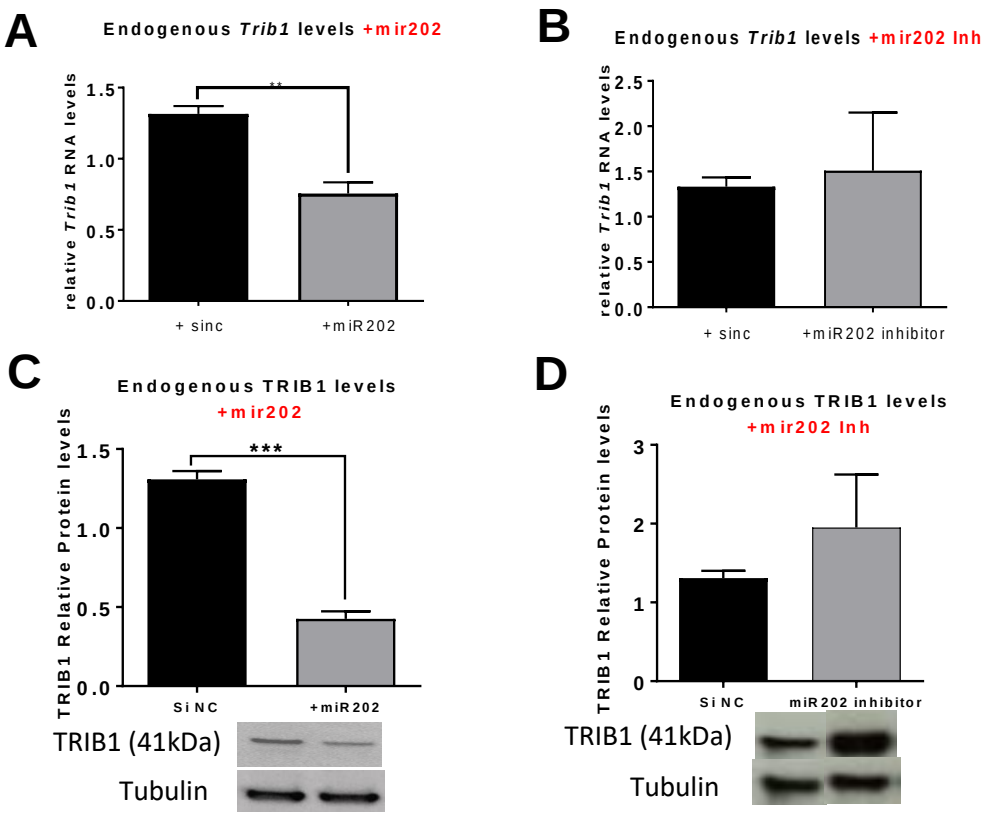

Figure 5.5: miR202 is expressed in HepG2's and is able to bind and modulate endogenous TRIB1 mRNA and protein levels.

A,B) Transiently transfected miR202 mimic and inhibitor in HepG2 cells. Normalised against B-actin. **C,D)** Western blot shows reduction in TRIB1 levels upon overexpression of miR202 and an increase TRIB1 levels upon addition of miR202 inhibitor. Normalised against Tubulin for western blot. (Mean ± SEM, P<0.01 for mimic, P<0.05 for inhibitor, Student t-test, N=6).

5.10 Reciprocal regulation of TRIB1 and miR202 in HepG2 cells by high glucose

Next, the impact of high glucose was tested to see miR202 and Trib1 levels. A metabolic stimulus were given to the HepG2 cells. Trib1 levels was reduced upon high glucose levels in HepG2s, with a concurrent increase in miR202 expression levels (**Figure 5.6**).

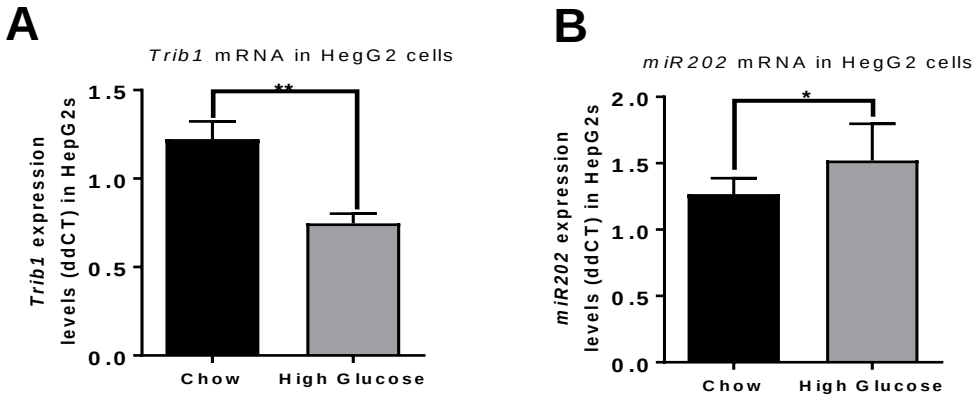

Figure 5.6: Trib1 is regulated upon High glucose in the HepG2 cells.

Reciprocal regulation of TRIB1 and miR202 RNAs in HepG2 cells by glucose. HepG2 cells were incubated in medium supplemented with glucose (25mM) for 48 hrs. Trib1 and miR202 RNA levels were quantified by RT-qPCR. Data are presented as mean ±SEM Student t-test, N=4, * p<0.05, *** p<0.001

5.11 Hepatic Trib1 levels reduced in mice fed on HFD

Having shown miR202 can bind and modulate TRIB1 levels in high glucose, it was tested to see if this changes with a HFD. The Trib1 level is reduced upon HFD in liver tissue, with a concurrent increase in miR202 expression levels. **Figure 5.7** also shows Trib1 is regulated in the liver tissue fed in HFD in the liver tissues. This suggests upon a change in metabolic environment, Trib1 levels shows a significant reduction in expression.

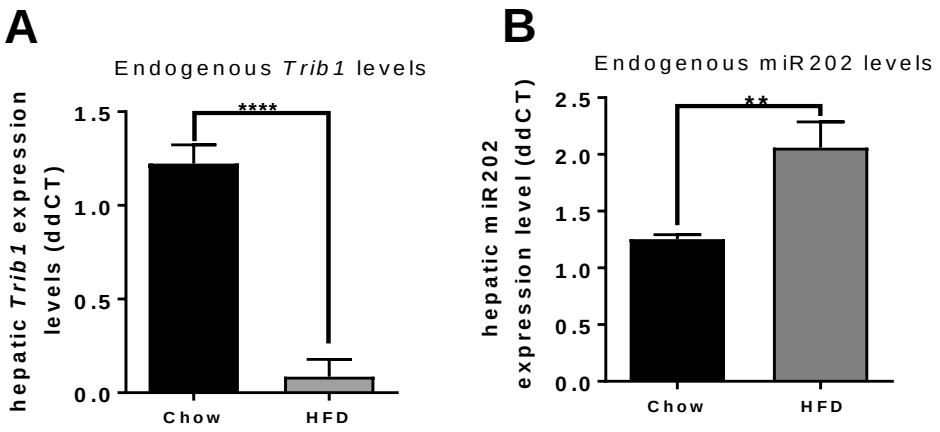

Figure 5.7: Trib1 is regulated upon HFD in the liver tissue.

Trib1 was reduced upon HFD in liver tissue 16 weeks old mice, with a concurrent increase in miR202 expression levels (Mean ± SEM P<0.0001) Student t-test, N=3.

5.12 Summary

- The bioinformatics database has shown the highest affinity predictions for the TRIB1 binding site. miR888-3p, miR129-3p and miR202-3p (TRIB1) have shown to be binding sites in the 3′UTR in the HepG2 cells.

- Mir202 has shown to bind with 3′UTR of TRIB1 and modulate a strong TRIB1 luciferase response. The mutants of TRIB1 have confirmed the binding site by showing mir202 was unable to bind to the mutant 3′UTR (negative control).

- MiR202 can modulate Trib1 mRNA and protein expression levels.

- Upon high glucose and HFD, Trib1 levels are reduced with a concurrent increase in miR202 expression levels.

5.13 Discussion

Trib1 is an important negative regulator in controlling inflammation and acts to lower plasma lipid levels. However, the half-life of TRIB1 is <1 hour (Sharova et al., 2009). Other studies have shown the half-life was due to proteasome-dependent degradation, facilitated by E3 ubiquitin ligases (Zhou et al., 2008). This chapter's aims is to use miRNA inhibitors to stabilise TRIB1 protein levels which could, therefore, have beneficial effects on the atheroma. The liver is the primary organ to modulate cholesterol levels, so we aim to stabilise TRIB1 levels in the liver, which would reduce VLDL production. miRNAs are small non-coding nucleotides that are important in regulating gene expression. It is shown that miRNAs regulate half of the protein-coding complex in a genome, hence, changes in miRNAs result in dysregulating of genes and therefore contribute to many types of disease (Kuret et al., 2018, Friedman RC, 2009). miRNAs have caused downregulation of many essential genes involved in lipid metabolism and fatty acid oxidation by the RISC complex.

It has been reported that miR27b can directly target PPARγ, which is an essential protein associated with the Trib family (Karbiener M, 2009). Another study has shown overexpression of miR51d reduces PPARα expression levels and is reported to cause a severe obese phenotype. miR-519 dose-dependently suppressed translation of the PPARα protein, and increased lipid accumulation during pre-adipocyte differentiation (Martinelli R, 2010). Furthermore miR-122 was shown to be predominantly expressed in the liver and can modulate cholesterol levels, shown to be involved in hepatic carcinoma and cancer progression (Hu et al., 2012). Furthermore, it was shown that inhibition of miR122 reduces expression of lipogenesis genes and a reduction in plasma cholesterol levels in chow and obese mice (Esau et al. 2006). Put together, the above literature makes a strong case that dysregulation of miRNA's has an impact on metabolic disease development and progression.

miRNA inhibitors are being used to stabilise protein levels that are important in metabolic and other processes which have shown positive effects. Although miRNA's are non-specific and can bind to and modulate different proteins, TSB is a specific oligo compound that can protect TRIB1 RNA specifically,

reducing off-target effects. It works by directly binding to the miRNA target site of an mRNA, preventing other miRNAs from gaining access to that site.

There have been some previous studies showing miRNA targeting TRIBs. It was shown that miR124 is upregulated in the livers of C57B/6 fed on HFD (Xing Liu et al., 2016). Upon overexpression of mir124, the mice had an excessive accumulation of triglycerides and had an increase in lipogenic genes in the liver. TRIB3 was shown to be a direct target of miR124, and the protein levels were reduced upon overexpression of miR124, with an increase in Akt phosphorylation. Interestingly, TRIB3 restoration on the liver of this overexpressed miR124 abolished the effects of miR124 suggesting TRIB3 plays a critical role in hepatic lipogenesis and TG accumulation.

Furthermore, studies by Tsai and colleagues showed miR-122 reduced TRIB1 levels in the liver, this is a tumour suppressor, highlighting TRIB1 importance in hepatic cancer pathogenesis (Tsai et al., 2009). Both TRIB1 and TRIB3 play essential roles in regulating different miRNAs and this has an impact on health and disease.

From this study, miRTarget database was used to predict miRNA bindings miR202 was highlighted as the most significant. Other databases such as miRNADA, Targetscan and miRscan were also used with similar outcomes. Selecting the top hit, and ordering the commercially made oligoes from Exicon. Dr Clint Millar have data showing miR202 to be important in maintenance of the double hairpin structure. Furthermore**,** the hairpin structure of TRIB1 and the location of miR202 binding site, reveals it is more accessible as it is located around the hairpin structure. The miR202 site is also very critical and polymorphic variants have been shown at the miR202 position.

Dual luciferase constructs were made, and co-transfected with miR202 mimics (50nM) and miR202 (100nM) inhibitors Renilla luciferase fused with truncated Trib1-3′UTR. A Renilla luciferase with no Trib1-3′UTR was used as a negative control. There was no significant change upon addition of miR202 mimic or miR202 inhibitor alongside the negative control. However, upon the addition of miR202mimic, a sharp reduction in Trib1-3′UTR levels and an increase in Trib1-3′UTR levels upon addition of the miR202 inhibitor. The impact of miR202 on Trib1-3′UTR was further validated by using a mutant Trib1-3′UTR which has a mutated site where miR202 binds to and the effect of miR202 mimic was observed.

Next, it was tested if Trib1 is expressed endogenously in HepG2 cells and if this is regulated upon miR202 mimic and miR0202 inhibitor. qPCR was used to measure Trib1 mRNA levels and normalised against B-actin, which acted as a housekeeping gene. Furthermore, a significant change in TRIB1 protein levels has been shown upon addition of miR202 mimic and miR202 inhibitor, suggesting miR202 to be an important miRNA in the post-translation modification.

Finally, in high glucose and HFD, Trib1 levels are reduced with a concurrent increase in miR202 expression levels showing Trib1 is regulated upon inflammation. It was also demonstrated that miRNA202 expression levels are regulated in HFD conditions.
All of these findings are novel because currently, the field of miRNA's with TRIB1 is relatively new. miRNA202 has been identified and tested as a novel small ncRNA that can modulate TRIB1 protein

levels. miR202 may represent a target by which TRIB1 levels could be raised *in vivo*, thereby providing a mechanism to regulate lipid and glucose levels and therefore augment the anti-atherosclerotic effects of this protein.

Chapter 6—Discussion

6.1 General discussion

Obesity is a driver of metabolic syndrome that is a global epidemic leading to an increased number of patients becoming obese and increasing the risk of diseases, including CVD, cancer and Type 2 diabetes. CVD is a leading cause of mortality and morbidity worldwide, with elevated levels of lipid in the arterial wall and inflammation. It is therefore important to understand the mechanisms that contribute to metabolic syndromes such as obesity and insulin resistance to provide better therapeutic treatments and reduce the risk of developing CVD. The main aim of this project was to characterise Trib3 dependent, tissue-specific regulatory mechanisms of metabolic tissues in male Trib3^{ko} compared with WT littermates. TRIBs have been described as fundamental regulators of the cell cycle, differentiation, metabolism, proliferation, and cell stress, as shown in many reviews and papers and discussed earlier. Previous studies have shown Trib3 to play important roles in core cell signalling pathways including those controlling insulin signalling and in lipid metabolism. However, even though several tissue-specific transgenic and knockdown experiments have recently been published; our knockout studies are the first to address this question at the level of the whole mouse. Furthermore, insight into the role of Trib3 in various organs remains limited. This study aimed to use a systemic approach, for the first time using whole body male Trib3^{ko} mice to decipher a role for Trib3 in metabolic dysfunction. Moreover, Trib1 was also studied because it has been shown to be a risk factor for hyperlipidaemia and previous studies have demonstrated Trib1 to be associated with plasma triglyceride and total cholesterol levels.

In this study, the consequences of full body male Trib3^{ko} mice on lipid profile and adipose tissue content were studied. It was shown that for full body male Trib3^{ko} mice, there is an elevated body weight compared with WT littermates at 13 weeks of age. Furthermore, in contrast, females do not show any weight difference compared with WT littermates. Upon dissection of the male Trib3^{ko} mouse, there was increased subcutaneous adipose tissue compared with the WT littermates. An MRI scan was carried out to look at the adipose distribution and location and an increase in body fat volume for the male Trib3^{ko} compared with WT littermates was observed. The anatomical position was shown to be around the abdominal region of the male Trib3^{ko} mice. The increased weight in the male Trib3^{ko} mice could be due to an increase in the volume of adipose tissue alongside other dense organs, e.g. liver, muscle. It was reported that adipose tissue-specific overexpression of Trib3 and noticed less WAT, slowed weight gain with an increase in dietary intake (Qi et al., 2006). A similar study by Weismann and colleagues reported a Trib3^{ko} via antisense oligo in rat livers had shown an elevated body weight and improved insulin sensitivity (Weismann et al., 2011). These studies confirm our finding that a full body male Trib3^{ko} leads to elevated body weight, alongside an increase in fat volume suggesting that Trib3 is involved in regulating lipid metabolism.

To understand further the dynamics and physiology of the male Trib3^{ko} compared with WT littermates, a metabolic cage experiment was carried out by our collaborators at NTU in Singapore. This is the first

time a metabolic cage experiment was conducted on a full body Trib3^{ko}. This experiment investigated the respiratory indexes, including sleeping, motion and energy expenditure of the mice. The male Trib3^{ko} mice have a clear circadian rhythm similar to the WT littermates. However, the male Trib3^{ko} mice eat and drink significantly less than the WT littermates and are much less active, with an RER less than that of WT. Their respiratory function is decreased but they require more oxygen and produce more carbon dioxide, for an activity that is in total decreased as compared with the WT littermates. This is an interesting observation, the male Trib3^{ko} seem to require more oxygen and have an RER ratio of 0.75, suggesting oxidation of the fat tissue. Having reduced movement and using more energy could suggest that the male Trib3^{ko} mice are using the energy from the stored fats or glucose. The metabolic cage experiment was carried out on male Trib3^{ko} mice that were 38 weeks old, hence the results could not be directly compared with the young Trib3^{ko} mice used in other experiments. Nevertheless, changes in metabolic physiology could be seen for male Trib3^{ko} compared with WT littermates, confirming an important function of this gene in energy homeostasis.

In **Chapter 4** tissue-specific consequences of the observed metabolic changes were characterised alongside tissue-specific mechanisms. A transcriptome analysis of the insulin-sensitive organs was conducted simultaneously and an attempt made to decipher a role for Trib3 in metabolic dysfunction. This is the first study to look at multiple tissues simultaneously and address the communication between the different insulin-sensitive organs. The study looked at the liver of the male Trib3^{ko} mice, an increase in lipid droplets was observed compared with the WT littermates, suggesting a fatty liver. A triglyceride assay was carried out for the liver and it showed elevated triglyceride levels in the liver of the male Trib3^{ko} mice compared with WT littermates. It has been reported that Trib3 to be upregulated in young mutant mice which have suffered from hypertriglyceridemia and fatty liver (Klingenspor et al., 1999). A transcriptome analysis of the liver was conducted and validated some of the genes using qRT-PCR and western blots. Lipid metabolism, Cholesterol metabolism and insulin signalling pathways were selected. There are increases in Akt phosphorylation in the liver, alongside a decrease in PPARα. PPARα is a member of the nuclear receptor family, which has been shown to be a major regulator of lipid metabolism. It is predominantly expressed in the liver and is a major activator of fatty acid oxidation. Furthermore, knockdown studies of PPARα have shown fasting-induced hypoglycaemia and reduction in hepatic glucose levels, suggesting its importance in glucose homeostasis (Sanders et al., 2014). Having shown an increase in LDLR mRNA and an increase in ApoE, this suggests a mechanism in which increased lipid levels are seen in the liver. Trib3 has been previously reported to influence Akt in the liver. Additionally, a study have shown overexpressing of Trib3 to the liver completely blocks insulin action through inhibition of Akt phosphorylation, suggesting Trib3 promotes glucose output from the liver under fasting conditions and that its abnormal expression may contribute to insulin resistance, thereby promoting hyperglycaemia (Du et al., 2003). Upon a GTT and ITT, male Trib3^{ko} mice had shown a quicker recovery of plasma glucose levels suggesting male Trib3^{ko} become glucose tolerant.

PPARγ and CEBPβ were highlighted genes in the adipose tissue. PPARγ is an important regulator of adipogenesis (Prudente et al., 2012). A previous study has reported Trib3 to suppress adipocyte differentiation in the 3T3-L1 cells via inhibiting ERK and prevents the phosphorylation and activation of

C/EBPβ, which in turn induces PPARγ. Furthermore, there is an increase in adipocyte differentiation marker PCNA and a reduction of pAKT in the adipose. Histological examination has shown no difference in adipocyte size, however, there is an increase in F480 marker, suggesting increased macrophages in the adipose tissue. The results suggest there is an increase in adipocyte differentiation in the adipose tissue with an influx of macrophages. Trib3 is influencing C/EBPβ and PPARγ in controlling adipogenesis. In the muscle, there is an increase in GLUT4 and pAKT suggesting an increase glucose uptake, which correlates with the microarray results.

Next, the plasma adipokine levels of male Trib3^{ko} mice were compared with the WT littermates and a slight reduction in Trib3^{ko} mice compared with the WT littermates was observed, however, this was not significant. Taken together, these observations suggest that Trib3 may be involved in the communication amongst different organs, including adipocyte differentiation and insulin signalling, to maintain lipid homeostasis and the major mechanisms that include PPARα in the liver, alongside PPARγ in the adipose tissue.

Having a strong metabolic phenotype upon a Trib3^{ko}, microarray analysis and subsequent validation have shown associations between Trib3 and a large number of dysregulated genes. Some of these genes have been identified in the literature. Having genes which have been shown by other groups gives us reassurance. Novel genes have also been identified, however, there has been no direct link to show whether Trib3 is able to bind directly or indirectly to those proteins. **Figure 6.1 shows a summary, of the impact of Trib3^{ko} on different insulin-sensitive tissues.**

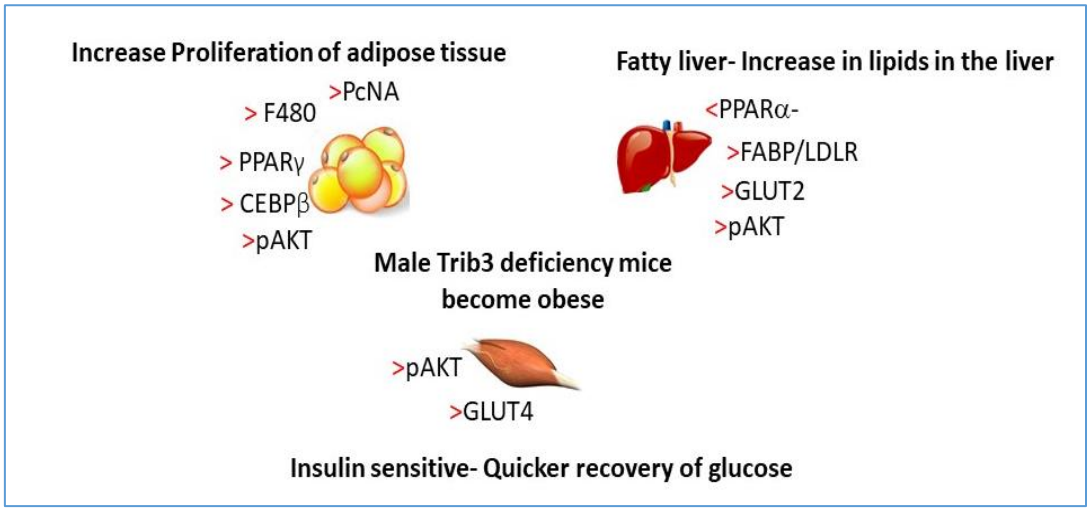

Figure 6.1 Summary, showing the impact of Trib3^{ko} on different insulin-sensitive tissues. Microarray analysis and subsequent validation have shown associations between Trib3 and a large number of dysregulated genes. Trib3 is influencing C/EBPβ and PPARγ in controlling adipogenesis. In the muscle, there is an increase in GLUT4 and pAKT suggesting an increase glucose uptake, which correlates with the microarray results. Furthermore, there is a reduction in PPARα in the live for the Trib3^{ko}. All of the dysregulated genes suggests with the phenotype that the adipose tissue is unable to store excess nutrient intake, which overloads and spills to the liver, which it cannot breakdown efficiently. This increases production of Apo-B, which transports the excess lipids to other organs and increases risk of developing CAD.

Chapter 6 next showed identification of miRNA's that are able to bind to the Trib 3′UTR using in silico analysis and the impact of miRNAs in Trib expression levels characterised. From this study, miRTarget database was used to predict miRNA bindings miR202 was highlighted as the most significant. Other databases such as miRNADA, Targetscan and miRscan were also used with similar outcomes. Selecting the top hit, and ordering the commercially made oligoes from Exicon. Dr Clint Millar have data showing miR202 to be important in maintenance of the double hairpin structure. Furthermore**,** the hairpin structure of TRIB1 and the location of miR202 binding site, reveals it is more accessible as it is located around the hairpin structure. The miR202 site is also very critical and polymorphic variants have been shown at the miR202 position.

Dual luciferase constructs were made, and co-transfected with miR202 mimics (50nM) and miR202 (100nM) inhibitors Renilla luciferase fused with truncated Trib1-3′UTR. A Renilla luciferase with no Trib1-3′UTR was used as a negative control. There was no significant change upon addition of miR202 mimic or miR202 inhibitor alongside the negative control. However, upon the addition of miR202mimic, a sharp reduction in Trib1-3′UTR levels and an increase in Trib1-3′UTR levels upon addition of the miR202 inhibitor. The impact of miR202 on Trib1-3′UTR was further validated by using a mutant Trib1-3′UTR which has a mutated site where miR202 binds to and the effect of miR202 mimic was observed.

Next, it was tested if Trib1 is expressed endogenously in HepG2 cells and if this is regulated upon miR202 mimic and miR0202 inhibitor. qPCR was used to measure Trib1 mRNA levels and normalised against B-actin, which acted as a housekeeping gene. Furthermore, a significant change in TRIB1 protein levels has been shown upon addition of miR202 mimic and miR202 inhibitor, suggesting miR202 to be an important miRNA in the post-translation modification.

Finally, in high glucose and HFD, Trib1 levels are reduced with a concurrent increase in miR202 expression levels showing Trib1 is regulated upon inflammation. It was also demonstrated that miRNA202 expression levels are regulated in HFD conditions.

Although miRNA's are non-specific and are able to bind to and modulate a number of different proteins, this is a limitation which can be overcome by using a TSB. Target Site Blockers are antisense oligonucleotides that bind to the miRNA target site of an mRNA, preventing miRNAs from gaining access to that site. This enables you to study the effects of an miRNA on a single target. The target site blockers outcompete miRNAs for their target sites.
Another important factor is the dose of the miR202, will it have sufficient upregulation of Trib1 levels, which in turn has an effect on lipid levels. A microarray would be ideal to look for different miRNA's that have been shown to bind to Trib1 levels and use a combination, giving a stronger response.

There have been approval for RNAi used as a therapy, Alnylam® is siRNA product Onpattro (patisiran), used in therapy for the rare hereditary disease transthyretin-mediated amyloidosis in adult patients.

Onpattro improved multiple clinical manifestations of the disease and demonstrated safe administration of a siRNA product

All of these findings are novel because currently, the field of miRNA's with TRIB1 is relatively new. miRNA202 has been identified and tested as a novel small ncRNA that can modulate TRIB1 protein levels. miR202 may represent a target by which TRIB1 levels could be raised *in vivo*, thereby providing a mechanism to regulate lipid and glucose levels and therefore augment the anti-atherosclerotic effects of this protein.

6.2 Future work

6.3 Characterising the metabolic activity of male Trib3^{ko} mice at 13 weeks of age

The metabolic cage experiment was carried out on male Trib3^{ko} that were 38 weeks old, hence it was not possible to compare the results with the 13 weeks Trib3^{ko} mice. Although they cannot be compared, changes in metabolic physiology for male Trib3^{ko} compared WT littermates could be seen. A metabolic cage experiment for both Trib3^{ko} male and female mice compared WT littermates, this can therefore be compared to the microarray data.

6.4 Measurements of lipolysis male Trib3^{ko} compared with WT littermates

Male Trib3^{ko} mice have an increase in adipocytes but do not show an increase in size. Markers such as PCNA, PPARγ and CEBPβ have shown to be differentially dysregulated, it would be interesting to measure the FFA, glycerol and other cytokines involved in the lipid metabolism. Studies have shown when there are defects in lipolysis, this can cause leaner mice but more fat in the liver because cells cannot store fat (Saponaro et al., 2015). Proliferation assay for adipose tissue, would be good to further validate the proliferation of the adipocytes.

6.5 Use of target site blocker (TSB) to increase endogenous Trib1 levels

TSBs are specific oligo compounds that are able to protect Trib1 RNA specifically, reducing off-target effects. Studies have shown TSB to have a high efficacy *in vitro* and *in vivo* with high protein *e*xpression due to lack of RNase H-dependent mRNA degradation (exicon.com).

6.6 Use of novel miRNA to regulate hepatic TRIB3 levels

Identify miRNA's that can bind to the Trib1 3′UTR using bioinformatics databases. Test and characterise the impact of miRNAs on Tribbles expression levels via Dual luciferase assay and qRT-PCR and western blots and use TSB to increase hepatic Trib3 levels and test for plasma lipid profile and triglyceride in the liver.

Chapter 7- References

ABDUL-GHANI, M. A. & DEFRONZO, R. A. 2010. Pathogenesis of insulin resistance in skeletal muscle. *J Biomed Biotechnol,* 2010**,** 476279.

ADIELS, M., TASKINEN, M. R. & BOREN, J. 2008. Fatty liver, insulin resistance, and dyslipidemia. *Curr Diab Rep,* 8**,** 60-4.

AGIANNITOPOULOS K, PAVLOPOULOU P, TSAMIS K, BAMPALI K, SAMARA P, NASIOULAS G, MERTZANOS G, BABALIS D & K., L. 2018. Expression of miR-208b and miR-499 in Greek Patients with Acute Myocardial Infarction. *In Vivo,* 32**,** 313-318.

AL-GOBLAN, AL-ALFI MA & MZ., K. 2014. Mechanism linking diabetes mellitus and obesity. *Diabetes Metab Syndr Obes.***,** 587-91.

ALBERTI & ZIMMET 1998. Definition, diagnosis and classification of diabetes mellitus and its complications. Part 1: diagnosis and classification of diabetes mellitus provisional report of a WHO consultation. *Diabet Med,* 15.

AMEER, F., SCANDIUZZI, L., HASNAIN, S., KALBACHER, H. & ZAIDI, N. 2014. De novo lipogenesis in health and disease. *Metabolism,* 63**,** 895-902.

AN, D., LESSARD, S. J., TOYODA, T., LEE, M. Y., KOH, H. J., QI, L., HIRSHMAN, M. F. & GOODYEAR, L. J. 2014. Overexpression of TRB3 in muscle alters muscle fiber type and improves exercise capacity in mice. *Am J Physiol Regul Integr Comp Physiol,* 306**,** R925-33.

ANGYAL, A. & KISS-TOTH, E. 2012. The tribbles gene family and lipoprotein metabolism. *Curr Opin Lipidol,* 23**,** 122-6.

ANSTEY, CHERBUIN N, BUDGE M & J., Y. 2011. Body mass index in midlife and late-life as a risk factor for dementia: a meta-analysis of prospective studies. *Obes Rev* 12.

ANTUNES, C. & BHIMJI, S. S. 2018. Fatty Liver. *StatPearls.* Treasure Island (FL).

APRAHAMIAN, T. R. & SAM, F. 2011. Adiponectin in cardiovascular inflammation and obesity. *Int J Inflam,* 2011**,** 376909.

ARDEKANI & NAEINI 2010. The Role of MicroRNAs in Human Diseases. *Avicenna J Med Biotechnol,* 2**,** 161–179.

ARYAL, B., SINGH, A. K., ROTLLAN, N., PRICE, N. & FERNANDEZ-HERNANDO, C. 2017. MicroRNAs and lipid metabolism. *Curr Opin Lipidol,* 28**,** 273-280.

AU, D. T., STRICKLAND, D. K. & MURATOGLU, S. C. 2017. The LDL Receptor-Related Protein 1: At the Crossroads of Lipoprotein Metabolism and Insulin Signaling. *J Diabetes Res,* 2017**,** 8356537.

AVRAMOGLU, R. K., BASCIANO, H. & ADELI, K. 2006. Lipid and lipoprotein dysregulation in insulin resistant states. *Clin Chim Acta,* 368**,** 1-19.

BANDIERA, PFEFFER, BAUMERT & ZEISEL 2015. miR-122 – A key factor and therapeutic target in liver disease. *J Hepatol.,* 62**,** 448-57.

BARROS, M. H., HAUCK, F., DREYER, J. H., KEMPKES, B. & NIEDOBITEK, G. 2013. Macrophage polarisation: an immunohistochemical approach for identifying M1 and M2 macrophages. *PLoS One,* 8**,** e80908.

BASSIOUNY, H. A. H. A. H. S. 2012. Pathophysiology of Carotid Atherosclerosis.

BAUER, R. C., SASAKI, M., COHEN, D. M., CUI, J., SMITH, M. A., YENILMEZ, B. O., STEGER, D. J. & RADER, D. J. 2015. Tribbles-1 regulates hepatic lipogenesis through posttranscriptional regulation of C/EBPalpha. *J Clin Invest,* 125**,** 3809-18.

BELTOWSKI, J., JAMROZ-WISNIEWSKA, A. & WIDOMSKA, S. 2008. Adiponectin and its role in cardiovascular diseases. *Cardiovasc Hematol Disord Drug Targets,* 8**,** 7-46.

BEZY, O., VERNOCHET, C., GESTA, S., FARMER, S. R. & KAHN, C. R. 2007. TRB3 blocks adipocyte differentiation through the inhibition of C/EBPbeta transcriptional activity. *Mol Cell Biol,* 27**,** 6818-31.

BLACKBURN, G. L., WOLLNER, S. & BISTRIAN, B. R. 2010. Nutrition support in the intensive care unit: an evolving science. *Arch Surg,* 145**,** 533-8.

BRAUN, HUNTZINGER E, FAUSER M & E., I. 2011. GW182 Proteins Directly Recruit Cytoplasmic Deadenylase Complexes to miRNA Targets. *Mol Cell,* 44**,** 120-33.

BRUCKERT, E. 2008. [Abdominal obesity: a health threat]. *Presse Med,* 37**,** 1407-14.

BURKHARDT, R., TOH, S. A., LAGOR, W. R., BIRKELAND, A., LEVIN, M., LI, X., ROBBLEE, M., FEDOROV, V. D., YAMAMOTO, M., SATOH, T., AKIRA, S., KATHIRESAN, S., BRESLOW, J. L. & RADER, D. J. 2010. Trib1 is a lipid- and myocardial infarction-associated gene that regulates hepatic lipogenesis and VLDL production in mice. *J Clin Invest,* 120**,** 4410-4.

BURNETT 2004. Lipids, Lipoproteins, Atherosclerosis and Cardiovascular Disease. *Clin Biochem Rev.,* 25.

CAI, Y., YU, X., HU, S. & YU, J. 2009. A brief review on the mechanisms of miRNA regulation. *Genomics Proteomics Bioinformatics,* 7**,** 147-54.

CALLE, RODRIGUEZ C, WALKER-THURMOND K & MJ., T. 2003. Overweight, Obesity, and Mortality from Cancer in a Prospectively Studied Cohort of U.S. Adults. *N Engl J Med,* 348**,** 1625-38.

CAMPFIELD, SMITH FJ, GUISEZ Y, DEVOS R & P., B. 1995. Recombinant mouse OB protein: evidence for a peripheral signal linking adiposity and central neural networks. *science,* 28**,** 546-9.

CAMUS, CHAPMAN MJ, FORGEZ P & PM., L. 1983. Distribution and characterization of the serum lipoproteins and apoproteins in the mouse,. *J Lipid Res,* 24**,** 1210-28.

CANI, POSSEMIERS S, VAN DE WIELE T, GUIOT Y, EVERARD A, ROTTIER O, GEURTS L, NASLAIN D, NEYRINCK A, LAMBERT DM, MUCCIOLI GG & NM., D. 2009. Changes in gut microbiota control inflammation in obese mice through a mechanism involving GLP-2-driven improvement of gut permeability. *gut,* 58.

CATALANOTTO, COGONI & ZARDO 2016. MicroRNA in Control of Gene Expression: An Overview of Nuclear Functions. *Int J Mol Sci,* 17.

CHAN, D. C., BARRETT, P. H. & WATTS, G. F. 2004. Lipoprotein transport in the metabolic syndrome: pathophysiological and interventional studies employing stable isotopy and modelling methods. *Clin Sci (Lond),* 107**,** 233-49.

CHAN, M. C., NGUYEN, P. H., DAVIS, B. N., OHOKA, N., HAYASHI, H., DU, K., LAGNA, G. & HATA, A. 2007. A novel regulatory mechanism of the bone morphogenetic protein (BMP) signaling pathway involving the carboxyl-terminal tail domain of BMP type II receptor. *Mol Cell Biol,* 27**,** 5776-89.

CHITTURI, S. & FARRELL, G. C. 2001. Etiopathogenesis of nonalcoholic steatohepatitis. *Semin Liver Dis,* 21**,** 27-41.

CHIU, J. J. & CHIEN, S. 2011. Effects of disturbed flow on vascular endothelium: pathophysiological basis and clinical perspectives. *Physiol Rev,* 91**,** 327-87.

CORNIER, M. A., DABELEA, D., HERNANDEZ, T. L., LINDSTROM, R. C., STEIG, A. J., STOB, N. R., VAN PELT, R. E., WANG, H. & ECKEL, R. H. 2008. The metabolic syndrome. *Endocr Rev,* 29**,** 777-822.

CYPESS & KAHN 2010 Brown fat as a therapy for obesity and diabetes. *Curr Opin Endocrinol Diabetes Obes,* 17**,** 143-9.

DAI, HUANG YS, TANG M, LV TY, HU CX, TAN YH, XU ZM & YB., Y. 2007. Microarray analysis of microRNA expression in peripheral blood cells of systemic lupus erythematosus patients. *Lupus,* 16**,** 939-46.

DAVIES, M. J., GRAY, L. J., AHRABIAN, D., CAREY, M., FAROOQI, A., GRAY, A., GOLDBY, S., HILL, S., JONES, K., LEAL, J., REALF, K., SKINNER, T., STRIBLING, B., TROUGHTON, J., YATES, T. & KHUNTI, K. 2017. *A community-based primary prevention programme for type 2 diabetes mellitus integrating identification and lifestyle intervention for prevention: a cluster randomised controlled trial.* Southampton (UK).

DE LUIS, D. A., PEREZ CASTRILLON, J. L. & DUENAS, A. 2009. Leptin and obesity. *Minerva Med,* 100**,** 229-36.

DEFRONZO, R. A. & ABDUL-GHANI, M. 2011. Assessment and treatment of cardiovascular risk in prediabetes: impaired glucose tolerance and impaired fasting glucose. *Am J Cardiol,* 108**,** 3B-24B.

DU, K., HERZIG, S., KULKARNI, R. N. & MONTMINY, M. 2003. TRB3: a tribbles homolog that inhibits Akt/PKB activation by insulin in liver. *Science,* 300**,** 1574-7.

EGLIT, RINGMETS I & M., L. 2013. Obesity, high-molecular-weight (HMW) adiponectin, and metabolic risk factors: prevalence and gender-specific associations in Estonia. *plos one,* 8.

ELLULU, PATIMAH I, KHAZA'AI H, RAHMAT A & Y., A. 2017. Obesity and inflammation: the linking mechanism and the complications *Arch Med Sci*.

ENGIN, A. 2017. Adiponectin-Resistance in Obesity. *Adv Exp Med Biol,* 960**,** 415-441.

ESTEVE RAFOLS, M. 2014. Adipose tissue: cell heterogeneity and functional diversity. *Endocrinol Nutr,* 61**,** 100-12.

FEHLMANN, T., SAHAY, S., KELLER, A. & BACKES, C. 2017. A review of databases predicting the effects of SNPs in miRNA genes or miRNA-binding sites. *Brief Bioinform*.

FELDMANN, H. M., GOLOZOUBOVA, V., CANNON, B. & NEDERGAARD, J. 2009. UCP1 ablation induces obesity and abolishes diet-induced thermogenesis in mice exempt from thermal stress by living at thermoneutrality. *Cell Metab,* 9**,** 203-9.

FERRO-LUZZI & MARTINO, L. 1996. The Origins and Consequences of Obesity.

FITZGERALD, M. L., MUJAWAR, Z. & TAMEHIRO, N. 2010. ABC transporters, atherosclerosis and inflammation. *Atherosclerosis,* 211**,** 361-70.

FREEMAN, A. M. & PENNINGS, N. 2018. Insulin Resistance. *StatPearls.* Treasure Island (FL).

FRIEDMAN RC, F. K., BURGE CB, BARTEL DP. 2009. Most mammalian mRNAs are conserved targets of microRNAs. *Genome Res,* 1**,** 92-105.

GATSELIS, N. K., NTAIOS, G., MAKARITSIS, K. & DALEKOS, G. N. 2014. Adiponectin: a key playmaker adipocytokine in non-alcoholic fatty liver disease. *Clin Exp Med,* 14**,** 121-31.

GEBERT & MACRAE 2018. Regulation of microRNA function in animals. *Nat Rev Mol Cell Biol.*

GILBY, D. C., SUNG, H. Y., WINSHIP, P. R., GOODEVE, A. C., REILLY, J. T. & KISS-TOTH, E. 2010. Tribbles-1 and -2 are tumour suppressors, down-regulated in human acute myeloid leukaemia. *Immunol Lett,* 130**,** 115-24.

GLASS, C. K. & WITZTUM, J. L. 2001. Atherosclerosis. the road ahead. *Cell,* 104**,** 503-16.

GOETTLER, ANNA GROSSE & SONNTAG, D. 2016. Productivity loss due to overweight and obesity: a systematic review of indirect costs. *BMJ,* 7.

GOLIA, E., LIMONGELLI, G., NATALE, F., FIMIANI, F., MADDALONI, V., RUSSO, P. E., RIEGLER, L., BIANCHI, R., CRISCI, M., PALMA, G. D., GOLINO, P., RUSSO, M. G., CALABRO, R. & CALABRO, P. 2014. Adipose tissue and vascular inflammation in coronary artery disease. *World J Cardiol,* 6**,** 539-54.

GONG, H. P., WANG, Z. H., JIANG, H., FANG, N. N., LI, J. S., SHANG, Y. Y., ZHANG, Y., ZHONG, M. & ZHANG, W. 2009. TRIB3 functional Q84R polymorphism is a risk factor for metabolic syndrome and carotid atherosclerosis. *Diabetes Care,* 32**,** 1311-3.

GORTMAKER, MUST A, SOBOL AM, PETERSON K, COLDITZ GA & WH., D. 1996. Television viewing as a cause of increasing obesity among children in the United States, 1986-1990. *Arch Pediatr Adolesc Med,* 150**,** 356-62.

GROSSHANS, J. & WIESCHAUS, E. 2000. A genetic link between morphogenesis and cell division during formation of the ventral furrow in Drosophila. *Cell,* 101**,** 523-31.

GUZIK, T. J., MANGALAT, D. & KORBUT, R. 2006. Adipocytokines - novel link between inflammation and vascular function? *J Physiol Pharmacol,* 57**,** 505-28.

HARP, J. B. 2004. New insights into inhibitors of adipogenesis. *Curr Opin Lipidol,* 15**,** 303-7.

HEGEDUS, Z., CZIBULA, A. & KISS-TOTH, E. 2006. Tribbles: novel regulators of cell function; evolutionary aspects. *Cell Mol Life Sci,* 63**,** 1632-41.

HEGEDUS, Z., CZIBULA, A. & KISS-TOTH, E. 2007. Tribbles: a family of kinase-like proteins with potent signalling regulatory function. *Cell Signal,* 19**,** 238-50.

HEILBRONN, NOAKES M & PM., C. 2001. Energy restriction and weight loss on very-low-fat diets reduce C-reactive protein concentrations in obese, healthy women. *Arterioscler Thromb Vasc Biol.,* 21.

HIMSWORTH & KERR 1939. Insulin-sensitive and insulin-insensitive types of diabetes mellitus. *Clinical Science,* 4**,** 120-152.

HOGARTH, ROY A & DL., E. 2003. Genomic evidence for the absence of a functional cholesteryl ester transfer protein gene in mice and rats. *Comp Biochem Physiol B Biochem Mol Biol.,* 135.

HOTAMISLIGIL, SHARGILL NS & BM., S. 1993. Adipose expression of tumor necrosis factor-alpha: direct role in obesity-linked insulin resistance. *science,* 1.

HOTAMISLIGIL, G. S. 2006. Inflammation and metabolic disorders. *Nature,* 444**,** 860-7.

HRUBY 2015. The Epidemiology of Obesity: A Big Picture. *Pharmacoeconomics* 33**,** 673-689.

HUANG, P. L. 2009. A comprehensive definition for metabolic syndrome. *Dis Model Mech,* 2**,** 231-7.

HUMPHREY, R. K., RAY, A., GONUGUNTLA, S., HAO, E. & JHALA, U. S. 2014. Loss of TRB3 alters dynamics of MLK3-JNK signaling and inhibits cytokine-activated pancreatic beta cell death. *J Biol Chem,* 289**,** 29994-30004.

ILLÁN-GÓMEZ, GONZÁLVEZ-ORTEGA M, OREA-SOLER I, ALCARAZ-TAFALLA MS, ARAGÓN-ALONSO A, PASCUAL-DÍAZ M, PÉREZ-PAREDES M & ML., L.-A. 2012. Obesity and inflammation: change in adiponectin, C-reactive protein, tumour necrosis factor-alpha and interleukin-6 after bariatric surgery. *Obes Surg,* 22.

JURA, M. & KOZAK, L. P. 2016. Obesity and related consequences to ageing. *Age (Dordr),* 38**,** 23.

KACHUR, S., LAVIE, C. J., DE SCHUTTER, A., MILANI, R. V. & VENTURA, H. O. 2017. Obesity and cardiovascular diseases. *Minerva Med,* 108**,** 212-228.

KADOMATSU, T., TABATA, M. & OIKE, Y. 2011. Angiopoietin-like proteins: emerging targets for treatment of obesity and related metabolic diseases. *FEBS J,* 278**,** 559-64.

KAHN, HULL RL & KM., U. 2006. Mechanisms linking obesity to insulin resistance and type 2 diabetes. *Nature,* 14.

KAHN, S. E., PRIGEON, R. L., SCHWARTZ, R. S., FUJIMOTO, W. Y., KNOPP, R. H., BRUNZELL, J. D. & PORTE, D., JR. 2001. Obesity, body fat distribution, insulin sensitivity and Islet beta-cell function as explanations for metabolic diversity. *J Nutr,* 131**,** 354S-60S.

KAPLAN, F., AL-MAJALI, K. & BETTERIDGE, D. J. 2001. PPARS, insulin resistance and type 2 diabetes. *J Cardiovasc Risk,* 8**,** 211-7.

KARBIENER M, F. C., NOWITSCH S, OPRIESSNIG P, PAPAK C, AILHAUD G, DANI C, AMRI EZ, SCHEIDELER M. 2009. microRNA miR-27b impairs human adipocyte differentiation and targets PPARgamma. *Res Commun,* 2**,** 247-251.

KATHIRESAN, MELANDER O, GUIDUCCI C, SURTI A, B. N., RIEDER MJ, COOPER GM, ROOS C, VOIGHT BF, HAVULINNA AS, WAHLSTRAND B, HEDNER T, CORELLA D, TAI ES, ORDOVAS JM, BERGLUND G, VARTIAINEN E, JOUSILAHTI P, HEDBLAD B, TASKINEN MR, NEWTON-CHEH C, SALOMAA V, PELTONEN L, GROOP L, ALTSHULER DM & M., O.-M. 2008. Six new loci associated with blood low-density lipoprotein cholesterol, high-density lipoprotein cholesterol or triglycerides in humans. *Nat Genet,* 40**,** 189-97.

KATO, S. & DU, K. 2007. TRB3 modulates C2C12 differentiation by interfering with Akt activation. *Biochem Biophys Res Commun,* 353**,** 933-8.

KATSIKI, N., MANTZOROS, C. & MIKHAILIDIS, D. P. 2017. Adiponectin, lipids and atherosclerosis. *Curr Opin Lipidol,* 28**,** 347-354.

KAUR, J. 2014. A comprehensive review on metabolic syndrome. *Cardiol Res Pract,* 2014**,** 943162.

KEESHAN, K., BAILIS, W., DEDHIA, P. H., VEGA, M. E., SHESTOVA, O., XU, L., TOSCANO, K., ULJON, S. N., BLACKLOW, S. C. & PEAR, W. S. 2010. Transformation by Tribbles homolog 2 (Trib2) requires both the Trib2 kinase domain and COP1 binding. *Blood,* 116**,** 4948-57.

KEESHAN, K., HE, Y., WOUTERS, B. J., SHESTOVA, O., XU, L., SAI, H., RODRIGUEZ, C. G., MAILLARD, I., TOBIAS, J. W., VALK, P., CARROLL, M., ASTER, J. C., DELWEL, R. & PEAR, W. S. 2006. Tribbles

homolog 2 inactivates C/EBPalpha and causes acute myelogenous leukemia. *Cancer Cell,* 10**,** 401-11.
KEESHAN, K., SHESTOVA, O., USSIN, L. & PEAR, W. S. 2008. Tribbles homolog 2 (Trib2) and HoxA9 cooperate to accelerate acute myelogenous leukemia. *Blood Cells Mol Dis,* 40**,** 119-21.
KISS-TOTH, E. 2011. Tribbles: 'puzzling' regulators of cell signalling. *Biochem Soc Trans,* 39**,** 684-7.
KISS-TOTH, E., BAGSTAFF, S. M., SUNG, H. Y., JOZSA, V., DEMPSEY, C., CAUNT, J. C., OXLEY, K. M., WYLLIE, D. H., POLGAR, T., HARTE, M., O'NEILL L, A., QWARNSTROM, E. E. & DOWER, S. K. 2004a. Human tribbles, a protein family controlling mitogen-activated protein kinase cascades. *J Biol Chem,* 279**,** 42703-8.
KISS-TOTH, E., BAGSTAFF, S. M., SUNG, H. Y., JOZSA, V., DEMPSEY, C., CAUNT, J. C., OXLEY, K. M., WYLLIE, D. H., POLGAR, T., HARTE, M., O'NEILL, L. A., QWARNSTROM, E. E. & DOWER, S. K. 2004b. Human tribbles, a protein family controlling mitogen-activated protein kinase cascades. *J Biol Chem,* 279**,** 42703-8.
KISS-TOTH, E., WYLLIE, D. H., HOLLAND, K., MARSDEN, L., JOZSA, V., OXLEY, K. M., POLGAR, T., QWARNSTROM, E. E. & DOWER, S. K. 2006. Functional mapping and identification of novel regulators for the Toll/Interleukin-1 signalling network by transcription expression cloning. *Cell Signal,* 18**,** 202-14.
KLADWANG, W., VANLANG, C. C., CORDERO, P. & DAS, R. 2011. A two-dimensional mutate-and-map strategy for non-coding RNA structure. *Nat Chem,* 3**,** 954-62.
KLINGENSPOR, M., XU, P., COHEN, R. D., WELCH, C. & REUE, K. 1999. Altered gene expression pattern in the fatty liver dystrophy mouse reveals impaired insulin-mediated cytoskeleton dynamics. *J Biol Chem,* 274**,** 23078-84.
KLOP, B., ELTE, J. W. & CABEZAS, M. C. 2013. Dyslipidemia in obesity: mechanisms and potential targets. *Nutrients,* 5**,** 1218-40.
KOO, S. H., SATOH, H., HERZIG, S., LEE, C. H., HEDRICK, S., KULKARNI, R., EVANS, R. M., OLEFSKY, J. & MONTMINY, M. 2004. PGC-1 promotes insulin resistance in liver through PPAR-alpha-dependent induction of TRB-3. *Nat Med,* 10**,** 530-4.
KOPELMAN 2000. Obesity as a medical problem. *Nature,* 6**,** 635-43.
KRATZER, A., GIRAL, H. & LANDMESSER, U. 2014. High-density lipoproteins as modulators of endothelial cell functions: alterations in patients with coronary artery disease. *Cardiovasc Res,* 103**,** 350-61.
KUHN, NUOVO GJ, MARTIN MM, MALANA GE, PLEISTER AP, JIANG J, SCHMITTGEN TD, TERRY AV JR, GARDINER K, HEAD E, FELDMAN DS & TS., E. 2008. Human chromosome 21-derived miRNAs are overexpressed in down syndrome brains and hearts. *Biochem Biophys Res Commun,* 370**,** 473-7.
KUO, C. H., MOROHOSHI, K., AYE, C. C., GAROON, R. B., COLLINS, A. & ONO, S. J. 2012. The role of TRB3 in mast cells sensitized with monomeric IgE. *Exp Mol Pathol,* 93**,** 408-15.
KURET, T., BURJA, B., FEICHTINGER, J., THALLINGER, G. G., FRANK-BERTONCELJ, M., LAKOTA, K., ZIGON, P., SODIN-SEMRL, S., CUCNIK, S., TOMSIC, M. & HOCEVAR, A. 2018. Gene and miRNA expression in giant cell arteritis-a concise systematic review of significantly modified studies. *Clin Rheumatol*.
KURODA, J. & KITAZONO, T. 2013. [Atherosclerosis: progress in diagnosis and treatments. Topics: II. Atherosclerosis -promoting factors; pathogenesis and pathophysiology; 1. Risk factors for cerebrovascular disease and carotid atherosclerosis]. *Nihon Naika Gakkai Zasshi,* 102**,** 289-96.
LACQUEMANT, C., VASSEUR, F., LEPRETRE, F. & FROGUEL, P. 2005. [Adipocytokins, obesity and development of type 2 diabetes]. *Med Sci (Paris),* 21 Spec No**,** 10-8.
LAU, D. C., DHILLON, B., YAN, H., SZMITKO, P. E. & VERMA, S. 2005. Adipokines: molecular links between obesity and atheroslcerosis. *Am J Physiol Heart Circ Physiol,* 288**,** H2031-41.
LAWRENCE & KOPELMAN 2004. Medical Consequences of Obesity. *Clin Dermatol.,* 22**,** 296-302.

LEE, FEINBAUM RL & V., A. 1993. The C. elegans heterochronic gene lin-4 encodes small RNAs with antisense complementarity to lin-14. *Cell,* 75**,** 843-54.
LIANG, K. L., RISHI, L. & KEESHAN, K. 2013. Tribbles in acute leukemia. *Blood,* 121**,** 4265-70.
LIBBY, RIDKER PM & GK., H. 2011. Progress and challenges in translating the biology of atherosclerosis. *nature,* 473**,** 317-25.
LIBBY, P. 2005. The forgotten majority: unfinished business in cardiovascular risk reduction. *J Am Coll Cardiol,* 46**,** 1225-8.
LIEW, C. W., BOCHENSKI, J., KAWAMORI, D., HU, J., LEECH, C. A., WANIC, K., MALECKI, M., WARRAM, J. H., QI, L., KROLEWSKI, A. S. & KULKARNI, R. N. 2010. The pseudokinase tribbles homolog 3 interacts with ATF4 to negatively regulate insulin exocytosis in human and mouse beta cells. *J Clin Invest,* 120**,** 2876-88.
LIHN, A. S., PEDERSEN, S. B. & RICHELSEN, B. 2005. Adiponectin: action, regulation and association to insulin sensitivity. *Obes Rev,* 6**,** 13-21.
LIU, J., WU, X., FRANKLIN, J. L., MESSINA, J. L., HILL, H. S., MOELLERING, D. R., WALTON, R. G., MARTIN, M. & GARVEY, W. T. 2010. Mammalian Tribbles homolog 3 impairs insulin action in skeletal muscle: role in glucose-induced insulin resistance. *Am J Physiol Endocrinol Metab,* 298**,** E565-76.
LIU, Y., HUO, X., PANG, X. F., ZONG, Z. H., MENG, X. & LIU, G. L. 2008. Musclin inhibits insulin activation of Akt/protein kinase B in rat skeletal muscle. *J Int Med Res,* 36**,** 496-504.
LIU, Y. C., ZOU, X. B., CHAI, Y. F. & YAO, Y. M. 2014. Macrophage polarization in inflammatory diseases. *Int J Biol Sci,* 10**,** 520-9.
LOHAN, F. & KEESHAN, K. 2013. The functionally diverse roles of tribbles. *Biochem Soc Trans,* 41**,** 1096-100.
LOWE, O'RAHILLY S & JJ., R. 2011. Adipogenesis at a glance. *J Cell Sci,* 16**,** 2681-6.
LUKIW 2007. Micro-RNA speciation in fetal, adult and Alzheimer's disease hippocampus. *Neuroreport,* 18**,** 297-300.
LUMENG, C. N. 2013. Innate immune activation in obesity. *Mol Aspects Med,* 34**,** 12-29.
LUO, L. & LIU, M. 2016. Adipose tissue in control of metabolism. *J Endocrinol,* 231**,** R77-R99.
MA, H., WU, Y., YANG, H., LIU, J., DAN, H., ZENG, X., ZHOU, Y., JIANG, L. & CHEN, Q. 2016. MicroRNAs in oral lichen planus and potential miRNA-mRNA pathogenesis with essential cytokines: a review. *Oral Surg Oral Med Oral Pathol Oral Radiol,* 122**,** 164-73.
MARANHAO, R. C., CARVALHO, P. O., STRUNZ, C. C. & PILEGGI, F. 2014. Lipoprotein (a): structure, pathophysiology and clinical implications. *Arq Bras Cardiol,* 103**,** 76-84.
MARTINELLI R, N. C., PILONE V, BUONOMO T, LIGUORI R, CASTANÒ I, BUONO P, MASONE S, PERSICO G, FORESTIERI P, PASTORE L, SACCHETTI L. 2010. miR-519d overexpression is associated with human obesity. *Obesity (Silver Spring),* 18**,** 2170-2176.
MATSUSHIMA, R., HARADA, N., WEBSTER, N. J., TSUTSUMI, Y. M. & NAKAYA, Y. 2006. Effect of TRB3 on insulin and nutrient-stimulated hepatic p70 S6 kinase activity. *J Biol Chem,* 281**,** 29719-29.
MATSUZAWA, Y. 2005. Adipocytokines and metabolic syndrome. *Semin Vasc Med,* 5**,** 34-9.
MATSUZAWA, Y. 2010. Adiponectin: a key player in obesity related disorders. *Curr Pharm Des,* 16**,** 1896-901.
MATSUZAWA, Y., FUNAHASHI, T., KIHARA, S. & SHIMOMURA, I. 2004. Adiponectin and metabolic syndrome. *Arterioscler Thromb Vasc Biol,* 24**,** 29-33.
MAURY, E. & BRICHARD, S. M. 2010. Adipokine dysregulation, adipose tissue inflammation and metabolic syndrome. *Mol Cell Endocrinol,* 314**,** 1-16.
MAYANS, L. 2015. Metabolic Syndrome: Insulin Resistance and Prediabetes. *FP Essent,* 435**,** 11-6.
MILLER, W. M., NORI-JANOSZ, K. E., LILLYSTONE, M., YANEZ, J. & MCCULLOUGH, P. A. 2005. Obesity and lipids. *Curr Cardiol Rep,* 7**,** 465-70.
MITCHELL, M. E. & SIDAWY, A. N. 1998. The pathophysiology of atherosclerosis. *Semin Vasc Surg,* 11**,** 134-41.

MONDA, K. L., NORTH, K. E., HUNT, S. C., RAO, D. C., PROVINCE, M. A. & KRAJA, A. T. 2010. The genetics of obesity and the metabolic syndrome. *Endocr Metab Immune Disord Drug Targets,* 10**,** 86-108.

MONTEIRO, R. & AZEVEDO, I. 2010. Chronic inflammation in obesity and the metabolic syndrome. *Mediators Inflamm,* 2010.

NAKAMURA, SHIMADA K, FUKUDA D, SHIMADA Y, EHARA S, HIROSE M, KATAOKA T, KAMIMORI K, SHIMODOZONO S, KOBAYASHI Y, YOSHIYAMA M, TAKEUCHI K & J., Y. 2004. Implications of plasma concentrations of adiponectin in patients with coronary artery disease. *heart,* 90.

NAMMI, KOKA S, CHINNALA KM & KM., B. 2004. Obesity: An overview on its current perspectives and treatment options. *Nutr J,* 14**,** 3.

NEUSCHWANDER-TETRI, B. A. 2007. Fatty liver and the metabolic syndrome. *Curr Opin Gastroenterol,* 23**,** 193-8.

NGUYEN, P., LERAY, V., DIEZ, M., SERISIER, S., LE BLOC'H, J., SILIART, B. & DUMON, H. 2008. Liver lipid metabolism. *J Anim Physiol Anim Nutr (Berl),* 92**,** 272-83.

NIKOLIC, D., KATSIKI, N., MONTALTO, G., ISENOVIC, E. R., MIKHAILIDIS, D. P. & RIZZO, M. 2013. Lipoprotein subfractions in metabolic syndrome and obesity: clinical significance and therapeutic approaches. *Nutrients,* 5**,** 928-48.

NISOLI, E., CLEMENTI, E., CARRUBA, M. O. & MONCADA, S. 2007. Defective mitochondrial biogenesis: a hallmark of the high cardiovascular risk in the metabolic syndrome? *Circ Res,* 100**,** 795-806.

O'CONNELL, TAGANOV KD, BOLDIN MP, CHENG G & D., B. 2007. MicroRNA-155 is induced during the macrophage inflammatory response. *Proc Natl Acad Sci U S A,* 104**,** 1604-9.

OBERKOFLER, H., PFEIFENBERGER, A., SOYAL, S., FELDER, T., HAHNE, P., MILLER, K., KREMPLER, F. & PATSCH, W. 2010. Aberrant hepatic TRIB3 gene expression in insulin-resistant obese humans. *Diabetologia,* 53**,** 1971-5.

OHOKA, N., YOSHII, S., HATTORI, T., ONOZAKI, K. & HAYASHI, H. 2005. TRB3, a novel ER stress-inducible gene, is induced via ATF4-CHOP pathway and is involved in cell death. *EMBO J,* 24**,** 1243-55.

OKAMOTO, H., LATRES, E., LIU, R., THABET, K., MURPHY, A., VALENZEULA, D., YANCOPOULOS, G. D., STITT, T. N., GLASS, D. J. & SLEEMAN, M. W. 2007. Genetic deletion of Trb3, the mammalian Drosophila tribbles homolog, displays normal hepatic insulin signaling and glucose homeostasis. *Diabetes,* 56**,** 1350-6.

ONO, K., KUWABARA, Y. & HAN, J. 2011. MicroRNAs and cardiovascular diseases. *FEBS J,* 278**,** 1619-33.

ORD, D. & ORD, T. 2003. Mouse NIPK interacts with ATF4 and affects its transcriptional activity. *Exp Cell Res,* 286**,** 308-20.

OSTROVSKY, SWENCIONIS C, WYLIE-ROSETT J & CR., I. 2013. Social anxiety and disordered overeating: An association among overweight and obese individuals

Eat Behav, 145**,** 2.

OUIMET, EDIRIWEERA H, AFONSO MS1, RAMKHELAWON B, SINGARAVELU R, LIAO X, BANDLER RC, RAHMAN K, FISHER EA, RAYNER KJ, PEZACKI JP, TABAS I & KJ., M. 2017. microRNA-33 Regulates Macrophage Autophagy in Atherosclerosis. *Arterioscler Thromb Vasc Biol.,* 37**,** 1058-1067.

OUIMET, M. 2013. Autophagy in obesity and atherosclerosis: Interrelationships between cholesterol homeostasis, lipoprotein metabolism and autophagy in macrophages and other systems. *Biochim Biophys Acta,* 1831**,** 1124-33.

PATEL, T. P., RAWAL, K., BAGCHI, A. K., AKOLKAR, G., BERNARDES, N., DIAS DDA, S., GUPTA, S. & SINGAL, P. K. 2016. Insulin resistance: an additional risk factor in the pathogenesis of cardiovascular disease in type 2 diabetes. *Heart Fail Rev,* 21**,** 11-23.

POONAWALLA, A. H., SJOBERG, B. P., REHM, J. L., HERNANDO, D., HINES, C. D., IRARRAZAVAL, P. & REEDER, S. B. 2013. Adipose tissue MRI for quantitative measurement of central obesity. *J Magn Reson Imaging,* 37**,** 707-16.

PRUDENTE, S., HRIBAL, M. L., FLEX, E., TURCHI, F., MORINI, E., DE COSMO, S., BACCI, S., TASSI, V., CARDELLINI, M., LAURO, R., SESTI, G., DALLAPICCOLA, B. & TRISCHITTA, V. 2005. The functional Q84R polymorphism of mammalian Tribbles homolog TRB3 is associated with insulin resistance and related cardiovascular risk in Caucasians from Italy. *Diabetes,* 54**,** 2807-11.

PRUDENTE, S., SESTI, G., PANDOLFI, A., ANDREOZZI, F., CONSOLI, A. & TRISCHITTA, V. 2012. The mammalian tribbles homolog TRIB3, glucose homeostasis, and cardiovascular diseases. *Endocr Rev,* 33**,** 526-46.

QATANANI & MA., L. 2007. Mechanisms of obesity-associated insulin resistance: many choices on the menu. *Genes Dev.,* 21.

QI, L., HEREDIA, J. E., ALTAREJOS, J. Y., SCREATON, R., GOEBEL, N., NIESSEN, S., MACLEOD, I. X., LIEW, C. W., KULKARNI, R. N., BAIN, J., NEWGARD, C., NELSON, M., EVANS, R. M., YATES, J. & MONTMINY, M. 2006. TRB3 links the E3 ubiquitin ligase COP1 to lipid metabolism. *Science,* 312**,** 1763-6.

QIN, L., WANG, Y., TAO, L. & WANG, Z. 2011. AKT down-regulates insulin-like growth factor-1 receptor as a negative feedback. *J Biochem,* 150**,** 151-6.

RAVUSSIN. 1995. Metabolic differences and the development of obesity. *Metabolism,* 4**,** 12-4.

RISSANEN, HELIÖVAARA M, KNEKT P, REUNANEN A & A., A. 1991. Determinants of weight gain and overweight in adult Finns. *Eur J Clin Nutr.,* 45**,** 419-30.

RØRTH, P., SZABO, K. & TEXIDO, G. 2000. The level of C/EBP protein is critical for cell migration during Drosophila oogenesis and is tightly controlled by regulated degradation. *Mol Cell,* 6**,** 23-30.

ROSEN & OA., M. 2006. Adipocyte differentiation from the inside out. *Nat Rev Mol Cell Biol.,* 12**,** 885-96.

ROSENKILDE, NORDBY P, NIELSEN LB, STALLKNECHT BM & JW., H. 2010 Fat oxidation at rest predicts peak fat oxidation during exercise and metabolic phenotype in overweight men. *Int J Obes (Lond),* 34**,** 871-7.

SAELY, GEIGER K & H., D. 2012. Brown versus White Adipose Tissue: A Mini-Review. *Gerontology,* 58**,** 15-23.

SAKA, Y. & SMITH, J. C. 2004. A Xenopus tribbles orthologue is required for the progression of mitosis and for development of the nervous system. *Dev Biol,* 273**,** 210-25.

SALAZAR, M., LORENTE, M., GARCIA-TABOADA, E., PEREZ GOMEZ, E., DAVILA, D., ZUNIGA-GARCIA, P., MARIA FLORES, J., RODRIGUEZ, A., HEGEDUS, Z., MOSEN-ANSORENA, D., ARANSAY, A. M., HERNANDEZ-TIEDRA, S., LOPEZ-VALERO, I., QUINTANILLA, M., SANCHEZ, C., IOVANNA, J. L., DUSETTI, N., GUZMAN, M., FRANCIS, S. E., CARRACEDO, A., KISS-TOTH, E. & VELASCO, G. 2014. Loss of Tribbles pseudokinase-3 promotes Akt-driven tumorigenesis via FOXO inactivation. *Cell Death Differ*.

SAPONARO, C., GAGGINI, M., CARLI, F. & GASTALDELLI, A. 2015. The Subtle Balance between Lipolysis and Lipogenesis: A Critical Point in Metabolic Homeostasis. *Nutrients,* 7**,** 9453-74.

SATOH, T., KIDOYA, H., NAITO, H., YAMAMOTO, M., TAKEMURA, N., NAKAGAWA, K., YOSHIOKA, Y., MORII, E., TAKAKURA, N., TAKEUCHI, O. & AKIRA, S. 2013. Critical role of Trib1 in differentiation of tissue-resident M2-like macrophages. *Nature,* 495**,** 524-8.

SCARBOROUGH, BHATNAGAR P, WICKRAMASINGHE KK, ALLENDER S, FOSTER C & M., R. 2011. The economic burden of ill health due to diet, physical inactivity, smoking, alcohol and obesity in the UK. *J Public Health (Oxf).* 44**,** 527-35.

SEEDORF, U. & ASSMANN, G. 2001. The role of PPAR alpha in obesity. *Nutr Metab Cardiovasc Dis,* 11**,** 189-94.

SELIM, E., FRKANEC, J. T. & CUNARD, R. 2007. Fibrates upregulate TRB3 in lymphocytes independent of PPAR alpha by augmenting CCAAT/enhancer-binding protein beta (C/EBP beta) expression. *Mol Immunol,* 44**,** 1218-29.

SHARMA AM1, S. B. 2007. Review: Peroxisome proliferator-activated receptor gamma and adipose tissue--understanding obesity-related changes in regulation of lipid and glucose metabolism. *J Clin Endocrinol Metab*.

SHAROVA, L. V., SHAROV, A. A., NEDOREZOV, T., PIAO, Y., SHAIK, N. & KO, M. S. H. 2009. Database for mRNA Half-Life of 19 977 Genes Obtained by DNA Microarray Analysis of Pluripotent and Differentiating Mouse Embryonic Stem Cells. *DNA Research,* 16**,** 45-58.

SHERLING, D. H., PERUMAREDDI, P. & HENNEKENS, C. H. 2017. Metabolic Syndrome. *J Cardiovasc Pharmacol Ther,* 22**,** 365-367.

SIERSBAEK R, N. R., MANDRUP S. 2010. PPARgamma in adipocyte differentiation and metabolism--novel insights from genome-wide studies. *FEBS Lett,* 584(15).

SOUBEYRAND, S., MARTINUK, A., NAING, T., LAU, P. & MCPHERSON, R. 2016. Role of Tribbles Pseudokinase 1 (TRIB1) in human hepatocyte metabolism. *Biochim Biophys Acta,* 1862**,** 223-32.

SUNG, H. Y., FRANCIS, S. E., ARNOLD, N. D., HOLLAND, K., ERNST, V., ANGYAL, A. & KISS-TOTH, E. 2012. Enhanced macrophage tribbles-1 expression in murine experimental atherosclerosis. *Biology (Basel),* 1**,** 43-57.

SUNG, H. Y., GUAN, H., CZIBULA, A., KING, A. R., EDER, K., HEATH, E., SUVARNA, S. K., DOWER, S. K., WILSON, A. G., FRANCIS, S. E., CROSSMAN, D. C. & KISS-TOTH, E. 2007. Human tribbles-1 controls proliferation and chemotaxis of smooth muscle cells via MAPK signaling pathways. *J Biol Chem,* 282**,** 18379-87.

SZCZYGIELSKA, WIDOMSKA S, JARASZKIEWICZ M, KNERA P & K., M. 2003. Blood lipids profile in obese or overweight patients. *Ann Univ Mariae Curie Sklodowska Med,* 58.

TAKAHASHI, S. & SAKAI, J. 2006. [PPARalpha, PPARgamma, PPARdelta]. *Nihon Rinsho,* 64 Suppl 9**,** 259-62.

TAKAHASHI, Y., OHOKA, N., HAYASHI, H. & SATO, R. 2008. TRB3 suppresses adipocyte differentiation by negatively regulating PPARgamma transcriptional activity. *J Lipid Res,* 49**,** 880-92.

TANAKA, N., AOYAMA, T., KIMURA, S. & GONZALEZ, F. J. 2017. Targeting nuclear receptors for the treatment of fatty liver disease. *Pharmacol Ther,* 179**,** 142-157.

THOMAS, D. & APOVIAN, C. 2017. Macrophage functions in lean and obese adipose tissue. *Metabolism,* 72**,** 120-143.

THUM, CATALUCCI D & J., B. 2008. MicroRNAs: novel regulators in cardiac development and disease. *Cardiovasc Res,* 79**,** 562-70.

TILI, MICHAILLE JJ, COSTINEAN S & CM., C. 2008. MicroRNAs, the immune system and rheumatic disease. *Nat Clin Pract Rheumatol,* 4**,** 534-41.

TOUSOULIS, D., KAMPOLI, A. M., PAPAGEORGIOU, N., ANDROULAKIS, E., ANTONIADES, C., TOUTOUZAS, K. & STEFANADIS, C. 2011. Pathophysiology of atherosclerosis: the role of inflammation. *Curr Pharm Des,* 17**,** 4089-110.

TYAGI, GUPTA P, SAINI AS, KAUSHAL C & S., S. 2011. The peroxisome proliferator-activated receptor: A family of nuclear receptors role in various diseases. *J Adv Pharm Technol Res,* 4**,** 236-40.

UENO, OH-ISHI S, SEGAWA M, NISHIDA M, FUKUWATARI Y, KIZAKI T, OOKAWARA T & H., O. 1998. Effect of age on brown adipose tissue activity in the obese (ob/ob) mouse. *Mech Ageing Dev.,* 12**,** 67-76.

VAN DEN BERG, VAN DAM AD, RENSEN PC, MP, D. W. & E, L. 2017. Immune Modulation of Brown(ing) Adipose Tissue in Obesity. *Endocr Rev,* 38**,** 46-68.

VAN MARKEN LICHTENBELT, VANHOMMERIG JW, SMULDERS NM, DROSSAERTS JM, KEMERINK GJ, BOUVY ND, SCHRAUWEN P & GJ., T. 2009. Cold-activated brown adipose tissue in healthy men. *N Engl J Med.,* 360**,** 1500-8.

VIRTANEN, LIDELL ME, ORAVA J, HEGLIND M, WESTERGREN R, NIEMI T, TAITTONEN M, LAINE J, SAVISTO NJ, ENERBÄCK S & P., N. 2009. Functional brown adipose tissue in healthy adults. *N Engl J Med,* 360**,** 1518-25.

WAHID, SHEHZAD A, KHAN T & YY., K. 2010. MicroRNAs: Synthesis, mechanism, function, and recent clinical trials. *Biochim Biophys Acta,* 1803**,** 1231-43.

WANG, S., HONG, X., TU, Z. & YUAN, G. 2017. Angiopoietin-like protein 8: An attractive biomarker for the evaluation of subjects with insulin resistance and related disorders. *Diabetes Res Clin Pract,* 133**,** 168-177.

WANG, Y. G., SHI, M., WANG, T., SHI, T., WEI, J., WANG, N. & CHEN, X. M. 2009. Signal transduction mechanism of TRB3 in rats with non-alcoholic fatty liver disease. *World J Gastroenterol,* 15**,** 2329-35.

WANG, Z. H., SHANG, Y. Y., ZHANG, S., ZHONG, M., WANG, X. P., DENG, J. T., PAN, J., ZHANG, Y. & ZHANG, W. 2012. Silence of TRIB3 suppresses atherosclerosis and stabilizes plaques in diabetic ApoE-/-/LDL receptor-/- mice. *Diabetes,* 61**,** 463-73.

WEISMANN, D., ERION, D. M., IGNATOVA-TODORAVA, I., NAGAI, Y., STARK, R., HSIAO, J. J., FLANNERY, C., BIRKENFELD, A. L., MAY, T., KAHN, M., ZHANG, D., YU, X. X., MURRAY, S. F., BHANOT, S., MONIA, B. P., CLINE, G. W., SHULMAN, G. I. & SAMUEL, V. T. 2011. Knockdown of the gene encoding Drosophila tribbles homologue 3 (Trib3) improves insulin sensitivity through peroxisome proliferator-activated receptor-gamma (PPAR-gamma) activation in a rat model of insulin resistance. *Diabetologia,* 54**,** 935-44.

WHITEHEAD, J. P., RICHARDS, A. A., HICKMAN, I. J., MACDONALD, G. A. & PRINS, J. B. 2006. Adiponectin--a key adipokine in the metabolic syndrome. *Diabetes Obes Metab,* 8**,** 264-80.

WILLETT, DIETZ WH & GA., C. 1999. Guidelines for healthy weight. *N Engl J Med,* 5.

WILLETT, L. L. & ALBRIGHT, E. S. 2004. Achieving glycemic control in type 2 diabetes: a practical guide for clinicians on oral hypoglycemics. *South Med J,* 97**,** 1088-92.

WU, M., XU, L. G., ZHAI, Z. & SHU, H. B. 2003. SINK is a p65-interacting negative regulator of NF-kappaB-dependent transcription. *J Biol Chem,* 278**,** 27072-9.

XING LIU, JIEJIE ZHAO, QI LIU, XUELIAN XIONG, ZHIJIAN ZHANG, YANG JIAO, XIAOYING LI, BIN LIU, LI, Y. & LU, Y. 2016. MicroRNA-124 promotes hepatic triglyceride accumulation through targeting tribbles homolog 3. *Scientific Reports,* 6.

XU, J., LV, S., QIN, Y., SHU, F., XU, Y., CHEN, J., XU, B. E., SUN, X. & WU, J. 2007. TRB3 interacts with CtIP and is overexpressed in certain cancers. *Biochim Biophys Acta,* 1770**,** 273-8.

YAMAMOTO, M., UEMATSU, S., OKAMOTO, T., MATSUURA, Y., SATO, S., KUMAR, H., SATOH, T., SAITOH, T., TAKEDA, K., ISHII, K. J., TAKEUCHI, O., KAWAI, T. & AKIRA, S. 2007. Enhanced TLR-mediated NF-IL6 dependent gene expression by Trib1 deficiency. *J Exp Med,* 204**,** 2233-9.

YAN, F., WANG, Q., XU, C., CAO, M., ZHOU, X., WANG, T., YU, C., JING, F., CHEN, W., GAO, L. & ZHAO, J. 2014. Peroxisome proliferator-activated receptor alpha activation induces hepatic steatosis, suggesting an adverse effect. *PLoS One,* 9**,** e99245.

YANG, Z., CAPPELLO, T. & WANG, L. 2015. Emerging role of microRNAs in lipid metabolism. *Acta Pharm Sin B,* 5**,** 145-50.

YKI-JARVINEN, H. 2010. Liver fat in the pathogenesis of insulin resistance and type 2 diabetes. *Dig Dis,* 28**,** 203-9.

YOKOYAMA, T., KANNO, Y., YAMAZAKI, Y., TAKAHARA, T., MIYATA, S. & NAKAMURA, T. 2010. Trib1 links the MEK1/ERK pathway in myeloid leukemogenesis. *Blood,* 116**,** 2768-75.

YU, CHEN Y, CLINE GW, ZHANG D, ZONG H, WANG Y, BERGERON R, KIM JK, CUSHMAN SW, COONEY GJ, ATCHESON B, WHITE MF, KRAEGEN EW & GI., S. 2002. Mechanism by which fatty acids inhibit insulin activation of insulin receptor substrate-1 (IRS-1)-associated phosphatidylinositol 3-kinase activity in muscle. *J Biol Chem,* 27.

ZANINOTTO, HEAD J, STAMATAKIS E, WARDLE H & J., M. 2009. Trends in obesity among adults in England from 1993 to 2004 by age and social class and projections of prevalence to 2012. *J Epidemiol Community Health,* 63**,** 140-6.

ZHANG, PROENCA R, MAFFEI M, BARONE M, LEOPOLD L & JM., F. 1994. Positional cloning of the mouse obese gene and its human homologue. *Nature,* 1.

ZHONG, PERSAUD L, MUHARAM H, FRANCIS A, DAS D, AKTAS, BH9 & M, S. 2018. Eukaryotic Translation Initiation Factor 4A Down-Regulation Mediates Interleukin-24-Induced Apoptosis through Inhibition of Translation. *Cancers* 10.

ZHOU, Y., LI, L., LIU, Q., XING, G., KUAI, X., SUN, J., YIN, X., WANG, J., ZHANG, L. & HE, F. 2008. E3 ubiquitin ligase SIAH1 mediates ubiquitination and degradation of TRB3. *Cell Signal,* 20**,** 942-8.

ZHUANG, L., LI, C., CHEN, Q., JIN, Q., WU, L., LU, L., YAN, X. & CHEN, K. 2019. Overexpression of fatty acid binding protein 3 promotes remodeling after myocardial infarction by inducing apoptosis. *Am J Physiol Heart Circ Physiol*.

Appendix I- Metabolic Syndrome Definition

	World Health organisation WHO 1998	International diabetes federation IDF	National Cholesterol Education Program Adult Treatment Panel III NCEP ATP III
Required criteria	Type 2 DM, impaired fasting glucose, impaired glucose tolerance or insulin resistance PLUS 2 of:	Waist circumference 90 cm (for Asian) PLUS 2 of:	3 of the following:
Fasting glucose	NA	Glucose 100 mg dl^{-1} or previously diagnosed as type 2 DM	Glucose □110 mg dl^{-} or previously diagnosed as type 2 DM
HDL-cholesterol	<35 mg dl^{-1} or specific treatment	<40 mg dl^{-1} or specific treatment	<40 mg dl^{-1} or specific treatment
Triglyceride	Triglyceride level 150 mg dl^{-1} or specific treatment	Triglyceride level 150 mg dl^{-1} or specific treatment	Triglyceride level □150 mg dl^{-1} or specific treatment
Hypertension	Blood pressure 140/90 mm Hg or receiving anti-hypertensive medication	Blood pressure 130/85 mm Hg or receiving anti-hypertensive medication	Blood pressure 130/85 mm Hg or receiving anti-hypertensive medication
Obesity	BMI>30 kg m^{-2} or WHR>0.9	NA	Waist circumference >90 cm (for Asian)
Urine protein	microalbuminuria (albumin/creatinine ratio □30 mg g^{-1})	NA	NA

Appendix II-Genotyping

DNA was extracted from the mouse ear clip and placed in the lysis buffer overnight at 56'C to digest in the tissue.

DNA isolation

1. Add Prot K solution to lysis buffer to a final concentration of 300 µg/ml (30 µl stock per ml lysis buffer)
2. Add 150 µl lysis+Prot K to each ear clip in 1.5 ml eppendorf tube
3. Incubate ON at 55°C in waterbath
4. Vortex briefly
5. Heat inactivate Prot K by incubating samples @ 100°C for 12 min (heat block)
6. Add 600 µl sterile H_2O to each tube
7. Vortex & store @ 4°C
8. Use 4 µl DNA per reaction

Trib3 primer specifications:

LEXKO-1947-3′: CCGCGACGAATGAAAGGTTTA
LEXKO-1947-5′: AGACTCCGAGAGCTGCTCAGTTAGG
LTR-2: AAATGGCGTTACTTAAGCTAGCTTGC

WT oligos: LEXKO-1947-3′ + LEXKO-1947-5′
KO oligos: LEXKO-1947-3′ + LTR-2

WT band: 483bp
KO band: 381bp

PCR & agarose gel analysis

1. Prepare PCR mix on ice. Per sample:

Biomix Red (2x)	12.5 µl
Primer 1	0.5 µl
Primer 2	0.5 µl
Primer 3	0.5 µl
H_2O	9.0 µl
DNA sample	2.0 µl

	25.0 µl

   in 0.5 ml eppendorf tubes or 8-tube strips.

2. Run PCR using the following settings:

Step 1:	5 min at 95 °C	1 cycle
Step 2:	30 sec at 95 °C	40 cycles
	30 sec at 65 °C	
	30 sec at 72 °C	
Step 3:	5 min at 72 °C	1 cycle
Step 4:	∞ at 10 °C	

3. Prepare 2 % agarose gel: 100 ml TAE buffer + 2g agarose + 14 µl ethidium bromide (*handle with care! Carcinogenic substance*)
4. Run PCR products and marker (100 bp DNA ladder; Geneflow) on gel @ 80 V, 10 µl sample / slot
5. Analyse gel using transilluminator with EtBr/UV filter

Materials

- Tribbles-3 primers (Sigma); all primers are 100 µM in H_2O
- Biomix Red (2x concentrated; Bioline Ltd)
- TAE buffer
- Agarose powder
- Ethidium bromide
- Lysis buffer:
  - 10 ml 1M Tris-HCl (pH 8.5)
  - 0.4 ml 0.5M EDTA (pH 8.0)
  - 10 ml 10% Tween-20
  - Add H_2O to 200 ml; filter & store @ -20°C in 20 ml aliquots
- Proteinase K (10 mg/ml stock):
  - 100 mg Prot K
  - 5 ml glycerol
  - 100 µl 1M TRIS-HCl (pH 7.5)
  - 29 mg $CaCl_2$
  - Add H_2O to 10 ml; store 1 ml aliquots @ -20°C

Appendix III-Metabolic cage experiment

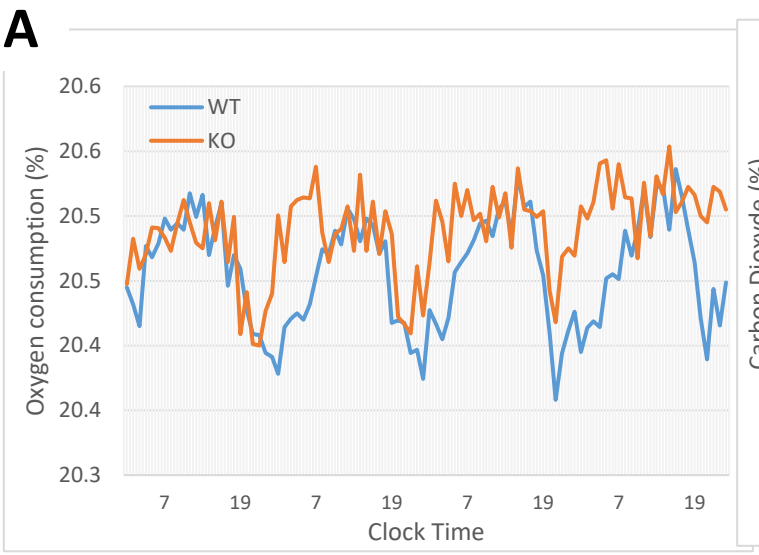

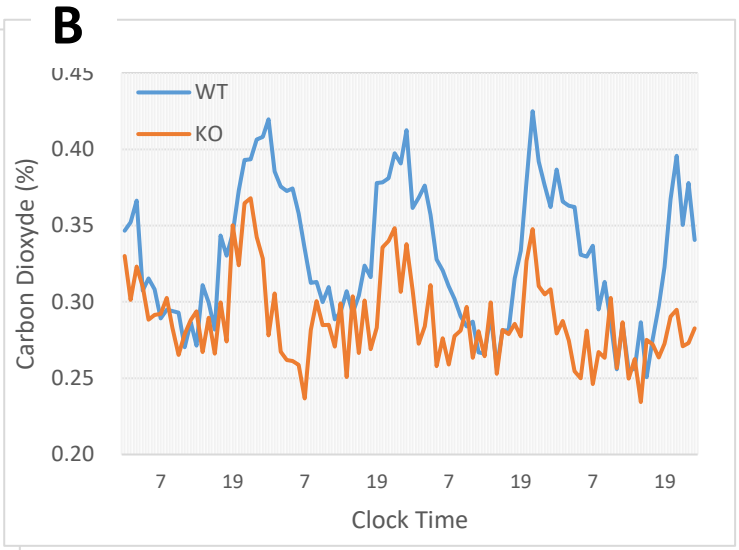

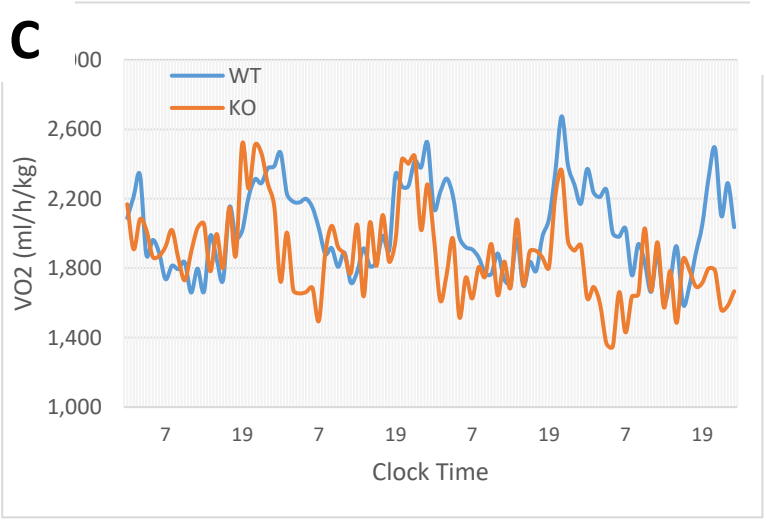

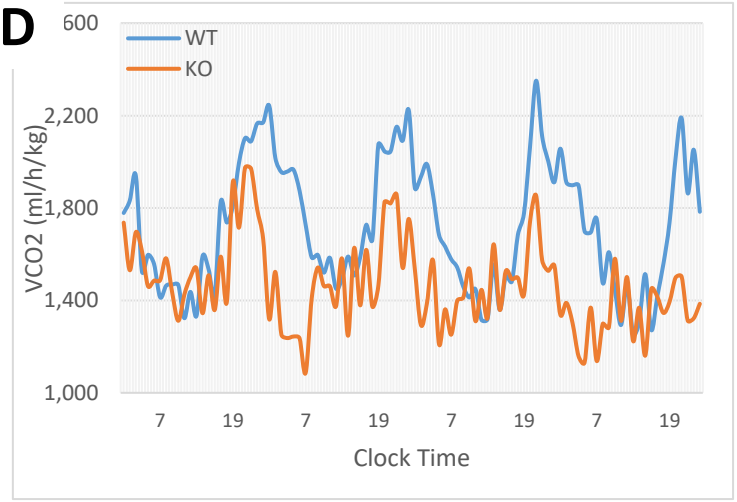

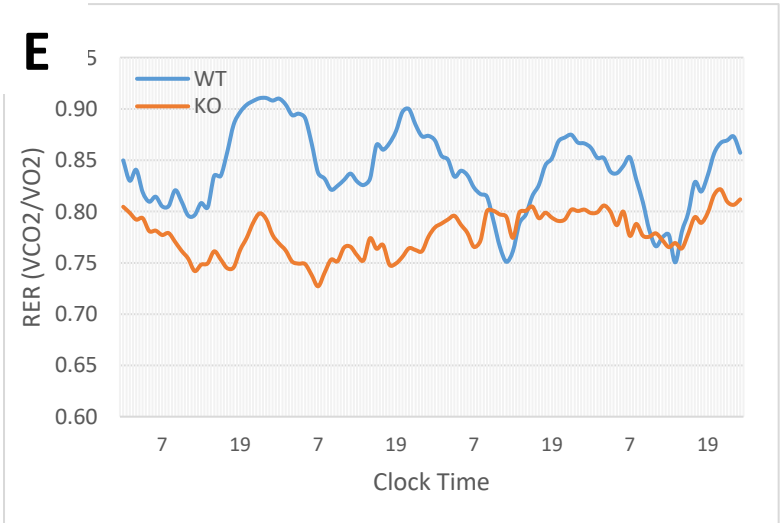

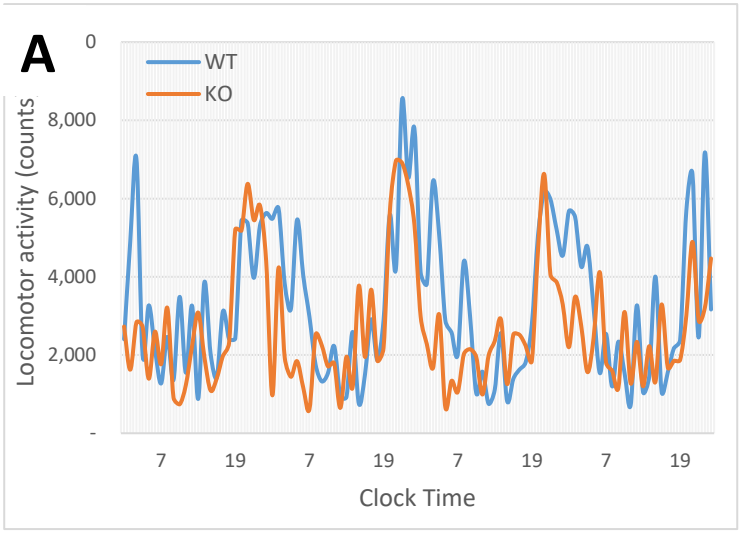
A
WT
KO
Locomotor activity (counts
0
8,000
6,000
4,000
2,000
-
7
19
7
19
7
19
7
19
Clock Time

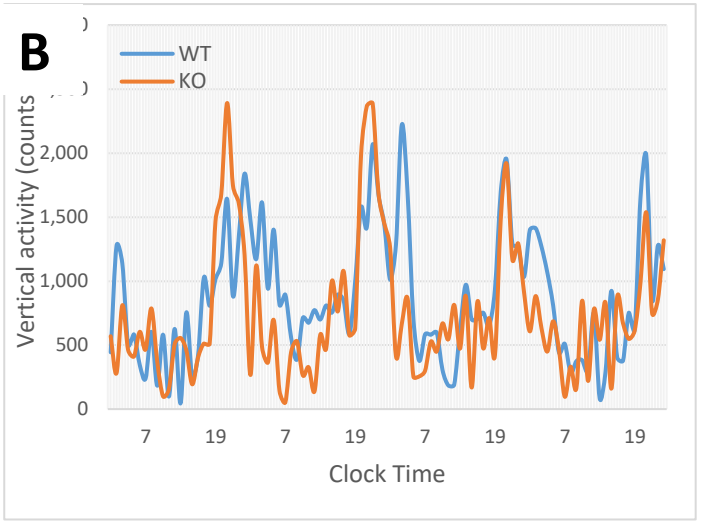
B
WT
KO
Vertical activity (counts
2,000
1,500
1,000
500
0
7
19
7
19
7
19
7
19
Clock Time

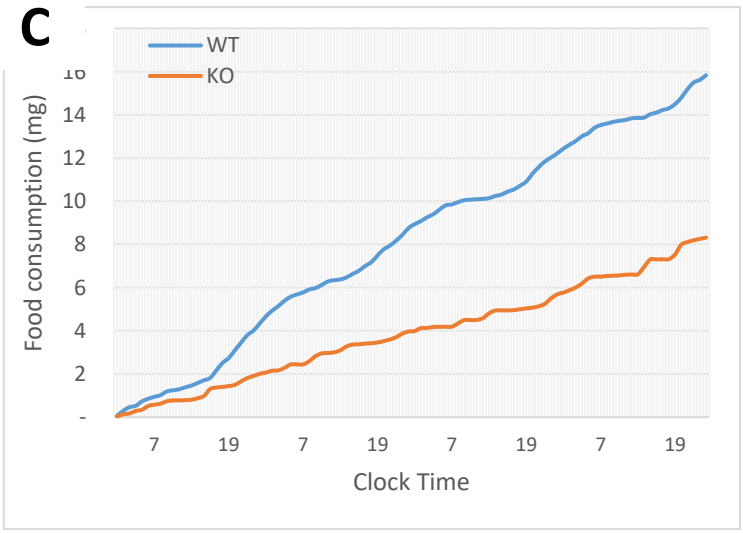
C
WT
KO
Food consumption (mg)
14
12
10
8
6
4
2
-
7
19
7
19
7
19
7
19
Clock Time

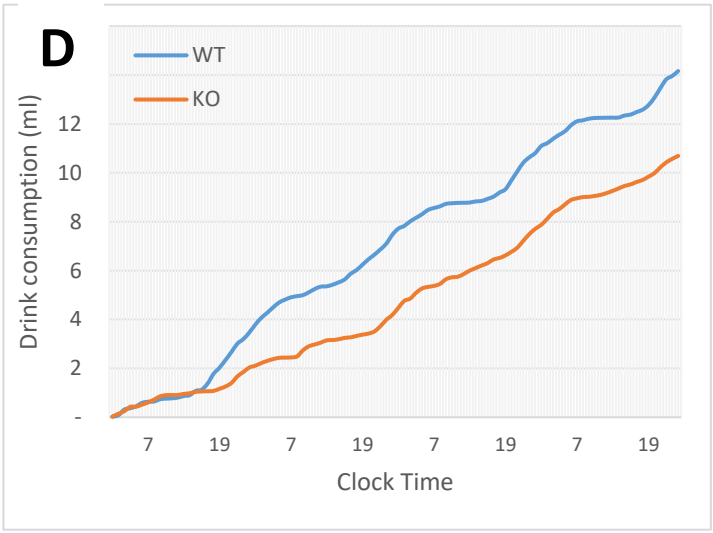
D
WT
KO
Drink consumption (ml)
12
10
8
6
4
2
-
7
19
7
19
7
19
7
19
Clock Time

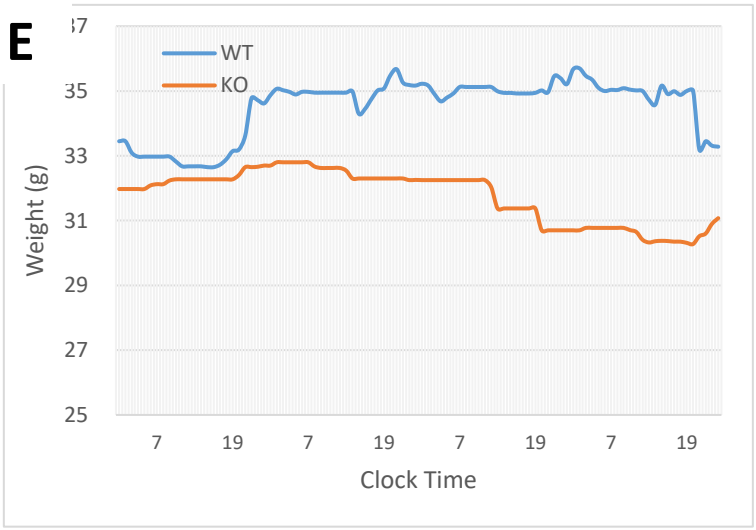
E
WT
KO
Weight (g)
35
33
31
29
27
25
7
19
7
19
7
19
7
19
Clock Time

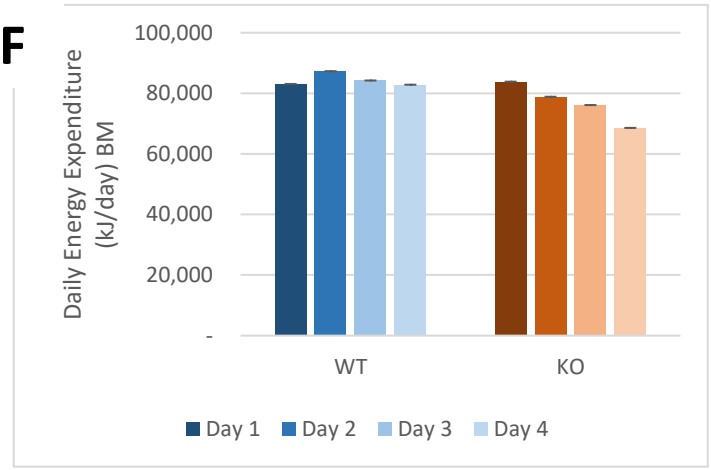
F
Daily Energy Expenditure (kJ/day) BM
100,000
80,000
60,000
40,000
20,000
-
WT
KO
Day 1
Day 2
Day 3
Day 4

Appendix VII-Trib3 RNA levels (QC)